SYNERGISTIC EFFECTS OF ALCOHOL-BASED RENEWABLE FUELS: FUEL PROPERTIES AND EMISSIONS

by

EKARONG SUKJIT

A thesis submitted to
The University of Birmingham
for the degree of

DOCTOR OF PHILOSOPHY

School of Mechanical Engineering
The University of Birmingham
November 2013

ABSTRACT

Biodiesel is known to improve the fuel properties of alcohol-diesel blends. However biodiesel is obtained from different feedstock and consequently the composition can be different, with varying fatty acid profiles resulting in different physical and chemical properties and a different response when blended with alcohol-diesel blends. To understand the effect of molecular structure of biodiesel on fuel properties and emissions, the most representative individual fatty acid methyl esters were added to alcohol-diesel blends. The results show that 15% of all methyl esters was enough to avoid phase separation of alcohol-diesel blends and keep the wear scar diameter of the blends below the limitation required by lubricity standards. Short carbon chain length and saturated methyl ester are recommended to improve emissions of alcohol-diesel blends. A comparison between two different alcohols used in the engine tests highlighted that butanol blends were more effective in reducing carbonaceous gas emissions and particulate matter emissions than ethanol blends. Further research on the effect of molecular structure of biodiesel on alcohol-diesel blends was conducted to understand influence of hydroxylated biodiesel which is derived from castor oil. The existence of hydroxyl group in biodiesel considerably improves the lubricity of alcohol-diesel blends. It was also shown to be beneficial in terms of engine-out emissions such as enhancing soot oxidation and reducing activation energy to oxidise soot emissions.

To counteract the likely increase in gaseous carbonaceous emissions with alcohol blends, the addition of hydrogen to replace part of the carbon within the liquid fuel was studied. The incorporation of hydrogen and alcohol blends indicates that there was a dramatic reduction in carbon dioxide, unburnt hydrocarbons and particulate matter emissions.

ACKNOWLEDGEMENTS

I would not have been able to complete my thesis without the support and contribution of a number of following individuals whom I would like to acknowledge.

I would like to express deepest gratitude to my advisors, Dr. Karl Dearn and Dr. Athanasios Tsolakis for their full support, productive guidance and invaluable advice throughout this research. I would also like to thank Dr. Jose Martin Herreros for his technical and moral support.

Special thanks go to the Royal Thai Government for the provision of the PhD scholarship and maintenance grant for the duration of my study.

I would like to be grateful to Spanish colleagues, Dr. Reyes García-Contreras (University of Castilla La-Mancha) and Dr. Sara Pinzi (University of Córdoba) for useful suggestions and advice on my thesis and the assistance in analysis of the fatty acid profile of methyl esters.

Finally, I would like to thank my parents for their support, encouragement and motivation throughout my study

Ekarong Sukjit

November 2013

TABLE OF CONTENTS

LIST OF FIGURES

LIST OF TABLES

LIST OF NOTATIONS

Symbol	Unit	
A	m^2	Area of piston head
A	s^{-1}	Pre-exponential factor of reaction
c	m/s	Speed of sound
C_p	J/(kg·K)	Specific heat capacity at constant pressure
C_v	J/(kg·K)	Specific heat capacity at constant volume
E_a	kJ/mol	Activation energy
$h_{fg\ H_2O}$	kJ/kg	Enthaphy of vaporisation of water
k_c		Chemical reaction rate constant
L	m	Stroke length
m	kg	Actual soot mass
m_{H_2O}	kg	Mass of water
m_f	kg	Mass of fuel burned
$\dot{m}_f$	kg/s	Mass flow rate of fuel
n		Number of cylinder
n		Reaction orders of soot
n_R		Number of crank revolutions per power stroke
N	rps	Engine speed

P	Pa	In-cylinder pressure
P_i	kW	Engine indicated power
P_{O_2}	Pa	Partial pressure of oxygen
Q_{LCV}	MJ/kg	Lower calorific value
r		Reaction orders of oxygen
R	kJ/(kmol·K)	Universal gas constant
t	s	Time
T	K	Temperature
V	m^3	Instantaneous volume of the engine cylinder
V_d	m^3	Displaced cylinder volume
$\dot{V}_i$	cm^3/s	Measured intake air volumetric flow rate with EGR
$\dot{V}_o$	cm^3/s	Measured intake air volumetric flow rate without EGR
w_i	N·m	Indicated work per cycle
β	MPa	Isentropic bulk modulus
γ		Ratio of specific heat
η_{th}	%	Engine thermal efficiency
θ	deg	Crank angle
ν		Parameter for relative humidity calculation
ρ	kg/m^3	Density
φ		Fuel-air equivalence ratio

LIST OF ABBREVIATIONS

A/F	Air to fuel ratio
AVP	Average vapour pressure
C	Atomic carbon
CAD	Crank angle degree
CI	Compression ignition
CLD	Chemiluminescence detection
CN	Cetane number
CO	Carbon monoxide
CO_2	Carbon dioxide
COME	Castor oil methyl ester
COV	Coefficient of variation
DC	Diffusion charging
DGM	Diethylene glycol dimethyl ether, Diglyme
DGE	Diethylene glycol diethyl ether
DI	Direct injection
DPF	Diesel particulate filter
EDS	Energy dispersive spectrometer
EGR	Exhaust gas recirculation
EN	European norm
EOC	End of combustion
EOI	End of injection
FAME	Fatty acid methyl ester
FID	Flame ionisation detection
GC	Gas chromatograph

GTL	Gas-to-liquid
H	Atomic hydrogen
H_2	Hydrogen
HCF	Humidity correction factor
HFRR	High frequency reciprocating rig
H_2O	Water
HO_2	Hydroperoxyl radicals
IC	Internal combustion
IMEP	Indicated mean effective pressure
ISFC	Indicated specific fuel consumption
ISO	International organization for standardization
MHRR	Maximum of heat release rate in premixed combustion
MICP	Maximum in-cylinder pressure
MWSD	Mean wear scar diameter
N_2	Nitrogen
NDIR	Non-dispersive infrared
NO	Nitric oxide or nitrogen monoxide
NO_2	Nitrogen dioxide
NO_X	Nitrogen oxides
O	Atomic oxygen
O_2	Oxygen
OH	Hydroxyl radicals
PAH	Polycyclic aromatic hydrocarbon
PM	Particulate matter
PPM	Parts per million
PTFE	Polytetrafluoroethylene, Teflon

RH	Relative humidity
RME	Rapeseed methyl ester
ROHR	Rate of heat release
SEM	Scanning electronic microscope
SI	Spark Ignition
SMPS	Scanning mobility particle sizer
SOC	Start of combustion
SOF	Soluble organic fraction
SOI	Start of injection
SOM	Soluble organic material
TDC	Top dead centre
TGA	Themogravimetric analyser
THC	Total hydrocarbons
UHC	Unburnt hydrocarbons
ULSD	Ultra low sulphur diesel
VOF	Volatile organic fraction
VOM	Volatile organic material
WS 1.4	Wear scar diameter at standard water vapour pressure of 1.4 kPa

CHAPTER 1

INTRODUCTION

1.1 Overview

The depletion of fossil diesel fuels, global warming concerns and the stricter limits on regulated pollutant emissions are encouraging the use of renewable fuels. Biodiesel is the most used renewable fuel in compression ignition (CI) engines. The majority of the literature agrees that particulate matter (PM), unburnt total hydrocarbons (THC) and carbon monoxide (CO) emissions from biodiesel are lower than from conventional diesel fuel. One of the most important reasons for this is the oxygen content of biodiesel, this induces a more complete and cleaner combustion process (Lapuerta et al., 2008b). In addition to this the absence of aromatic compounds in biodiesel leads to particulate matter reduction of biodiesel with respect to diesel fuel.

The potential emission benefits induced by the presence of oxygen in fuel molecules, has increased the interest in using bio-alcohols fuel blends in compression ignition engines such as ethanol. However butanol can be considered as an alternative due to some favourable properties like higher energy density, being less prone to water contamination, less corrosive, having a better blending stability and higher cetane number with respect to ethanol. Although longer-chain alcohols are more suitable for blending with diesel, properties like lubricity, viscosity and cetane number of alcohol-diesel blends still requires improvement. One approach to address this is the

addition of biodiesel which can improve all of these properties forming diesel-biodiesel-alcohol ternary blends.

Biodiesel is a mixture of mono-alkyl esters of different chain length and saturated fatty acids. As biodiesel can be obtained from various sources such as rapeseed oil, used vegetable oil, animal fats, etc., their composition can be different with varying fatty acid profiles. Variation in biodiesel composition results in different physical and chemical properties, affecting fuel miscibility, lubricity, engine performance, exhaust emissions, etc. Consequently, understanding the effect of molecular structure of methyl esters on diesel engine exhaust emissions and performance is necessary, leading to the development of specific fatty acid profiles of biodiesel which lead to advantages in the biodiesel used for alcohol-diesel blends.

1.2 Research objectives

The overall aim of this research focuses on finding ways to enhance the use of alcohol fuels in compression ignition engines. To meet this aim, biodiesel produced from edible and non-edible sources including several types of individual methyl esters, and hydrogen based on the amount obtained by on-board fuel reforming process were studied. The fuel properties, combustion and engine-out emissions are parameters used to justify the performance. The objectives of this research are to:

a) Demonstrate the beneficial effect of the lubricating properties of biodiesel fuel when added to poor lubricity fuels such as ultra low sulphur (ULSD) diesel and low temperature Fisher-Tropsch (GTL).

b) Understand the effect of carbon chain length and unsaturation degree of individual fatty acid methyl esters on the lubricity, combustion and emissions of alcohol-diesel blends.

c) Investigate the physical and chemical properties, combustion and emissions of using the hydroxylated biodiesel to improve the performance of the diesel fuel blended with alcohols.

d) Study the effect of hydrogen on alcohol-biodiesel blends to improve carbonaceous gas emissions.

1.3 The thesis outline

This thesis is divided into eight chapters in which the research objectives have been presented. A brief description of the remainder of the thesis is given below and the research outline is shown in Figure 1.1.

Chapter 2: Literature review

The fundamentals of the diesel engine, which includes operation, engine-out emissions and the legislation as prescribed by European standards, are reviewed. An overview of using alcohol in diesel engines is also presented, including alcohol effects on fuel properties, engine performance and regulated exhaust emissions. Finally, a brief review of the use of hydrogen as a combustion enhancer for diesel engines is given.

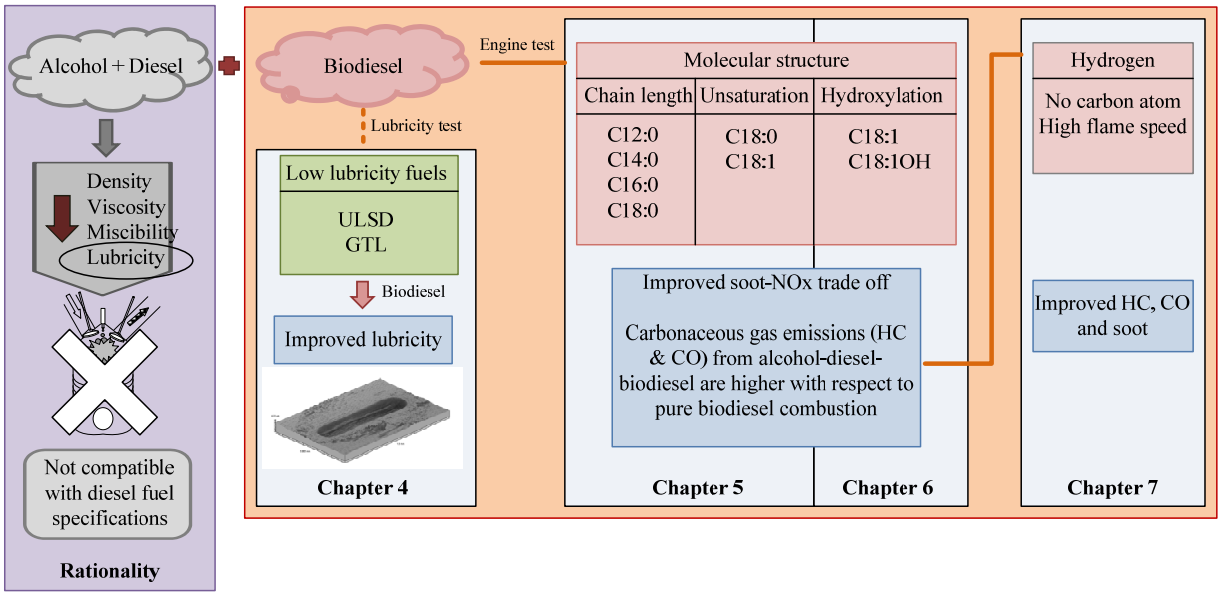

Figure 1.1: Research outline

Chapter 3: Experimental facilities

A description of the test fuels including methods used to investigate fuel properties is described. The details of the experimental engine, instrumentation and exhaust gas analysers are also given.

Chapter 4: The effects of blended diesel fuels on lubricity

Covers the investigations conducted to assess the use of biodiesel derived from rapeseed oil (RME) as lubricity enhancer to improve lubricating properties of the ultra low sulphur diesel (ULSD) and synthetic diesel fuel known as gas-to-liquid (GTL). Lubricity tests are conducted on a high frequency reciprocating rig (HFRR) according to the diesel fuel lubricity standard. The analysis of worn surface comprising of the wear scar profile, microscopic topography and deposit composition is also presented in this chapter.

Chapter 5: The effect of the addition of individual methyl esters on the combustion and emissions of ethanol and butanol-diesel blends

The most representative individual fatty acid methyl esters (FAMEs) are selected to study the effect of carbon chain length and unsaturation degree on fuel properties (focusing on stability and lubricity), combustion and emissions of alcohol-diesel blends. Two types of alcohols, ethanol and butanol, are tested to evaluate the presence of alcohol in fuel blends.

Chapter 6: Hydroxylated biodiesel effects on butanol-diesel blends

Literature suggests that ethanol is a viable fuel additive in diesel engines, however research on butanol is more scarce, but is novel and potentially challenging. Consequently, butanol is used in this chapter for further study on the effect of molecular structure of biodiesel on alcohol-diesel blends. Castor oil methyl ester (COME) is selected to study the effect of the hydroxyl group in biodiesel, on fuel properties and emissions of butanol-diesel blends. RME, used as a base line test, consists mainly of methyl oleate (C18:1) with the same number of carbon and unsaturation degree compared to methyl ricinoleate (C18:1 OH), the main composition of COME and so is a good comparator. Therefore the performance of the hydroxyl group in biodiesel is assessed.

Chapter 7: Effect of hydrogen on butanol-bidiesel blends in compression ignition engines

The potential benefits of using renewable fuel blends (butanol and RME) in terms of combustion characteristics and emissions are presented. Hydrogen with no carbon atoms and high flame speed is applied as a combustion improver to further reduce carbonaceous emissions and to find any synergetic effects between hydrogen and oxygenated fuels.

Chapter 8: Conclusions

A summary of the principal conclusions from the research are discussed along with recommendations of the potential areas for future research.

CHAPTER 2

LITERATURE REVIEW

2.1 Diesel engine operation

The higher thermal efficiency, enhanced fuel economy, engine durability, reliability and lower carbon dioxide (CO_2) emission are some of the advantages of diesel engines with respect to gasoline engines, which encourages their use in on-road vehicles. During the intake stroke in diesel engines, only air is inducted into the cylinders. This allows diesel engines to operate at high compression ratios. Subsequently, the inducted air is compressed in the cylinders to high pressure and temperature. Once the air temperature is above the fuel ignition point, fuel is injected into the cylinders as the injector atomises the fuel into fine droplets to mix with the compressed air. After a short delay the spontaneous auto-ignition of the fuel-air mixture initiates the combustion process. Rate of heat release (ROHR) analysis can be used to describe the overall diesel combustion process. The typical diesel combustion phase of a 4-stroke cycle compression ignition engine is shown in Figure 2.1 which includes four main characteristics. The ignition delay phase is defined as a period of time between the start of fuel injection (SOI) and the start of combustion (SOC). This includes the time required for the droplet of fuel to heat, vaporise and mix with the hot air in the cylinder and results in the negative ROHR. Once a quantity of the air-fuel mixture achieves its flammability limit, it begins to auto-ignite and burn within a few crank angle degrees leading to an increased rate of heat release (premixed combustion). Afterwards, the heat release rate is controlled by the rate at which the mixture becomes available to burn (diffusion controlled combustion). Combustion extends into the expansion stroke and heat release

during this period may be due to a small amount of unburnt fuel and incomplete combusted products (late combustion). The end of injection (EOI) defines the end of the diffusion phase and the beginning of late combustion. The heat release rate during late combustion will be at lower levels as the in-cylinder pressure and temperature reduces due to the expansion of the stroke and is approximately zero at the end of combustion (EOC).

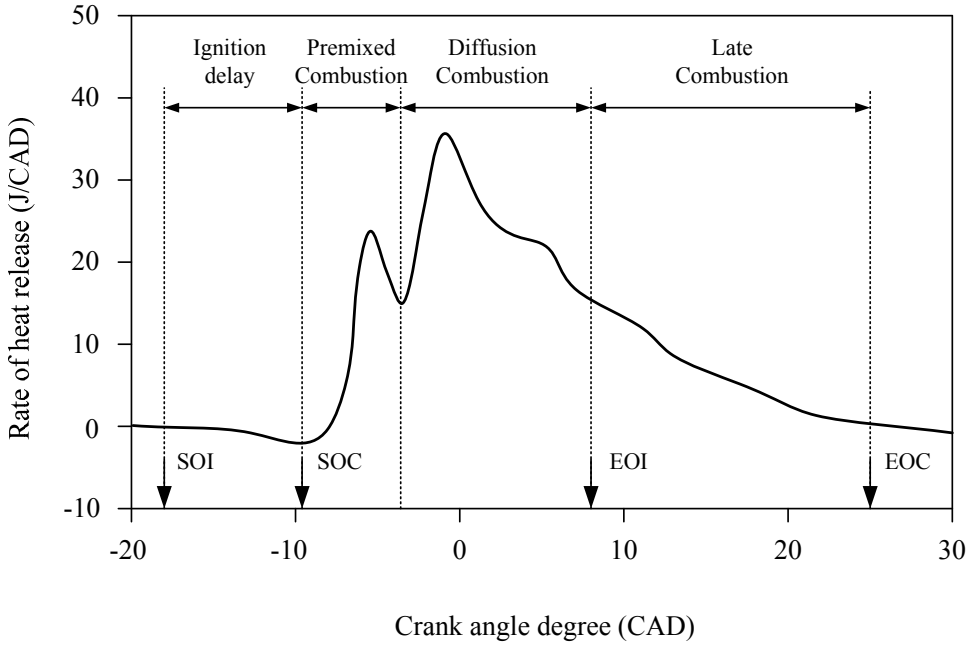

Figure 2.1: Diesel combustion phases of a typical direct injection diesel engine

An idealised cross-sectional slice of a diesel fuel jet is illustrated by Dec's conceptual model in Figure 2.2 (Dec, 1997, Mueller et al., 2003). This flame occurs during the diffusion combustion phase where the bulk of fuel is burnt. Oxygen will be entrained into the jet and mixed forming a vaporised fuel as the temperature of the vapour is 700-900K. An exothermic reaction occurs around the fuel-rich mixture as the available oxygen is consumed resulting in the start of soot formation. On the periphery of the fuel jet where there is readily available oxygen from the

surrounding air, combustion will be close to stoichiometric conditions and nitrogen oxides are formed on the lean side of the diffusion flame. As a result of diesel combustion the most relevant regulated emissions are nitrogen oxides (NO_X) and particulate matter (PM). An overview of the European emission standards, that regulate these emissions is shown in Figure 2.3 where, the most recent, Euro 6 regulations for light-duty and heavy-duty diesel vehicles have been finalised for implementation in 2014 and 2013 respectively.

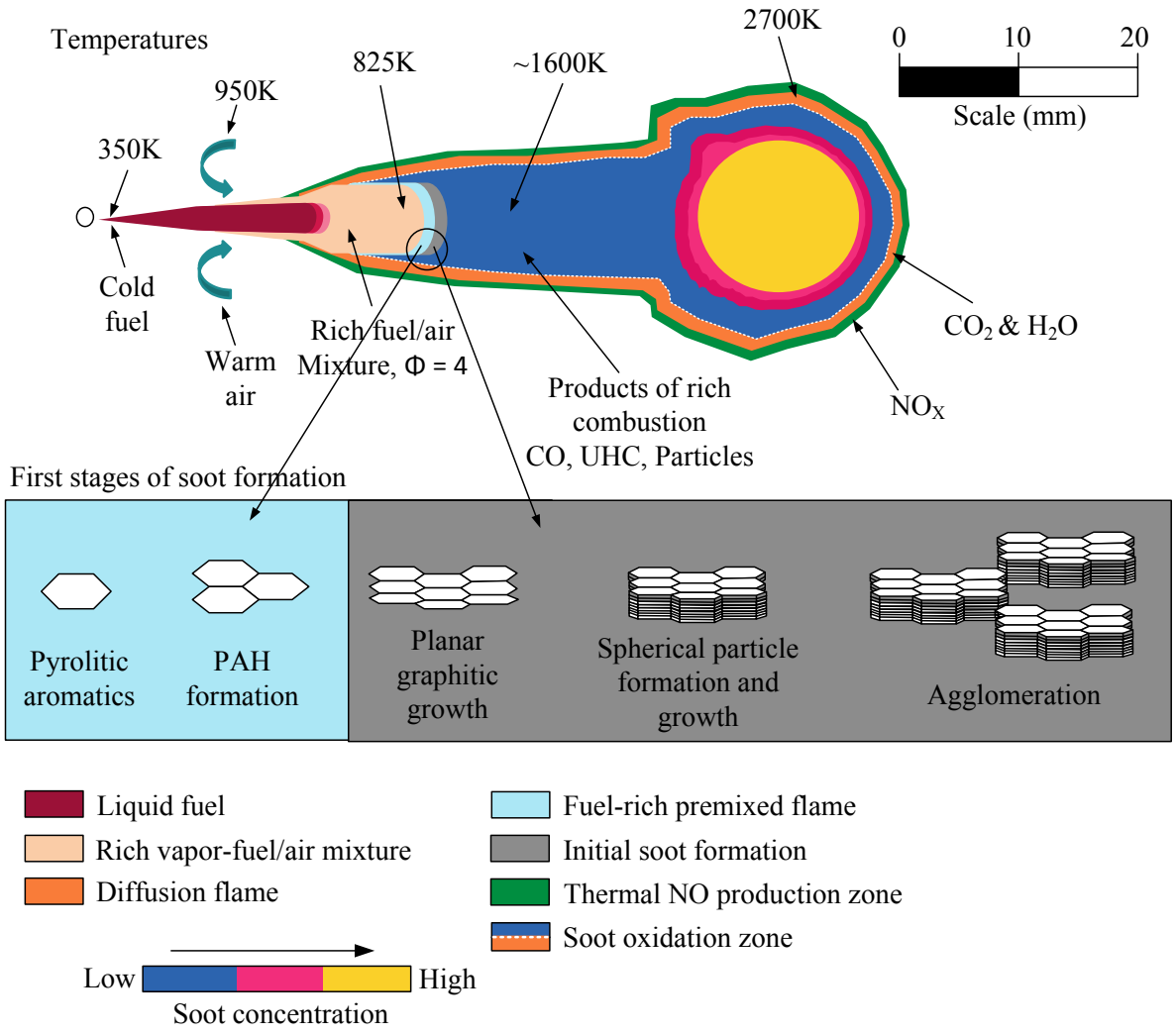

Figure 2.2: Dec's conceptual model of DI combustion during the quasi-steady period

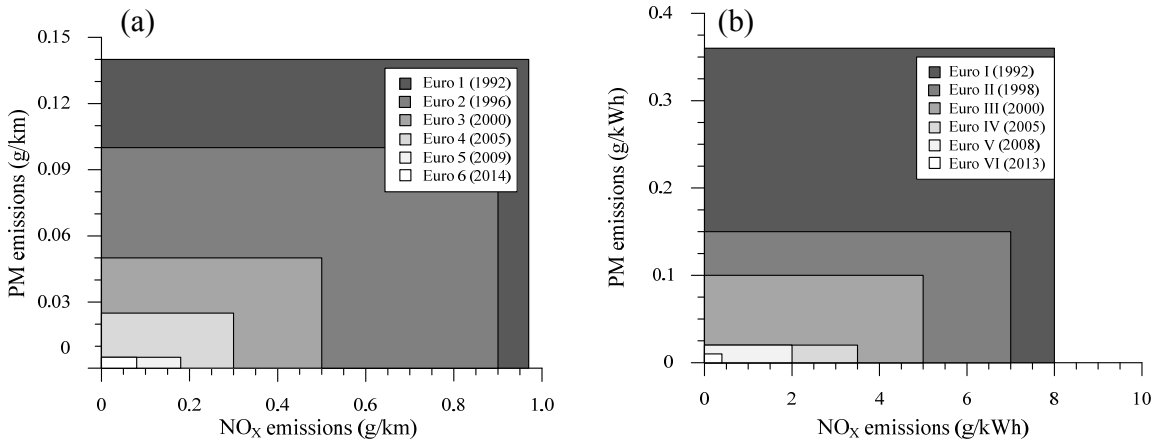

Figure 2.3: European emission standards for (a) diesel passenger cars (b) heavy-duty diesel engines (Rodríguez-Fernández et al., 2009)

2.2 Engine exhaust emissions

It is well-known that water and carbon dioxide (CO_2) are inherent to all combustion processes of hydrocarbon fuels. However, there are other products produced by combustion due to different conditions such as non-stoichiometric fuel-air ratios and heterogeneous mixtures. The regulated emissions of internal combustion engines prescribed by the European Union are carbon monoxide (CO), total hydrocarbons (THC) or unburnt hydrocarbons (UHC), nitrogen oxides (NO_X) and particulate matter (PM).

Exhaust emissions have different physiologic and environmental impacts which are the motivators for more stringent legislation to control these emissions. THC emissions can cause a variety of negative environmental effects as the main concern is precursors of photochemical smog and ozone levels when they react with NO_X (Majewski and Khair, 2006). CO emissions are strongly associated with human health problems, and can accumulate in red blood cells reducing

their capability to carry oxygen to cells and resulting in asphyxiation (Strauss et al., 2004). In environmental pollution CO emissions can also contribute to low-level ozone and to global warming. In the case of NO_X emissions, they are hazardous to haemoglobin and can result in respiratory illness. Combustion products of nitrogen compounds and sulphur contained in diesel fuel can be the principal cause of acid rain (Fernando et al., 2006). Additionally, NO_X emissions can also contribute to the formation of low-level ozone (Majewski and Khair, 2006). The serious effects of PM on human health, depend on the size of the particles, leading predominately to lung cancer and other cardiopulmonary mortality (Cohen et al., 2005). Smaller particles are more harmful to the environment and health as they are more difficult to trap, have a longer residence time in the atmosphere and are more reactive (higher surface to volume ratio). A particle size of 10 μm or less can penetrate the deepest part of the lungs (bronchioles or alveoli). Ultrafine particles (< 100nm) can be easily deposited in the human respiratory tract leading to respiratory diseases and damage to the lungs (Lakkireddy et al., 2006). Heavy organic compounds (i.e. PAH) increase carcinogenic potential (Krahl et al., 2003).

2.3 Regulated emissions formation

2.3.1 Carbonaceous gas emissions

THC emissions in diesel exhaust gases consist of unburnt hydrocarbon fuel, decomposed fuel molecules and recombined intermediate compounds. The composition and quality of the THC emissions depend on fuel composition as fuel containing a high proportion of aromatics and olefins produce relatively higher concentrations of hydrocarbon emissions (Heywood, 1988). There are two critical sources for the THC formation in diesel engine combustion, which are an

over-lean fuel-air mixture during the ignition delay and an over-rich mixture during combustion (Yu and Shahed, 1981). Some of the vaporised fuel with a lower equivalence ratio than the lean limit ($\phi \approx 0.3$) will not auto-ignite and support flame propagation resulting in fuel which escapes from the normal combustion process (Ferguson, 1986). The fuel leaving the injector nozzle at slow velocity and the fuel retained in the injector sac volume causes an over-rich mixture during combustion leading to THC emissions. Flame quenching on the combustion chamber surfaces and lubricant film on the cylinder wall can participate in THC formation. It is reported that hydrocarbon fuels produce shorter carbon chain hydrocarbons in exhaust gases and lubricating oil generate heavier longer hydrocarbon emissions (Majewski and Khair, 2006).

Carbon monoxide is a result of oxygen deficient combustion and is most prominent in the fuel rich combustion regions. CO emissions are low in diesel combustion engines because the mixture is globally lean. The formation of CO is controlled by the fuel-air equivalence ratio and is accompanied by the combustion of hydrocarbon radicals (Ṙ) as follows (Bowman, 1975):

$$\dot{R}H \rightarrow \dot{R} \rightarrow \dot{R}O_2 \rightarrow \dot{R}CHO \rightarrow \dot{R}CO \rightarrow CO \tag{2.1}$$

During lean burn combustion, the temperature may be high enough for oxygen and carbon monoxide to form carbon dioxide through the following equation:

$$CO + O_2 \rightarrow CO_2 + O \tag{2.2}$$

Once the reaction above is slowed the oxidation of CO can occur through the equation as shown below:

$$CO + OH \rightarrow CO_2 + H \quad (2.3)$$

where hydroxyl radicals (OH) are produced by the following equation:

$$O + H_2O \rightarrow 2OH \quad (2.4)$$

$$H + O_2 \rightarrow OH + O \quad (2.5)$$

2.3.2 Nitrogen oxides

Nitrogen oxides (NO_X) are considered as one of the most critical emissions produced from diesel engines (Heywood, 1988). NO_X is a mixture of nitric oxide (NO) and nitrogen dioxide (NO_2) in automotive aftertreatment. NO is generally the main component of the total NO_X emissions emitted from diesel combustion engines. NO formation consists of three primary mechanisms, namely, thermal NO mechanism (the reaction of atmospheric nitrogen and oxygen at high temperature), fuel NO mechanism (the oxidation of nitrogen contained in the fuel) and the prompt NO mechanism (the reaction of nitrogen with radicals derived from the fuel). The thermal NO mechanism is considered as the main source of NO formation which can be explained through the extended Zeldovich mechanism (Heywood, 1988). The primary pathway of NO formation is the oxidation of atmospheric nitrogen molecules and the chain reaction is initiated by the dissociation of oxygen molecules at high temperature during the combustion process:

$$O + N_2 \rightarrow NO + N \quad (2.6)$$

$$N + O_2 \rightarrow NO + O \quad (2.7)$$

The thermal NO mechanism can be extended by the reaction of the hydroxyl radicals with nitrogen (Lavoie et al., 1970):

$$N + OH \rightarrow NO + H \quad (2.8)$$

Although NO emissions are the main component of nitrogen oxides in diesel combustion NO_2 can be formed by the reaction of NO and hydroperoxyl radicals (HO_2) at low temperature:

$$NO + HO_2 \rightarrow NO_2 + OH \quad (2.9)$$

However NO_2 emissions can be converted back to NO at high temperature through the following reactions:

$$NO_2 + O \rightarrow NO + O_2 \quad (2.10)$$

$$NO_2 + H \rightarrow NO + OH \quad (2.11)$$

2.3.3 Particulate matter

PM emissions result from the incomplete combustion of hydrocarbon fuel where some fuel droplets cannot burn and are emitted as heavy liquid droplets or solid carbonaceous matter. Also, some of the lubricating oil on the cylinder wall is partially burned and contributes to particle matter. PM can be classified into three categories based on the diameter (Kittelson, 1998). The nuclei mode refers to nanoparticles with a diameter below 50 nm. The accumulation mode is defined by particle diameters in the range of 50 nm and 1000 nm. Particle diameters larger than 1000 nm are classified as coarse mode particles. In general, most particles from diesel combustions have diameters less than 100 nm.

PM formation begins in the fuel-rich premixed zone when the formation of the first aromatic structure resulting from the decomposition of fuel molecules is initiated (Richter and Howard, 2000). This is followed by subsequent phase PAH growth and particle nucleation. After primary particles are formed during the early stages of particle formation, they can grow by three mechanisms; surface growth (attachment of gas phase species), coagulation (collision between particles) and agglomeration (contact with other particles with weak cohesive bonding). The process of particle formation is shown alongside Dec's conceptual model in Figure 2.2. The main particle composition consists of carbonaceous soot, organic fraction and sulphur compounds. The unburnt fuel and evaporated lubricating oil generally appear as the volatile organic fraction (VOF) or soluble organic fraction (SOF) in exhaust gases (Lapuerta et al., 2007). The composition and particle size strongly depend on diffusion combustion (i.e. the duration and temperature) and the exhaust gas process (i.e. hydrocarbon condensation). It is reported that some volatile materials are vaporised at elevated temperatures, then condense on the surface of elementary carbon formed particles when the exhaust gas cools down (Burtscher et al., 1998).

2.4 Alternatives fuels for diesel engines

An alternative fuel is defined as a fuel which replaces the commonly accepted fuel on a potentially permanent basis with no adverse effects on engine operation and maintenance. An ideal alternative fuel is not only renewable and environmental friendly in terms of exhaust emissions but also economical, sustainable and able to deliver similar performance to conventional fossil fuels. Biofuels are derived from natural sources which are associated with living organisms and can be considered as short/medium term alternatives to fossil fuels in the transport sector.

The most common process to produce biofuels is the transformation of vegetable oils by means of a tranesterification process to form biodiesel and the use of sugar rich cereal crops to obtain bio-alcohol through fermentation (first generation). One crucial concern related to first generation biofuels which are generally made from edible feedstock is the competition with food production. As a consequence, new production technologies are being developed for the second generation biofuels which will be produced from non-edible feedstock. These include the transformation of lignocellulosic material to liquid fuels by means of thermochemical or biological processes, the use of non-food derived fuels from jathropa, waste cooking oil, castor oil and grease tallow.

2.4.1 Biodiesel

A sample form of biodiesel production is outlined in Figure 2.4. The aim of the process is to reduce the viscosity and degradation of renewable feedstock in the form of triglycerides by reacting them with short chain alcohols (e.g. methanol or ethanol) in the presence of a catalyst to yield biodiesel with a high oxygen content, no aromatic and sulphur content, good lubricating properties and enhanced cold flow properties. In Europe, rapeseed is the principle crop for the production of first generation biodiesel. Neat biodiesel used as an automotive fuel is required to meet the European standard EN 14214: Automotive fuels-fatty acid methyl esters (FAME) which are given in Table 2.1.

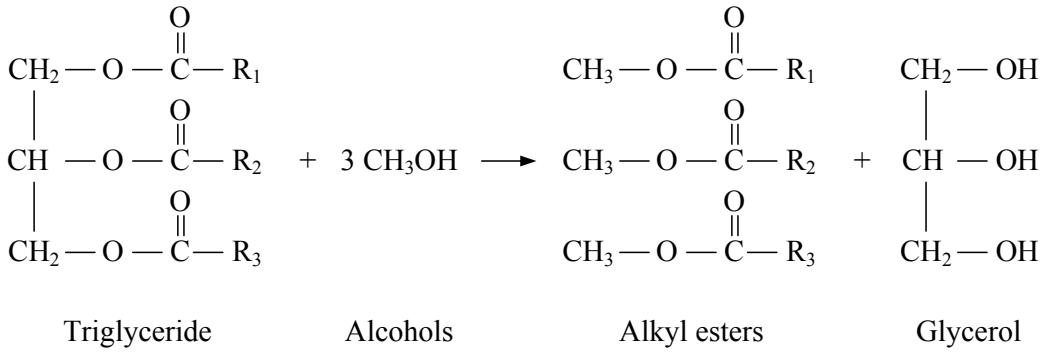

Figure 2.4: Transesterification reaction

Table 2.1: Requirements and test methods for FAME

Property	Test method	Min	Max	Unit
Viscosity @ 40 ^{o}C	EN 3104	3.5	5	mm^2/s
Flash point	EN 3679	120	-	^{o}C
Sulphur content	EN 20846/84	-	10	mg/kg
Carbon residue, (on 10% distillation residue)	EN 10370	-	0.3	% (m/m)
Cetane number	EN 5165	51.0	-	-
Oxidation stability @ 110 ^{o}C	EN 14112	6.0	-	Hours
Acid value	EN 14104	-	0.50	Mg KOH/g
Free glycerol	EN 14105/06	-	0.02	% (m/m)
Total glycerol	EN 14105	-	0.25	% (m/m)

2.4.1.1 Engine performance and emissions from biodiesel combustion

The lower heating value of biodiesel compared to diesel fuel causes the higher fuel consumption needed to produce the same power output due to the presence of oxygen in the fuel molecules (Graboski et al., 1996, Haas et al., 2001, Lapuerta et al., 2009b, Senatore et al., 2000).

Other fuel properties of biodiesel can create power losses in the engine. For example, the lower heating value, or the higher viscosity can make atomization of the fuel more difficult resulting in a worse mixing and evaporation process in the combustion chamber (Yücesu and İlkiliç, 2006). Nevertheless the power loss caused by such deficient properties can be recovered by the higher bulk modulus and higher cetane number of biodiesel which can produce an advance in the start of combustion (especially in pump-line-nozzle systems for the case of bulk modulus), leading to an improvement in the combustion process. Consequently, most of the published studies report that the thermal efficiency of the engine operating with biodiesel is similar to that of diesel fuel (Canakci, 2007, Dorado et al., 2003, Graboski and McCormick, 1998, Tsolakis, 2006).

The majority of publications agree that unburnt total hydrocarbon emissions with the biodiesel combustion are lower than those with diesel fuel (Monyem et al., 2001, Schmidt and Van Gerpen, 1996, Staat and Gateau, 1995), although there are some articles which show an increase in THC emissions or no differences with biodiesel compared to diesel fuel (Labeckas and Slavinskas, 2006). The existence of oxygen in the fuel seems to be an important factor in the reduction of THC emissions. This can be attributed to a more complete and cleaner combustion process (Rakopoulos et al., 2004). In addition, the higher cetane number and bulk modulus of biodiesel with respect to diesel fuel, advances the injection and combustion timing which tends to reduce THC emissions (Abd-Alla et al., 2001). Also the final distillation point of biodiesel is lower than that of diesel (Murillo et al., 2007, Turrio-Baldassarri et al., 2004).

In general, biodiesel combustion produces lower CO emissions than the case of diesel (Rakopoulos et al., 2008, Shi et al., 2005), although there is a minor number of studies which do not find those CO reductions (Labeckas and Slavinskas, 2006, Serdari et al., 1995). The presence

of oxygen in biodiesel leads to complete combustion reducing CO emissions. The advance of injection and combustion caused by the higher bulk modulus and cetane number of biodiesel tends to lower CO because the possibility of fuel-rich zones which are responsible for CO formation are decreased (Pinto et al., 2005, Ullman et al., 1994).

Although the engine operating conditions, injection strategy, engine technology and biodiesel feedstock can be factors affecting combustion performance and emissions, most of studies agree that higher nitrogen oxides emissions can be found with the biodiesel combustion rather than the diesel (Di et al., 2009, Schönborn et al., 2009). Reasons for this include: higher bulk modulus of biodiesel results in a quicker fuel pressure rise from the fuel pump to injector and as a consequence advances injection timing. On a common rail system, this effect is minimised. The earlier fuel injection and the higher cetane number of biodiesel promotes an advance in the start of combustion which usually leads to a higher mean peak temperature and higher local temperatures favouring NO_X formation (Murillo et al., 2007). In addition, biodiesel has a higher flame temperature than that of diesel which is responsible for higher NO_X emissions (Nabi et al., 2006). It is also reported that the presence of oxygen in biodiesel can enhance the NO reaction (Schmidt and Van Gerpen, 1996). Finally, some fuel properties such as viscosity, surface tension and boiling temperature can influence spray characteristics which modify the delay period and premixed combustion affecting the local temperature and the formation of NO_X emissions (Graboski and McCormick, 1998).

According to the majority of studies, particulate matter emissions with biodiesel are lower than those obtained with diesel fuel (Cardone et al., 2002, Lapuerta et al., 2005). However an increase in PM emissions with biodiesel can be possible and has been reported (Munack et al.,

2001). This increase in PM emissions is usually due to a significant increase in volatile organic material when using biodiesel. The lower volatility of biodiesel makes unburnt hydrocarbons condense easier to and are absorbed by particle surfaces, this can be used to justify this increase in organic material. Also the lower volatility can cause slower evaporation and mixing with air when compared to diesel fuel. On the other hand, it is evident that the use of biodiesel reduces soot emissions (Lapuerta et al., 2008c, Tsolakis et al., 2007, Yoon et al., 2009, Zheng et al., 2008).

The most likely reason for the decrease in PM emissions with biodiesel is the oxygen content of biodiesel. The presence of oxygen results the more complete combustion, especially in regions with fuel-rich diffusion flames where the particulate matter formation starts (Armas et al., 2006, Pradeep and Sharma, 2007). The benefit of oxygen in fuel molecules is mainly on soot emissions, inhibiting soot formation and enhancing soot oxidation. The absence of aromatic compounds in biodiesel also contributes to this (Haas et al., 2001).

2.4.1.2 Effect of molecular structure of biodiesel on emissions

There are a few of investigations with different individual fatty acid methyl esters on diesel exhaust emissions when they are used as neat component and blends in diesel engine (Graboski et al., 2003, Knothe et al., 2006, Schönborn et al., 2009). It has been found that an increase in chain length leads to an increase in carbonaceous gas emissions (THC and CO emissions) as a consequence of a reduction in the oxygen content. Also, methyl esters with a longer carbon chain length have higher boiling and melting points which makes fuel evaporation and burning more difficult resulting in less complete combustion (Hansen and Jensen, 1997). The increase in chain

length does not produce a clear trend in NO_X emissions. Statistical analysis shows that the formation of NO_X emissions with biodiesel is mainly controlled by the cetane number and bulk modulus (Pinzi et al., 2013). These two properties demonstrate the conflicting results in NO_X emissions and can be compensated for. The higher cetane number of longer chain methyl esters reduces ignition delay which tends to decrease NO_X emissions. Conversely, the higher bulk modulus of longer chain length results in the advance in injection timing which usually promotes an advance in the start of combustion. Consequently, the residence time of the burning mixture is increased so that NO_X formation is higher (Szybist et al., 2005b). In terms of particulate matter emissions, it is found that the increase in carbon chain length produces an increase in PM emissions. This is mainly due to the lower oxygen content when chain length increases.

Although the increase in carbonaceous gas emissions with the longer chain methyl esters has been reported, no clear conclusion related to unsaturation degree of methyl esters has been reached. On the other hand, unsaturation degree produces a clear trend in NO_X emissions. This trend is mainly explained by an increase in bulk modulus and decrease in cetane number when the unsaturation degree increases (Knothe et al., 2006). As the oxygen content seems to be similar for each compound other parameters such as viscosity and melting point can play an important role to explain the trends in PM emissions. The increase in unsaturation degree results in lower viscosity and lower melting point which can enhance fuel atomisation and evaporation, resulting in lower soot emissions (Williams et al., 2006).

2.4.2 Alcohols

Apart from biodiesel the most widely used liquid biofuels are the primary alcohols (produced from renewable feedstocks) which can be obtained from biomass or fossil fuels including gases (Herreros, 2010). Although traditionally they have been used as fuels in spark ignition engines, they have also been considered in compression ignition engines. One of the alcohols which has been used as a fuel for CI engines is ethanol which can be produced from edible and non-edible feedstocks classified. First generation ethanol can be obtained from sugar cane, sugar beet, corn and other grains while second generation can be produced from woody and herbaceous crops. The use of blends with high percentages of ethanol is limited because of its poor miscibility with conventional diesel, low cetane number, low energy density, low viscosity, low lubricity and high volatility (Lapuerta et al., 2010a, Lapuerta et al., 2010b). The most critical property that should be taken into account is the miscibility of ethanol with diesel fuel. This may result in phase separation with catastrophic consequences for the engine (e.g. high water absorption tends to corrode metal parts of fuel injection components) (Wadumesthrige et al., 2010).

Butanol is a feasible alternative to ethanol due to its higher energy density, being less prone to water contamination, less corrosive, better blending stability and higher cetane number with respect to ethanol. Butanol contains more carbon atoms than ethanol which makes it more complex as carbon atoms can form either straight or branched structures. The butanol produced from biomass tends to yield straight chain structures named 1-butanol or n-butanol. The drawback of using butanol includes higher production costs compared to ethanol. However the production sustainability depends on the feedstock and the process. Feedstock (maize, sugar cane,

sugar beets) and conventional production process used to produce ethanol can be adapted to produce butanol. Additionally sustainable production can be improved by the use of lignocellulosic material through fermentation to produce butanol. Unfortunately, this technology not well developed and more research is needed. Furthermore, butanol can be produced by anaerobic fermentation of crude glycerol which is the main co-product of the tranesterification reaction of biodiesel production (Rakopoulos et al., 2011). This route seems to be a viable approach to reduce the problems associated with the disposal of crude glycerol. Recent studies suggest that butanol can be a better alternative biofuel than ethanol for use in CI engines (Miers et al., 2008, Weiskirch et al., 2008, Zoldy et al., 2010). Although longer-chain alcohols are more suitable to use for blending with diesel, properties like lubricity, viscosity and cetane rating of butanol-diesel blends still need to be improved (Lapuerta et al., 2010b) when they are used in high percentage blends with diesel fuels.

2.4.2.1 Engine performance and emissions from alcohol-diesel blend combustion

Cetane number of alcohols is lower than in the case of diesel fuel resulting in a high probability of diesel knock at high compression ratios. For this reason it is expected that the output power of an engine fuelled with alcohol blends will be lower than diesel. Moreover the lower energy density of alcohols increases the brake specific fuel consumption which increases the fuel mass needed to obtain the same power output. Nonetheless the lower engine output can be compensated for by lowering the heating value to obtain similar diesel thermal efficiency. The application of using ethanol (Lapuerta et al., 2008a, Lapuerta et al., 2008c, Li et al., 2005) and butanol (Karabektas and Hosoz, 2009, Rakopoulos et al., 2010) in compression ignition engines showed similar thermal efficiency compared to that of diesel fuel, although an improvement in

thermal efficiency with high butanol percentages has been reported due to the presence of oxygen and high burning velocity of butanol (Lujaji et al., 2011).

Although oxygen content yields a cleaner and more complete combustion, THC emissions are usually higher in the case of alcohol blends than that of diesel fuel, especially in engine operating modes with low combustion temperatures where hydrocarbon emissions are significant. This increase is mainly due to the higher heat of vaporization of alcohols which causes the slower evaporation and poorer fuel-air mixing, particularly with ethanol. The slower air mixing process leads to an increase in spray penetration resulting in unwanted fuel impingement on the combustion chamber walls. This increases the lean outer flame zone where a flame is unable to exist (Rakopoulos et al., 2007). In addition, at the end of fuel injection process the alcohol fuel left in the nozzle sac volume could escape into the combustion chamber. This is because it can evaporate from the blend as it is heated, and can consequently be transported into the cylinder at low velocity and late in the expansion stroke (Ferguson, 1986, Heywood, 1988). Some research also reported that the lower cetane number of alcohols in the blend can prolong the ignition delay allowing more time for fuel blends to evaporate which tends to increase THC emissions (Doğan, 2011). Comparing ethanol to butanol blends THC emissions obtained with ethanol blends are higher than those obtained with butanol blends as a consequence of the higher heat of vaporization of ethanol (Sukjit et al., 2012).

Carbon monoxide is the one of the emissions, which is generally used as an indicator of incomplete combustion. The existence of oxygen content in fuel molecule favours a more complete combustion as a consequence of a lower level of CO emissions with alcohol blends (Can et al., 2004). The benefit in CO emissions when alcohol blends can be due to the lower C/H

ratio of alcohols. It is suggested that an increase in CO emissions due to higher heat of vaporization of alcohols resulting in a lower in-cylinder temperature and a thick quenching layer can be obtained (He et al., 2003). However this effect will be compensated for by the effects of the oxygen and lower C/H ratio of alcohols which tend to enhance the complete combustion. Alcohols, by comparison show higher CO emissions, and these are higher with ethanol than butanol blends according to the higher heat of vaporization of ethanol.

Research suggests conflicting effects on NO_X emissions from the use of alcohols in diesel engines. The low cetane number of alcohol blends tends to increase ignition delay and so leads to higher local combustion temperatures in a premixed combustion mode which results in higher NO_X emissions. Also, the oxygen content of alcohols can assist in the formation of NO_X emissions. Conversely, the high heat of vaporization of alcohols reduces the flame temperature in the cylinder resulting in lower NO_X emissions (Li et al., 2005, Xing-Cai et al., 2004). These opposing effects can be compensated for and the final results may depend on injection strategies and engine operating conditions, generally NO_X emissions reduce with increasing blend percentages (Rakopoulos et al., 2011). In the case of ethanol it is implied that the higher heat of vaporization could display a higher decrease in NO_X emissions than in the case of butanol, especially at low engine loads where the heat vaporization is significant compared to the combustion temperature.

The reduction of soot emissions with the use of alcohols in the internal combustion engine is evident and clear. The most common reason for this soot reduction is the oxygen content which diminishes soot precursors and enhances oxidation, although other reasons such as more premixed combustion, lower C/H ratio and the lack of aromatic compounds can be used to

support the decrease in soot emissions. However in the case of particulate matter, it is not as clear because the organic fraction of PM can be higher with the use of alcohols, especially during low temperature engine operating conditions (Song et al., 2007). Comparing the different alcohols, it is reported that the soot emissions with ethanol blends are lower than those obtained from butanol blends when they are used in heavy duty diesel engines. The higher temperatures contribute to higher oxidation rates inside the crucial zones in addition to the lower C/H ratio (Rakopoulos et al., 2011). However some parameters such as the heat of vaporisation and cetane number of alcohols may lower soot oxidation resulting in an increase in emitted soot emissions.

2.4.2.2 Fuel properties of alcohol-diesel blends

The stability of alcohol-diesel blends depends on temperature, humidity, and fuel composition. Alcohol and diesel blends may separate into different liquid phases under certain conditions. Generally, ethanol is immiscible in diesel over wide range of temperatures and water content because of the difference in chemical structure and characteristics. Phase separation can generate different types of unstable blends such as two liquid phases, a gelatinous interphase, or the formation of gelatinous phase. As reported by Lapuerta et al. (2009a) at positive temperatures and when blends contain between 15% and 75% by volume of anhydrous ethanol (99.7%), two different liquid phases are distinguishable after the separation. At temperatures below 0 °C and when blends contain between 10% and 60% ethanol, a gelatinous phase is generated and is located in the interphase between two liquid phases. To prevent the phase separation between ethanol and diesel fuel, biodiesel can act as an additive in stabilising ethanol in diesel blends as it contains a polar head that is chemically attracted to ethanol and a non-polar tail that is chemically attracted to diesel fuel leading to a homogeneous blend (Kwanchareon et al., 2007). As the cost

of commercially available additives is very high, the use of biodiesel is a feasible way to improve blending stability between ethanol and diesel fuel. Generally, alcohols containing higher carbons can decrease the blending stability problem when they are blended with diesel fuel because of their lower polarity which means they are more soluble in diesel fuel. This makes butanol preferable to ethanol for blending with diesel fuel. It is reported that butanol can be blended with diesel fuel at any percentage without blend stability problem when the blend temperature is tested at a positive temperature (Lapuerta et al., 2010b).

Many fuel properties such as cetane number, heating value and bulk modulus are related to the density which has direct effects on engine performance characteristics. The change in density will influence fuel injection systems resulting in a different mass of fuel injected to combustion chamber. Blended alcohols show a delay in the start of combustion due to the low density of alcohols. The use of ethanol in diesel engines which does not require any engine modification can be up to 20% ethanol in diesel fuel by volume concentration (Agarwal, 2007). Although this ethanol percentage provides the blend density in the acceptable range prescribed by diesel fuel requirements (820-845 kg/m^3) (Barabás and Todoruț, 2009). To avoid any problems caused by the density of alcohol/ diesel blends, biodiesel may be added. Another feasible way to improve the density is to use alcohols with higher carbon numbers.

Viscosity affects the quality of fuel atomisation, the size of fuel droplets and the penetration of fuel spray. The acceptable range of diesel fuel viscosity is 2-4.5 mm^2/s (EN-590, 2009). Leakage in the fuel system can be caused by low fuel viscosity. Ethanol lowers blended fuel viscosity. Barabás et al. (2009) reported that blending diesel fuel with 25% ethanol by volume did

not meet the diesel fuel specification. In case of butanol, it can be blended with diesel fuel in any concentration to meet the range of the recommended standard in EN 590.

The use of alcohols as a blend component for diesel engines will reduce cetane number of blends as a result of the low centane number of alcohols and is not recommended for use directly without engine modification. It was reported that more than 10% reduction in cetane number of the blend was obtained when 10% ethanol by volume was added to diesel fuels (He et al., 2003). To compensate for the loss of cetane number biodiesel can also be used as an ignition improver for alcohol blends due to its higher cetane number. Moreover, the replacement of ethanol by longer carbon chain alocohols such as butanol may be more attractive for use in diesel engines because they have a higher cetane number than shorter carbon chain alcohols.

2.4.2.3 Lubricating properties of alcohol-diesel blends

The introduction of low sulphur diesel fuel brings about some serious problems in fuel properties due to the desulphurization process, which eliminates not only quantities of sulphur in diesel fuel but also that of lubricity-imparting compounds such as polyaromatics and oxygen containing compounds (Bhatnagar et al., 2006, Nikanjam and Rutherford, 2006, Wei et al., 1996). This reduction in lubricity can have a damaging effect on the fuel injection equipment. To prevent metal-to-metal contact that leads to premature failures of this equipment, several standards have been developed to ensure lubricity levels in diesel fuels are maintained at acceptable standards. The standard test for diesel fuel lubricity is based on the high frequency reciprocating rig (HFRR) and a generated wear scar, which under specified conditions must not exceed 460 μm by European regulations.

In general, the addition of alcohol to diesel fuels decreases the lubricity of the blend due to the low lubricity of alcohols. There is no a clear effect on lubricity obtained when 10% ethanol was added to diesel fuel (Corkwell and Jackson, 2002). As the ethanol concentration in the blend continues increasing from 3%-50% at 60 °C, the lubricity remains within a small variation range and the wear scar generated under these blends is under the acceptable maximum limit of diesel fuel lubricity standard (Lapuerta et al., 2010a). The reason for the expected loss of lubricity, caused by the presence of ethanol, is compensated for due to evaporation of ethanol from the lubricating layer, resulting in better lubricating properties of the remaining diesel-rich fuel.

Although the lubricity of pure alcohols will improve as the molecular weight of alcohol increases, the diesel fuel blended with intermediate ethanol contents shows better lubricity than that butnaol blends due to evaporation. The limit of blending ethanol and butanol with diesel fuel to fulfill the lubricity requirement standard is 92% ethanol and 35% butanol by volume with the initial wear scar diameter of 315 μm (Lapuerta et al., 2010b).

Biodiesel has successfully been used as lubricity enhancer because oxygen containing moieties, particularly carboxylic acid groups, in this biodiesel improve the lubricity. Numerous studies have investigated the lubricating properties of biodiesel and subsequent fuel blends. Most studies agree that the addition of 1% to 2% (v/v) of biodiesel to diesel fuel improves the blended fuel lubricity and there is no further improvement in lubricity when a certain concentration is reached. The optimal concentration of biodiesel to restore low sulphur diesel fuel is between 2% to 15% (Anastopoulos et al., 2001, Suarez et al., 2009, Sulek et al., 2010, Wadumesthrige et al., 2009). Geller and Goodrum reported that the methyl esters obtained from vegetable oils, composed of a mixture of several fatty acids, had better lubrication performance than the single

fatty acid methyl esters when they were added to low sulfur diesel fuel (Geller and Goodrum, 2004). Moreover the addition of biodiesel produced from hydroxylated oils (lesquerella and castor oils), reduced the wear scar much more than the case of nonhydroxylated oils (rapeseed and soybean) (Goodrum and Geller, 2005). Knothe and Steidley (2005) compared the lubricity of individual fatty compounds that comprise biodiesel and some hydrocarbons that comprise diesel fuel. According to their study, fatty compounds with polarity-imparting oxygen atoms show better lubricity than hydrocarbons and an order of oxygenated moieties enhancing lubricity (COOH > CHO > OH > $COOCH_3$ > C-O > C-O-C) was obtained from studying various oxygenated C10 compounds. The molecular structure of fatty compounds, such as saturation and chain length, could influence the lubricity performance. It is observed that lubricity enhancement increases as unsaturation of these fatty compounds increases. Nonetheless there is no correlation between fatty acid chain length and lubricity enhancing properties (Geller and Goodrum, 2004).

In order to improve the lubricity of alcohol blends a small number of studies on the use of biodiesel as a lubricity enhancer have been reported. Polar molecules of the mixture of the fatty acids within the biodiesel will be absorbed on to metallic surfaces such that strong and stable fluid films will be formed to prevent wear of moving parts resulting in an improvement of alcohol blends lubricity. Although an increase in biodiesel concentration tends to increase the lubricity of alcohol-diesel blend, Lapuerta et al. (2010) reported that the addition of 2% biodiesel produced from a blend of soybean oil with palm oil (with the optimal percentage around 2% biodiesel by volume) to a fixed 7.7% ethanol-diesel blend is an optimal percentage to decrease corrected wear scar under lubricity test (Lapuerta et al., 2010a). Another work concerned with the use of soybean oil based biodiesel to enhance the lubricity of alcohol blends was studied by

(Wadumesthrige et al., 2010). According to their results, the ratio of biodiesel to butanol should be 1:1 in order to meet a dramatic improvement of blend lubricity when high butanol concentration blended with diesel fuel was tested. An investigation confirmed the beneficial effect of biodiesel lubricity added into alcohol blends in a current common rail injection system used in light duty diesel vehicles (Armas et al., 2011).

2.4.3 Hydrogen

Hydrogen is considered to be a potential alternative fuel, which can used to control diesel exhaust emissions. The use of hydrogen as a fuel can avoid the formation of carbonaceous gas emissions because it does not have a carbon atom in the fuel molecule. The partial replacement of hydrocarbon fuels with hydrogen has shown to be beneficial in terms of brake power, thermal efficiency and reduction of THC, CO, CO_2 and PM (Tsolakis and Megaritis, 2004). However the potential of using hydrogen will depend on the production processes and storage. Hydrogen can be produced from many methods such as conversion of petroleum fuels and biomass, electrolysis and direct solar conversion by thermo-chemical means (Goswami et al., 2003). To alleviate the lack of fueling infrastructure and difficulties of storage in the transport section, a way of producing hydrogen to allow partial fueling with hydrogen in dual fuel systems can be made by the on-board exhaust gas fuel reforming process (Panuccio and Schmidt, 2007, Tsolakis et al., 2005). The process involves a catalytic reaction of engine exhaust gas which contains both oxygen and high temperatures, with hydrocarbon fuel to produce hydrogen-rich gas.

The clear benefit of using hydrogen as an engine fuel is that hydrogen contains no carbon. Carbon in hydrocarbon fuels is a major source of greenhouse gases. Hydrogen can be inducted

into the cylinder with either port fuel injection or in-cylinder injection but the literature shows that a higher thermal efficiency is obtained with the intake port injection at all equivalence ratios (Yi et al., 2000). A number of studies have reported the benefits of the partial replacement of diesel fuel by hydrogen in dual fuel engine systems (Korakianitis et al., 2010, Lata and Misra, 2010). There are improvements in terms of THC, CO and particulate matter emissions due to diesel fuel replacement (Bika et al., 2008, Lambe and Watson, 1992, Senthil Kumar et al., 2003). Also beneficial effects due to the hydrogen characteristics such as the absence of carbon, high flame speed, higher diffusivity and broad flammability limits are also found. Although nitrogen oxides emissions with hydrogen fuel can increase or decrease depending on engine operating conditions and injection timing (Tomita et al., 2001), the addition of hydrogen fuel tends to increase NO_X emissions (Chae et al., 1994, Varde and Frame, 1983). This is attributed to the increased rate of heat release which elevates the peak cycle temperature. On the other hand, there are studies which report that the addition of hydrogen reduces NO_X emissions (Saravanan et al., 2007). The reason used to justify this reduction is an enhancement of turbulent mixing in-cylinder caused by the injection of pressurised hydrogen through the intake valve (Saravanan and Nagarajan, 2008). In terms of nitrogen dioxide (NO_2), the addition of hydrogen significantly increases NO_2 emissions compared to only liquid fuel combustion. The main route in the production of NO_2 is via the oxidation of NO with the hydroperoxyl (HO_2) radical. Hydrogen combustion increases the HO_2 level, as shown experimentally by Bika et al. (2008) and numerically by Lilik et al. (2010), which in turn results in the increase in NO_2 emissions. The addition of hydrogen is combined with the exhaust gas recirculation technique to obtain a simultaneous reduction of both NO_X and smoke emissions (Tsolakis et al., 2003).

CHAPTER 3

EXPERIMENTAL FACILITIES

The experimental facilities that have been used for this research are introduced in this chapter. This includes information on tested fuels and their properties, the specification of the diesel engine, instruments, and emission analysers.

3.1 Fuels

The fuels used in this research were ultra low sulphur diesel (ULSD) and rapeseed methyl ester (RME) provided by Shell Global Solutions UK. The synthesis diesel known as gas-to-liquid (GTL) was employed as a base fuel to investigate the ability of biodiesel to act as a lubricity enhancer and was also provided by Shell Global Solutions UK. The two alcohols used in this study were ethanol and n-butanol from Sigma-Aldrich. The biodiesel containing hydroxyl group, castor oil methyl ester (COME), was supplied from Hampshire Commodities Limited in order to study the hydroxylated biodiesel effects on alcohol-diesel blends. All mono-alkyl esters of fatty acids, used to evaluate the effects of fatty ester compositions (carbon chain length and unsaturation degree) were also acquired from Sigma-Aldrich. The esters selected were: methyl laurate (C12:0), methyl myristate (C14:0), methyl palmitate (C16:0), methyl stearate (C18:0) and methyl oleate (C18:1). The purity of these esters was > 96%, except in the case of technical grade methyl oleate (approximately ~77%).

3.2 Fuel properties

The basic properties of tested fuels are given in Table 3.1 and Table 3.2. The density and kinematic viscosity were measured according to ISO 12185 and ISO 3150 respectively. An IKA C200 calorimeter was employed to measure the higher calorific value (Q_{HCV}) of tested fuels, and then the lower calorific value (Q_{LCV}) of each fuel can be determined using the following equation:

$$Q_{HCV} = Q_{LCV} + \left(\frac{m_{H_2O}}{m_f}\right) h_{fg\,H_2O} \tag{3.1}$$

where $\left(\frac{m_{H_2O}}{m_f}\right)$ is the ratio of mass of water produced to mass of fuel burned and $h_{fg\,H_2O}$ is enthaphy of vaporisation of water.

The cetane number of COME and methyl esters was taken from Berman et al. (2011) and (Knothe, 2005) respectively. The information published in Graboski and McCormick (1998) was used to represent the boiling and melting point of individual methyl esters. The latent heat of vaporisation of ethanol and butanol was taken from Goodger (2000) and Rakopoulos et al. (2010), respectively. The adiabatic flame temperature of methyl esters was calculated at constant pressure with a stoichiometric air–fuel mixture ($\phi = 1$), no dissociation, combustion starting at 881 K and 4.5 MPa, enthalpy of formation of the FAME taken from Osmont et al. (2007) and specific heat capacity of the products taken from Turns (1996). Bulk modulus of methyl esters was calculated by the following equation:

$$\beta = c^2\rho \tag{3.2}$$

where β is the isentropic bulk modulus (Mpa), c is the speed of sound (m/s) in the sample, and ρ is the density (kg/m^3). Data of speed of sound and density (at 40 °C) were obtained from Gouw

and Vlugter (1964b and 1964a). In case of technical grade methyl oleate the data of neat methyl esters was used to calculated the adiabatic flame temperature and bulk modulus.

Table 3.1: Physical and chemical properties of fuels

Properties	ULSD	GTL	RME	COME	Ethanol	Butanol
Purity (% v/v)	100	100	100	100	99.7	99
Cetane number	53.9	80	54.7	48.9	8	17
Density at 15 ^{o}C (kg/m^{3})	827.1	784.6	883.7	928.7	789.4	809.7
Kinematic viscosity at 40 ^{o}C (cSt)	2.47	3.50	4.48	16.67	1.13	2.22
Lower heating value (MJ/kg)	43.3	43.9	37.8	37.6	26.83	33.09
Latent heat of vaporisation (kJ/kg)	243	-	216	-	858	585
Bulk modulus (Mpa)	1410	-	1553	-	1320	1500
Melting point (^{o}C)	-	-	-	-	-114	-90
Boiling point (^{o}C)	-	-	-	-	78.3	117.5
Lubricity at 60 ^{o}C (μm)	275	290	205	-	656	620
Sulphur (mg/kg)	46	0.05	5	-	-	-
-Aromatics (% wt)	24.4	0.3	0	-	-	-
Molecular weight (kg/kmol)	194.4	-	295.1	309.8	46.07	74.12
C (% wt)	86.4	85	77.1	73.5	52.14	64.82
H (% wt)	13.6	15	12.1	11.7	13.13	13.60
O (% wt)	0	0	10.8	14.8	34.73	21.58

Table 3.2: Physical and chemical properties of individual fatty acid methyl esters

Properties	C12:0	C14:0	C16:0	C18:0	C18:1
Purity (% v/v)	>98	>98	>97	>96	>70
Cetane number	61.4	66.2	74.5	86.9	55.0
Density at 15 ^{o}C (kg/m^{3})	871	868	-	-	878.5
Density at 40 ^{o}C (kg/m^{3})	853.3	851.7	850.5	849.6	859.6
Kinematic viscosity at 40 ^{o}C (cSt)	2.23	2.96	4.38	5.58	4.11
Lower heating value (MJ/kg)	35.3	36.3	37	37.7	37.5
Adiabatic flame temperature (K)	2828	2833	2837	2840	2860
Bulk modulus (MPa)	1393	1438	1477	1511	1539
Melting point (^{o}C)	5.2	19	30	39.1	-19.9
Boiling point (^{o}C)	262	295	338	352	349
Lubricity at 60 ^{o}C (μm)	330	299	148	243	232
Molecular weight (kg/kmol)	214.3	242.4	270.5	298.5	296.5
C (% wt	72.9	74.3	75.5	76.4	76.9
H (% wt)	12.2	12.5	12.7	12.9	12.1
O (% wt)	14.9	13.2	11.8	10.7	11.0

Assessment of the lubrication properties of the tested fuels was carried out on a high frequency reciprocating rig (HFRR). This is shown schematically in Figure 3.1. The test specimens comprised of a 6 mm diameter steel ball and steel disc. All tests were conducted according to the EN ISO 12156-1:2006 standard (ISO12156-1, 2006). This included the fuel temperature maintained at 60 ^{o}C and the volume of the fuel sample used, set at 2 ml. A humidity and temperature controlled cabinet was employed to provide the laboratory air conditions as

shown in Figure 3.2. During the test the disc was fully submerged in the tested fuels at a reciprocating frequency of 50 Hz lasting 75 min. At the conclusion of each test, all components were cleaned using toluene and acetone respectively. The HFRR reported the friction coefficient and lubricant film concentration.

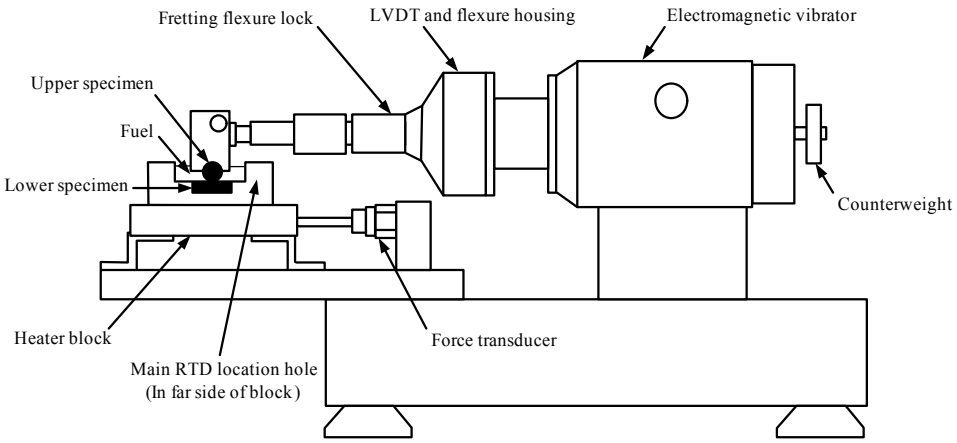

Figure 3.1: Schematic diagram of HFRR

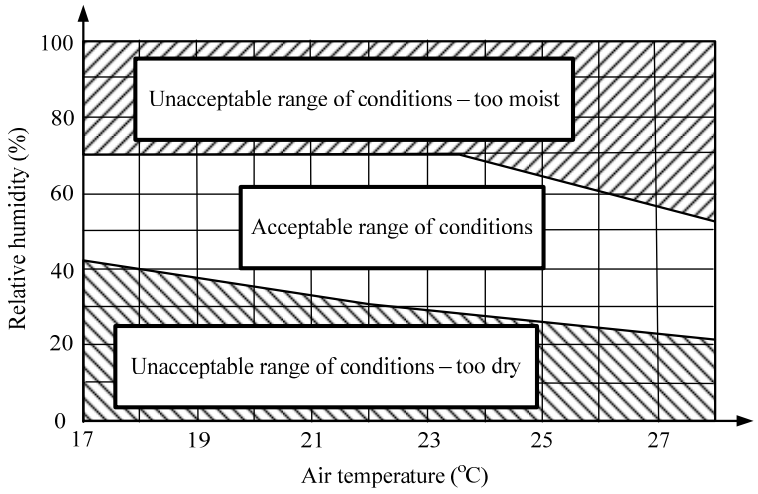

Figure 3.2: Acceptability map of laboratory air conditions

To investigate the size of the wear scar of the ball in micrometers an optical microscope was used together with a 100x magnification lens. From this the average wear scar diameter was calculated and corrected to normalize for the standard water vapour pressure of 1.4 kPa (WS1.4). This considers the effect of the air conditions on the fuel's lubricating performance while the HFRR was operating, as defined by ISO 12156-1. The corrected wear scar diameter can be determined using the following equation:

$$\text{WS1.4 } (\mu\text{m}) = \text{MWSD } (\mu\text{m}) + \text{HCF} \times (1.4\text{-AVP (kPa)}) \tag{3.3}$$

where MWSD is the mean wear scar diameter, humidity correction factor (HCF) is 60 as mentioned in the standard and AVP is the mean absolute vapour pressure and can be calculated as follows:

$$\text{AVP} = \frac{\text{AVP}_1 + \text{AVP}_2}{2} \tag{3.4}$$

where the subscript 1 and 2 are the initial and final absolute vapour pressure, respectively and can be expressed by the following equation:

$$\text{AVP} = \frac{\text{RH} \times 10^{\nu}}{750} \tag{3.5}$$

where RH is the relative humidity and ν is the function of temperature (T) in degrees Celsius as described below.

$$\nu = 8.017352 - \frac{1705.984}{231.864 + \text{T}} \tag{3.6}$$

All of the lubricity experiments were repeated twice and repeatability was demonstrated to be less than 20 μm. After two independent experiments the results were reported in the calculated mean values and standard deviation. The HFRR was modified to account for fuel evaporation due to the high volatility of the alcohol fuels when alcohol fuels were tested. The fuel holder was deeper with respect to that used for the diesel fuel lubricity test and was covered with a close-fitting PTFE lid (Figure 3.3).

In order to analyse the wear scar perpendicular to the sliding direction on the lower specimen as well as measure the wear scar depth, measurements of the worn disc surface were made using a Talysurf-120 profilometer. A Philips XL-30 scanning electron microscopy (SEM) fitted with an Oxford Instruments INCA energy dispersive spectrometer (EDS) system was employed to investigate the microscopic topography and elemental chemical compositions of the worn surfaces.

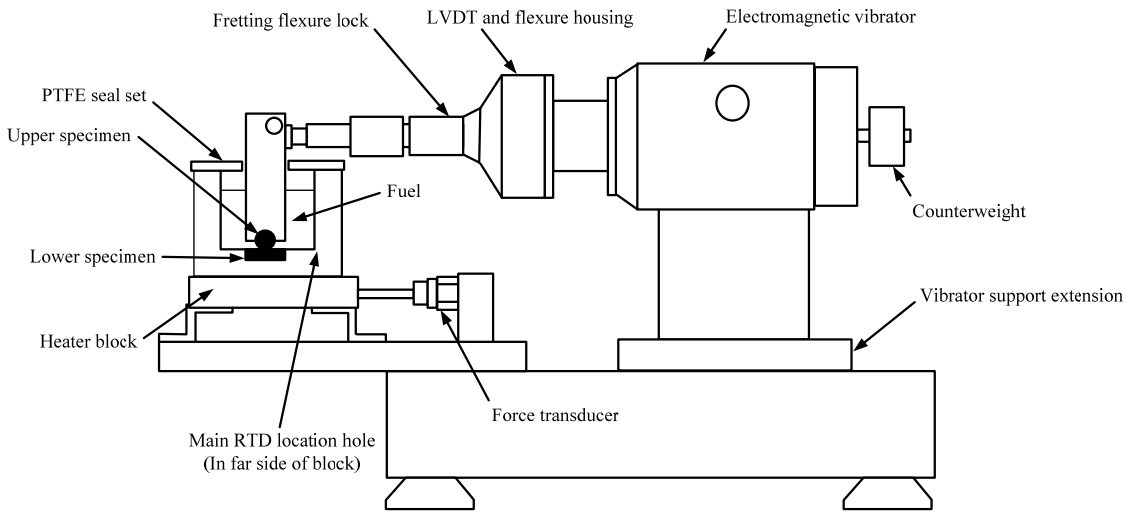

Figure 3.3: Schematic diagram of modified HFRR

Other properties of tested fuels which are shown in the fuel properties table were obtained from suppliers. The fatty acid profiles of the technical grade methyl oleate (TG C18:1), RME and COME were determined using a Perkin Elmer Clarus 500 chromatograph equipped with a FID as shown in Table 3.3.

Table 3.3: Fatty acid profiles of RME, COME and TG C18:1, % wt

Methyl esters		RME	COME	TG C18:1
Lauric	C12:0	-	-	1.96
Myristic	C14:0	-	-	1.75
Palmitic	C16:0	4.51	1.17	4.07
Palmitoleic	C16:1	-	1.22	5.24
Stearic	C18:0	1.47	-	1.13
Oleic	C18:1	63.12	3.85	77.62
Ricinoleic	C18:1 OH	-	87.90	-
Linoleic	C18:2	19.85	4.97	8.23
Linolenic	C18:3	9.03	0.89	-
Gadoleic	C20:1	0.55	-	-
Erucic	C22:1	1.47	-	-

3.3 Test engine and instrumentation

The experiments were carried out on a single cylinder experimental test rig as shown in Figure 3.4. This engine is a Lister Petter model TR1 diesel engine which employs a pump-line-nozzle direct injection system. The technical data and engine specifications are given in Table 3.4. It has to be clarified that the results which were obtained in this research are specific for this type of engine (mechanical injection system, single injection and naturally aspirated), where the

physical properties of the fuel (such as density or bulk modulus) are expected to affect the injection process to a greater extent in modern systems.

A thyristor-type air cooled DC electric dynamometer was used to motor and load the engine. To record in-cylinder pressure traces, a Kistler 6125B pressure transducer mounted at the cylinder head and connected via a Kistler 5011 charge amplifier to a data acquisition board (National Instruments PCI-MIO-16E-4) was used. The crankshaft position was measured using a 360-ppr incremental shaft encoder. The schematic diagram of experimental installation including a wiring diagram of measuring in-cylinder pressure and crankshaft position is shown in Figure 3.5. An in-house developed LabVIEW based programme was employed to analyse combustion parameters. Outputs from the analysis of engine cycles included the in-cylinder pressure, indicated mean effective pressure (IMEP), percentage coefficient of variation (COV) of IMEP and peak cylinder pressures, average crank angle for ignition delay and other combustion characteristic information. The data of 100 engine cycles was collected and then averaged to get rid of noise problems in the data signals and acquisition system. The COVs of IMEP and peak cylinder pressure were used as criteria for combustion stability (cyclic variability). All experiment tests were acceptable with the COVs below 5%. Other standard engine test rig instrumentation used to monitor intake air, exhaust gas recirculation (EGR), temperatures (oil, air, inlet manifold and exhaust) and pressures were included in the test rig.

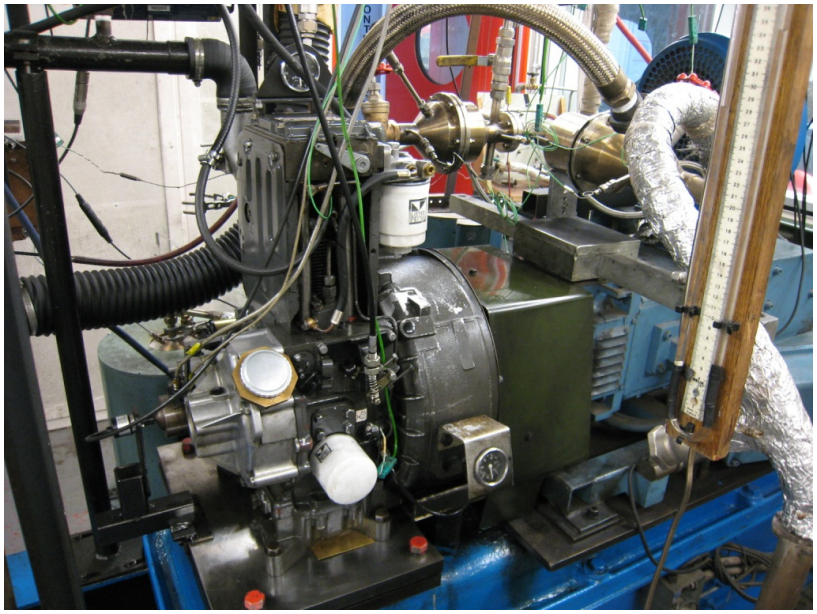

Figure 3.4: The single cylinder diesel engine test rig

Table 3.4: Engine specifications

Engine specification	
Number of cylinders	1
Bore (mm)	98.4
Stroke (mm)	101.6
Connecting rod length (mm)	165
Displacement volume (cm^3)	773
Maximum torque (N.m) @ 1800rpm	39.2
Maximum power (kW) @ 2500 rpm	836
Compression ratio	15.5:1
Injection timing (^{o}bTDC)	22
Maximum injection pressure (bar)	180
Injection system	Three holes pump-line-nozzle
Engine piston	Bowl-in-piston

The volumetric flow rate of the EGR was determined according to the reduction in the volumetric air flow rate as defined by

$$\text{EGR (\%vol)} = \frac{\dot{V}_O - \dot{V}_i}{\dot{V}_O} \times 100 \tag{3.7}$$

where $\dot{V}_i$ and $\dot{V}_O$ are the measured intake air volumetric flow rate with and without EGR, respectively.

The IMEP is the work transfer from fuel to piston over displaced volume and can be determined using the following equation:

$$\text{IMEP} = \frac{w_i}{V_d} = \frac{\oint p dV}{V_d} \tag{3.8}$$

where w_i is the indicated work per cycle. The p and V represent the in-cylinder pressure and corresponding cylinder volume, respectively. The V_d is the displaced volume and can be calculated as follows:

$$V_d = A \times L \times n \tag{3.9}$$

where A is the area of piston head, L is the stroke length and n is the number of cylinders.

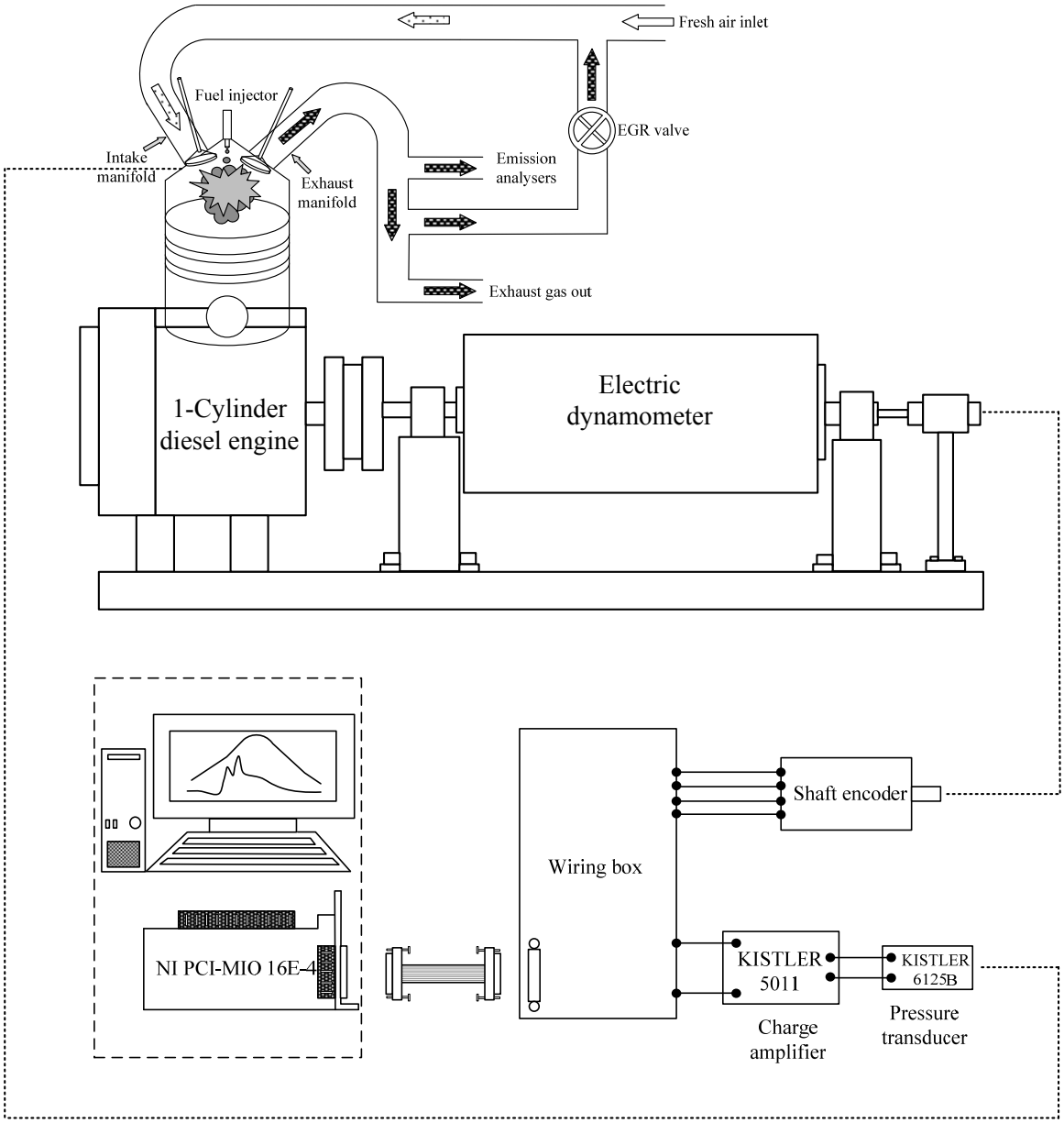

Figure 3.5: Schematic diagram of experimental installation

In this study the engine efficiency and the specific engine emissions were calculated using the indicated power (P_i) which is shown in the following equation:

$$P_i(\text{kW}) = \frac{\text{IMEP (Pa)} \times V_d\,(\text{m}^3) \times \text{N (rpm)}}{n_R \times 60 \times 1000} \tag{3.10}$$

where N is the engine speed and n_R is the number of crank revolutions for each power stroke per cylinder ($n_R = 2$ for four-stroke engine).

The indicated specific fuel consumption (ISFC) is the mass fuel flow rate per unit power output and can be calculated using the following equation:

$$\text{ISFC (g/kWh)} = \frac{\dot{m}_f\,(\text{g/h})}{P_i\,(\text{kW})} \tag{3.11}$$

where $\dot{m}_f$ is the mass fuel flow rate.

The engine thermal efficiency (η_{th}) is the ratio of the work produced per cycle to the fuel energy supplied per cycle and can be expressed by the equation as shown below.

$$\eta_{th} = \frac{P_i}{\dot{m}_f Q_{LCV}} \tag{3.12}$$

The measured pressure in the combustion chamber was processed for the heat release rate. By combining the first law of thermodynamics, the perfect gas equation of state and ideal gas assumption, the model used to calculate heat release rate in this research is expressed by the following equation:

$$\frac{dQ}{d\theta} = \frac{\gamma}{\gamma\text{-}1} p \frac{dV}{d\theta} + \frac{\gamma}{\gamma\text{-}1} V \frac{dp}{d\theta} \tag{3.13}$$

where γ is the ratio of specific heats (C_p/C_v), p is the instantaneous in-cylinder pressure and V is the instantaneous engine cylinder volume. The value of γ was calculated by interpolation based on the actual p-V diagrams.

3.4 Emission analyser

A Horiba MEXA 7100DEGR analyser was employed to measure gaseous emissions. The exhaust gas was sampled through the heated line at 190 ^oC to avoid the condensation of gaseous emissions. The method of non-dispersive infrared (NDIR) where the detector calculates the concentration of gaseous emissions by measuring its energy absorption at specific wavelengths in the infrared spectrum was used to measure CO and CO_2 emissions. The flame ionization detector (FID) was employed to measure THC emissions by detecting ions using a metal collector when any hydrocarbons in the sample are burnt in hydrogen flame inside the FID. The chemiluminescence detector (CLD) was used to determine NO_X emissions by measuring the amount of light emitted when NO molecules react with ozone and is oxidized to NO_2. A MultiGas 2030 based on the fourier transform infrared (FTIR) spectrometer technique was also used for the measurement of diesel emissions alongside the Horiba MEXA 7100DEGR to remove experimental bias.

A Horiba MEXA 1230 PM was employed to analyse soot emissions by the diffusion charging method with a 1:40 (exhaust:air) dilution ratio of soot diluter and to measure soluble organic material (SOM) by a dual FID method equipped with a 47mm diameter Teflon (PTFE)-coated glass fibre filter. The configuration of the Horiba PM which is mainly composed of a diffusion charger (DC) detector and two FIDs is shown in Figure 3.6. To measure soot emissions

the sample of exhaust gas is introduced into the heated diluter (200 ^{o}C) which is positioned before the DC unit to eliminate the condensation of volatile hydrocarbons. The amount of charge for each particle is measured by the detector resulting from the irons attached onto the particle surface area which relates to averaged discharge values. In case SOM the sample gas is induced to the heated filter which is positioned before the FIDs to trap soot emissions, resulting in the passing of only gaseous phase in sampling exhaust. The sample is then divided by two sample lines which are maintained at 47 ^{o}C and 191 ^{o}C based on the fact that the compounds of gaseous hydrocarbons vaporise. The difference between the FIDs can be used to calculate the SOM with the technique that shows a good correlation to the conventional gravimetric method followed by the soxhlet extraction method (Fukushima et al., 2000). The soluble organic fraction (SOF) representing the portion of organic material which forms the particulate matter can be analysed using the following equation:

$$SOF = \frac{SOM}{SOM + soot} \tag{3.14}$$

To study the size distribution of particulate matter, a scanning mobility particle sizer (SMPS), model TSI/3080, fitted with thermodiluter was employed. The sample and sheath flow rates were set to obtain the range of measured particle size diameters between 10.4 and 379 nm. The dilution ratio was set at 1:200. The air dilution temperature was maintained constant at 150 ºC in order to prevent hydrocarbon condensation and nucleation which can occur during sampling. The particle mass distribution was estimated from the particle number distribution using an agglomerate density function which decreases as agglomerate size increases (Lapuerta et al., 2003).

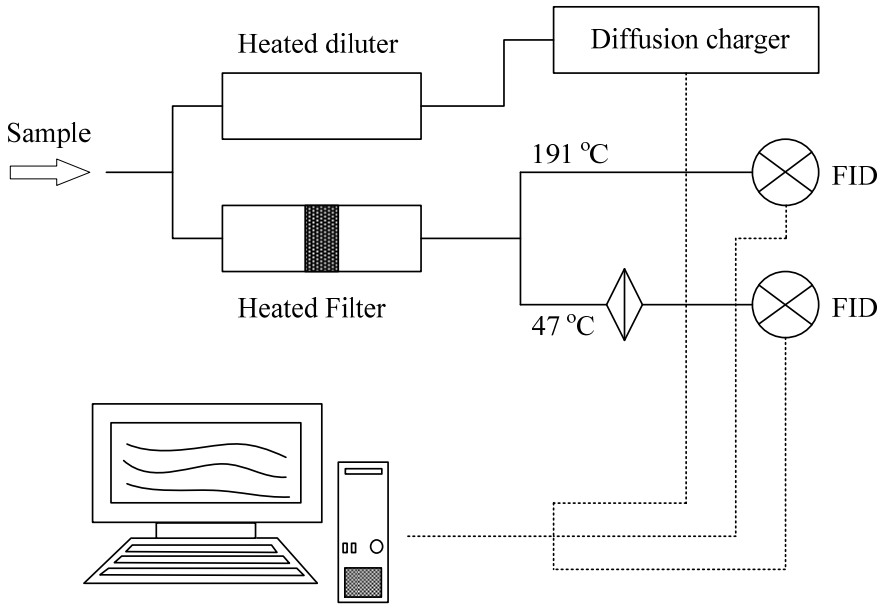

Figure 3.6: System configuration of Horiba PM

PM emissions were collected on 47 mm diameter glass micro-fibre filters (Whatman-without a PTFE coating) using an in-house built venture nozzle diluter with a dilution ratio of 1:10. The sample gas flow rate was set at 10 l/min and the PM was loaded on the filter for 1 hour. Analysis of collected PM composition and the rate of soot oxidation were carried out on a thermo gravimetric analyser (TGA) according to the method listed in Table 3.5. Regarding the method the first step is the heating programme with the isothermal process (40 ^{o}C) for 10 minutes to avoid any undesirable movement of the TGA robot arm and the sample holder when transferred to the furnace. Secondly, the sample is heated from 40 ^{o}C to 400 ^{o}C at a slow rate of 3 ^{o}C/min under a nitrogen atmosphere to allow sufficient time for the vaporisation of volatile organic material (VOM). When the temperature reaches 400 ^{o}C, the isothermal process is conducted for 30 minutes to fully vaporise VOM. However before the oxidation process is introduced, the furnace temperature is cooled down to 350 ^{o}C to broaden the soot oxidation window. The

temperature is ramped up to 600 ^{o}C at a heating rate of 3 ^{o}C/min under an air atmosphere to oxidise soot. Finally, the temperature is maintained at 600 ^{o}C for 60 minutes to complete the soot oxidation. It is notable that temperatures above 600 ^{o}C can decompose the sample filter resulting in the errors of the soot oxidation results. Volatile organic fraction (VOF) is obtained by comparing the mass of particulate matter which is lost in the nitrogen atmosphere (volatile organic material) with the mass of total particulate matter (volatile organic material and soot). The activation energy used to oxidise soot emissions of tested fuels can be modeled through an Arrhenius-type reaction as follows:

$$-\frac{dm}{dt} = k_c m^n p_{O_2}{}^r = A \exp\left(\frac{-E_a}{RT}\right) m^n p_{O_2}{}^r \tag{3.15}$$

where m is the actual soot mass, t is the time, k_c is the reaction rate constant, A is the pre-exponential factor, Ea is the activation energy of the reaction, p_{O_2} is the partial pressure of oxygen, n is the reaction orders of soot and r is the reaction orders of oxygen. When logarithms are taken from the equation above and the reaction orders of soot and oxygen are supposed to be unity (Rodríguez-Fernández et al., 2011), the simplified equation to estimate the activation energy can be expressed by the following equation:

$$\ln\left(-\frac{dm}{dt}\right) = \ln\left(Ap_{O_2}\right) - \frac{E_a}{R}\frac{1}{T} \tag{3.16}$$

Table 3.5: TGA heating programme

	Initial temp. (^oC)	Final temp. (^oC)	Heating rate (^oC/min)	Duration (min)	Atmosphere gas
1	40	40	Isothermal	10	Nitrogen
2	40	400	3	-	Nitrogen
3	400	400	Isothermal	30	Nitrogen
4	400	350	3	-	Nitrogen
5	350	600	3	-	Air
6	600	600	Isothermal	60	Air

CHAPTER 4

THE EFFECT OF BLENDED DIESEL FUELS ON LUBRICITY

The lubricating properties of two sustainable alternative diesels blended with ultra low sulphur diesel (ULSD) were investigated. The candidate fuels were a biodiesel consisting of fatty acid methyl esters derived from rapeseed (RME) and gas-to-liquid (GTL). Lubricity tests were conducted on a high frequency reciprocating rig (HFRR). The mating specimen surfaces were analysed using optical microscopy and profilometery for wear scar diameters and profiles respectively. Microscopic surface topography and deposit composition was evaluated using a scanning electronic microscope (SEM) with an energy dispersive spectrometer (EDS).

A series of six lubricity tests were conducted. The first focused solely on the base fuels by way of a benchmark for the blended fuel tests. The second to the fourth tests were conducted using dual blends viz. ULSD/RME, GTL/RME and ULSD/GTL with a 10% (v/v) increase of the second fuel to study the effect of blend volumes on lubricity. The fifth and sixth series focused on three-way blends where the content of the principle fuel (i.e. ULSD and GTL) was fixed at 70% with the proportion of RME varied at 5%, 10%, 15%, 20%, 25% and 30% (v/v).

4.1 Lubricating properties

Figure 4.1 shows the measured tribological properties obtained from the HFRR tests for the base fuels. They show that RME possesses the best lubricity when compared to ULSD and GTL. This is due to the combination of oxygen-containing compounds and a variety of fatty acids in methyl

esters being adsorbed on the rubbing surfaces to reduce friction and improve the lubrication film (shown in figure 4.1d).

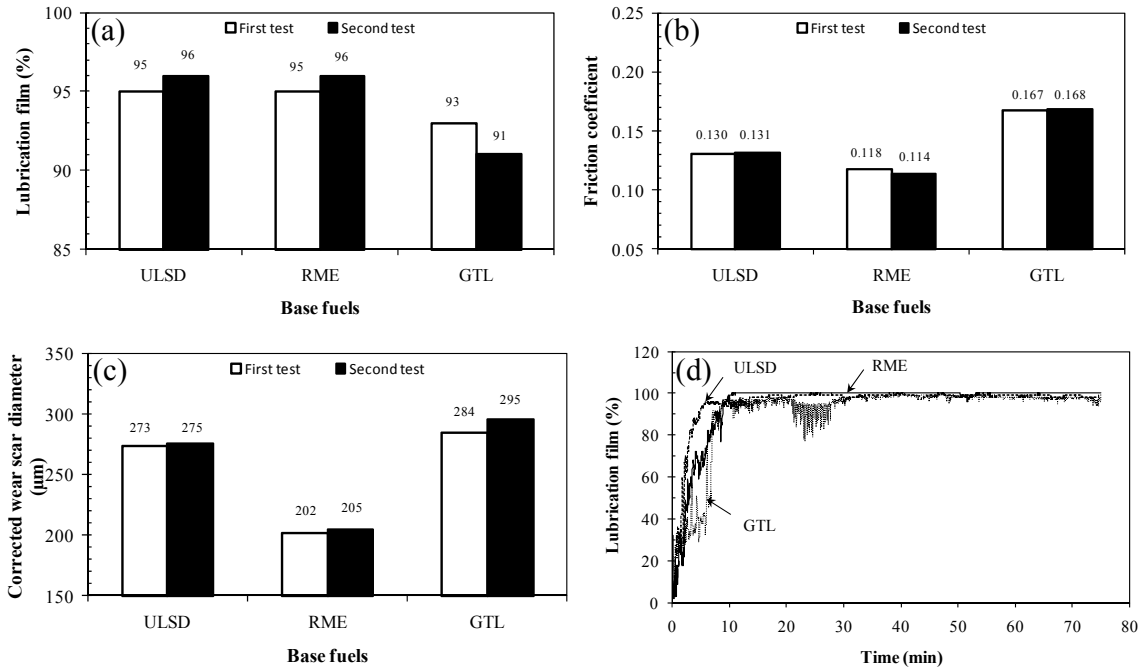

Figure 4.1: Tribological results for the base fuels (a) lubrication film, (b) friction coefficient, (c) WS1.4 (d) transient lubrication film

A correlation was obtained between the lubricating properties and the percentage content of RME blended with ULSD and GTL. The mean values and standard deviation of the lubrication film concentration and friction coefficient against RME percentage are shown in Figure 4.2a for ULSD/RME blends. The lubricant film of the blended fuels fluctuates around 96% and the friction decreases slightly to minimum of 0.116 in pure RME. Figure 4.2b shows the corrected wear scar diameter. A 10% addition of RME decreased wear scar diameters by approximately 27%. This reduction in tribological damage on the upper specimen was maximized at RME blends of 20%.

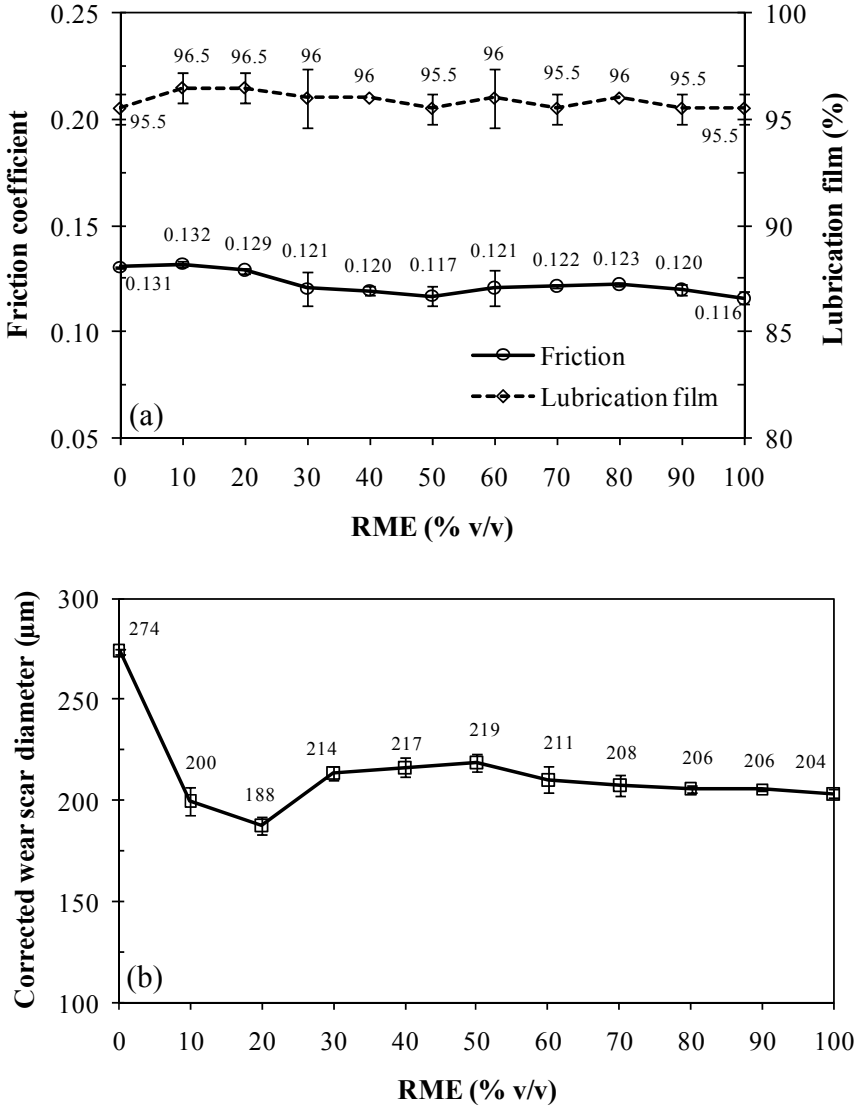

Figure 4.2: Tribological results for ULSD/RME blends (a) friction coefficient and lubrication film (b) WS1.4

The same three tribological parameters for the blends of GTL/RME are shown in Figure 4.3. Again, a 10% addition of RME is shown to improve the lubricity of GTL significantly. This result is in agreement with others and proves that GTL responds well to typical lubricity additives (Fukumoto et al., 2003, Oguma et al., 2004). The wear scar diameter for these blends reduced by

approximately 100 µm compared to that of the base GTL. This is likely to have been caused by an increase the viscosity and surface tension that can improve fluid film lubrication. To confirm this hypothesis the surface tension of GTL/RME blends were investigated using a tensiometer.

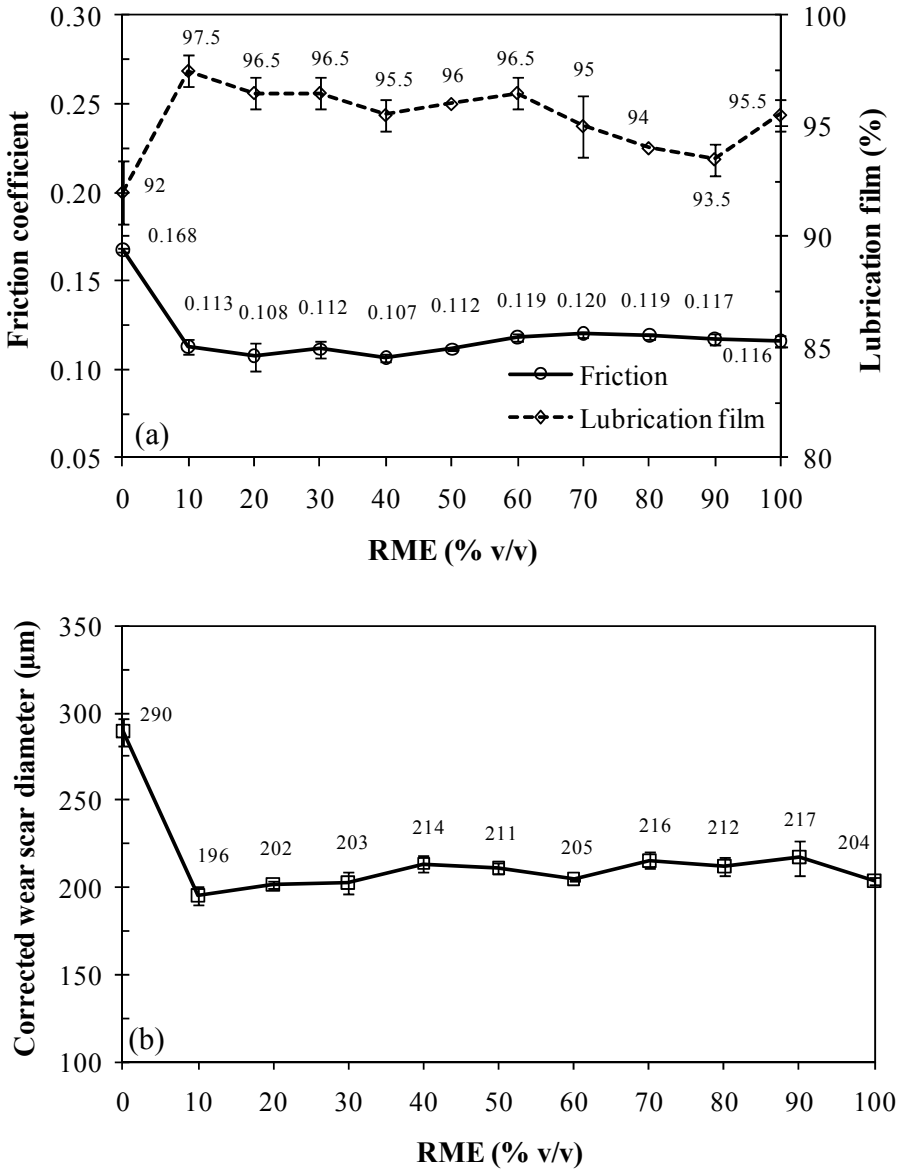

Figure 4.3: Tribological results for GTL/RME blends (a) friction coefficient and lubrication film (b) WS 1.4

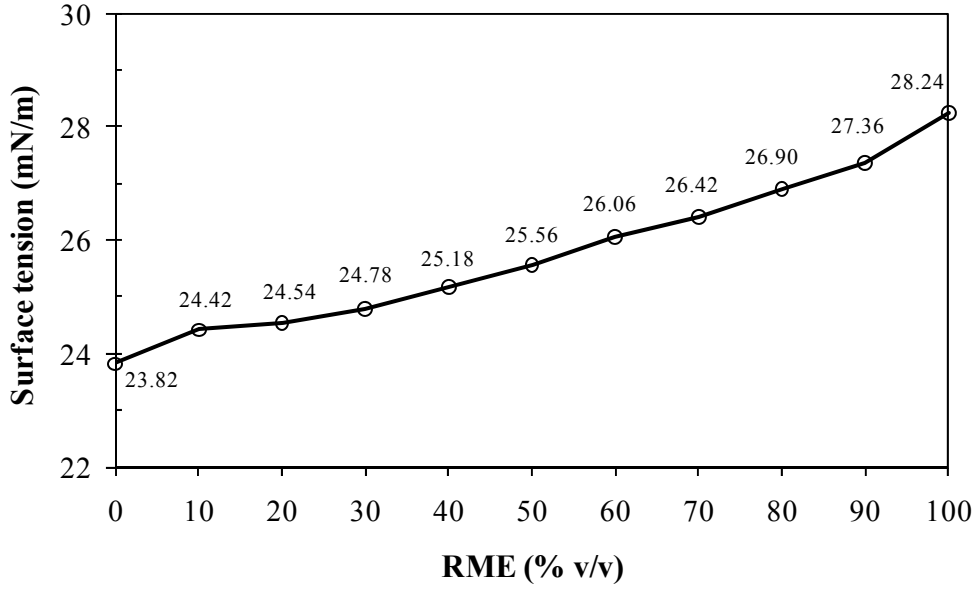

Figure 4.4: Surface tension for GTL/RME blends

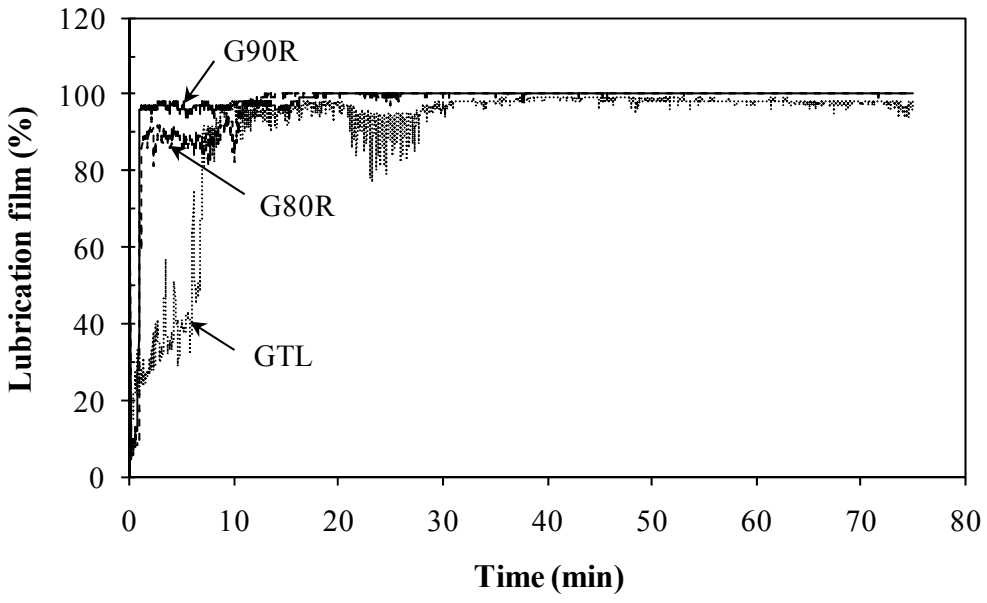

Figure 4.5: Lubrication film for GTL/RME blends

The results, shown in Figure 4.4, demonstrate that the surface tension increased linearly with an increase in the proportion of RME. In addition the mixture of fatty acids of RME can enhance the boundary lubrication by an increase in the polar-containing compounds, leading to improved stability of the lubrication film as shown in Figure 4.5. The friction coefficient and corrected wear scar diameter became approximately constant after the optimal proportion, 10% of RME in fuel blends, at approximately 0.112 and 210 μm respectively. It is useful to note that the almost all of the GTL/RME blends posed better lubricating ability than that of the ULSD/RME blends. This is likely to be caused by the better compatibility of biofuels to induce fluid film lubrication and form stronger boundary lubrication conditions.

The effect of GTL on the ULSD lubricity was also examined. Figure 4.6 shows that a 10% blend of GTL with ULSD decreased the lubrication film, directly affecting the corrected wear scar diameter by approximately 9%. The lubricity of the higher blends (above approximately 60%) reverted to behaviour similar to that of GTL. The GTL fuel demonstrated inferior lubricating characteristics when compared to ULSD and no benefit in overall lubricity was evident when the two fuels were blended.

To improve the lubricity of blending GTL and ULSD the tribological properties of three-way blends were studied respectively. The results for the ULSD and GTL biased tests are shown in Figure 4.7 and 4.8. It can be observed that as little as 5 % RME can improve the lubricity of ULSD/GTL blends dramatically. The lubrication film, which has a direct bearing on the generated wear scar, increased correspondingly from 90% to 97% and 92% to 98% for the 70% fixed concentration of ULSD and GTL. This resulted in a decrease of approximately 36% and 33% of the wear scar diameter for each composition. It can be seen that proportions of RME

higher than 10% (v/v) in blended fuels had no significant effect on lubricity. The optimal proportion of the ULSD biased blends that created the smallest corrected wear scar, was 70% ULSD, 15% GTL and 15% RME (D70G15R). Previous work at Birmingham has shown that this proportion can produce similar combustion characteristics to ULSD (Rounce et al., 2009). For the 70% biased GTL blends, the optimum blend proportion was at 70% GTL, 20% ULSD and 10% RME (G70D20R). Furthermore the corrected wear scar diameter under the lubrication of this blend was smallest compared to all tests. This demonstrates the synergistic effect of biofuels on lubrication properties, when the synthetic diesel and biodiesel fuels are blended with conventional diesel to achieve fuel substitution targets.

4.2 Wear scar profile

The wear scar profiles of the base fuels perpendicular to sliding direction on lower specimen are illustrated in Figure 4.9. The wear scar depths are 2.15 μm, 1.33 μm and 2.28 μm under the lubrication of ULSD, RME and GTL fuel respectively. 3-D topography measurements suggest that there was a deposit build-up on the periphery of the wear scar for the ULSD and RME specimens. This residue increased the surface roughness around the worn zone under fuel lubrication. It was absent in the GTL tests. Considering RME as a lubricity enhancer, the wear scar profiles are shown in Figures 4.10 and 4.11 for the 70% fixed ULSD and GTL blends respectively. They show a direct correlation to that of wear scar diameter, i.e. the bigger wear scar diameter, the deeper the wear scar depth. As little as 5% RME blended with ULSD/GTL can reduce the depth of wear damage by 54% and 49% respectively. Consequently, the optimal proportion of three-way blends possessing the shallowest wear scar depth was the same blend combination as the wear scar diameter, namely G70D20R.

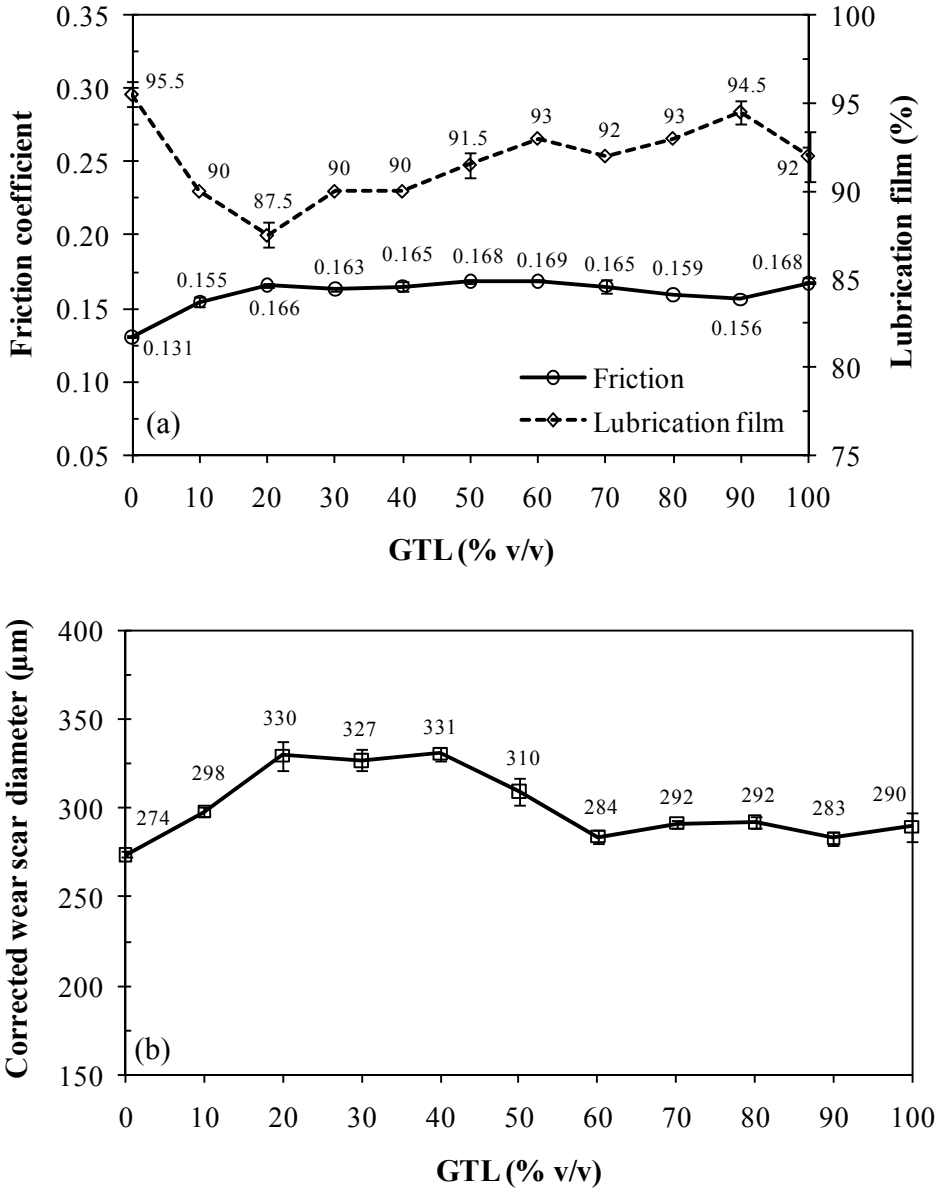

Figure 4.6: Tribological results for ULSD/GTL blends (a) friction coefficient and lubrication film (b) WS1.4

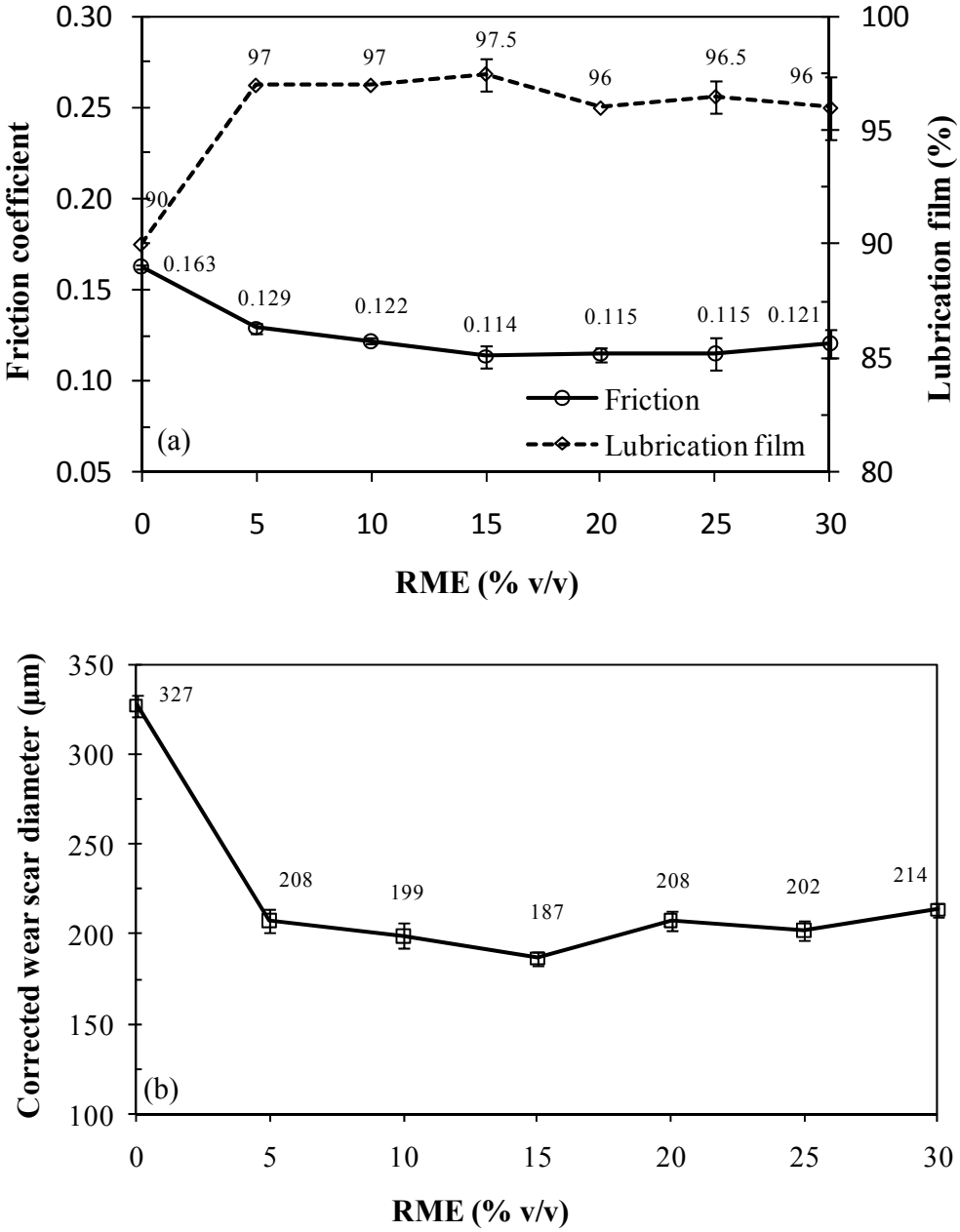

Figure 4.7: Tribological results for ULSD biased blends (ULSD fixed at 70% v/v) (a) friction coefficient and lubrication film (b) WS 1.4

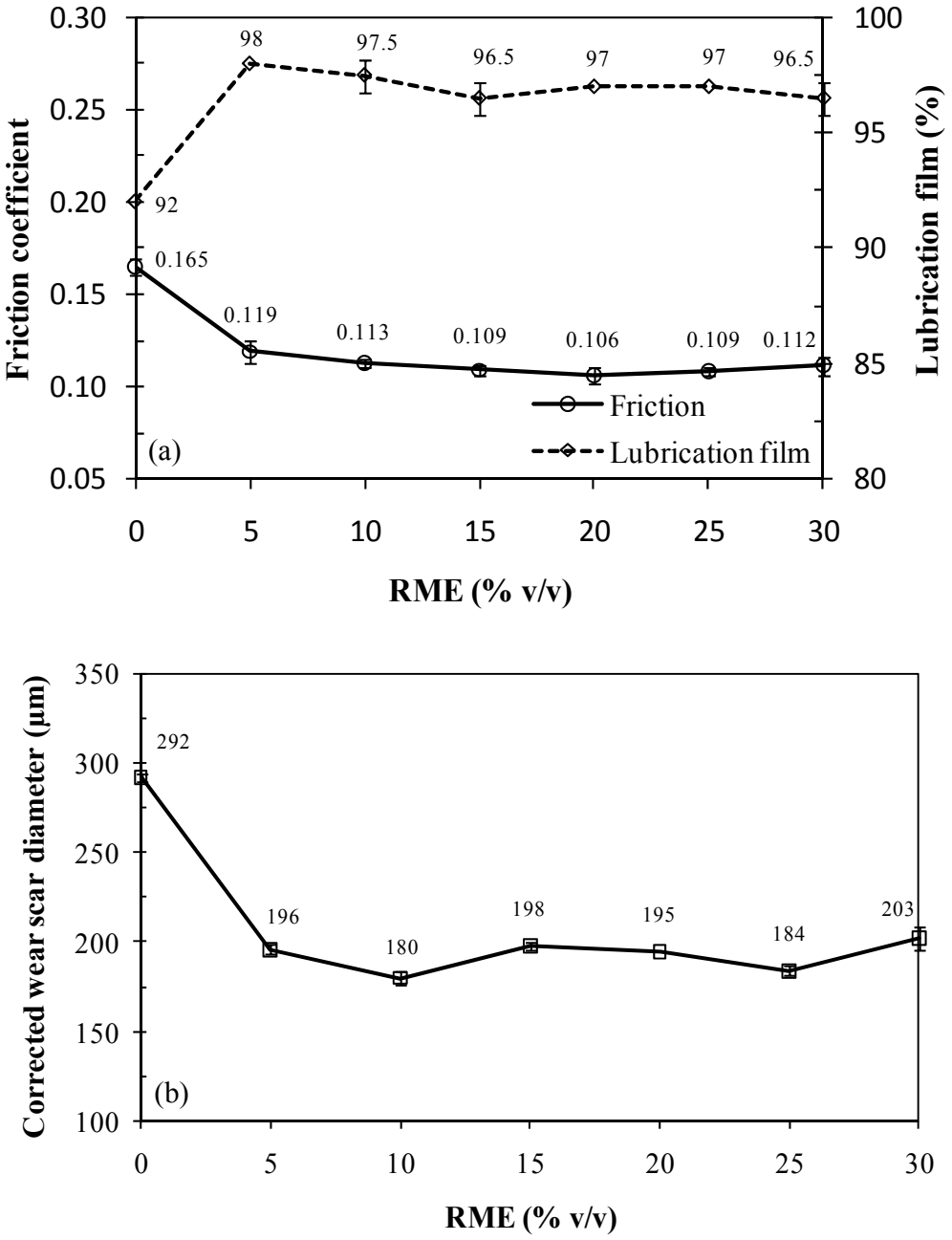

Figure 4.8: Tribological results for GTL biased blends (GTL fixed at 70% v/v) (a) friction coefficient and lubrication film (b) WS 1.4

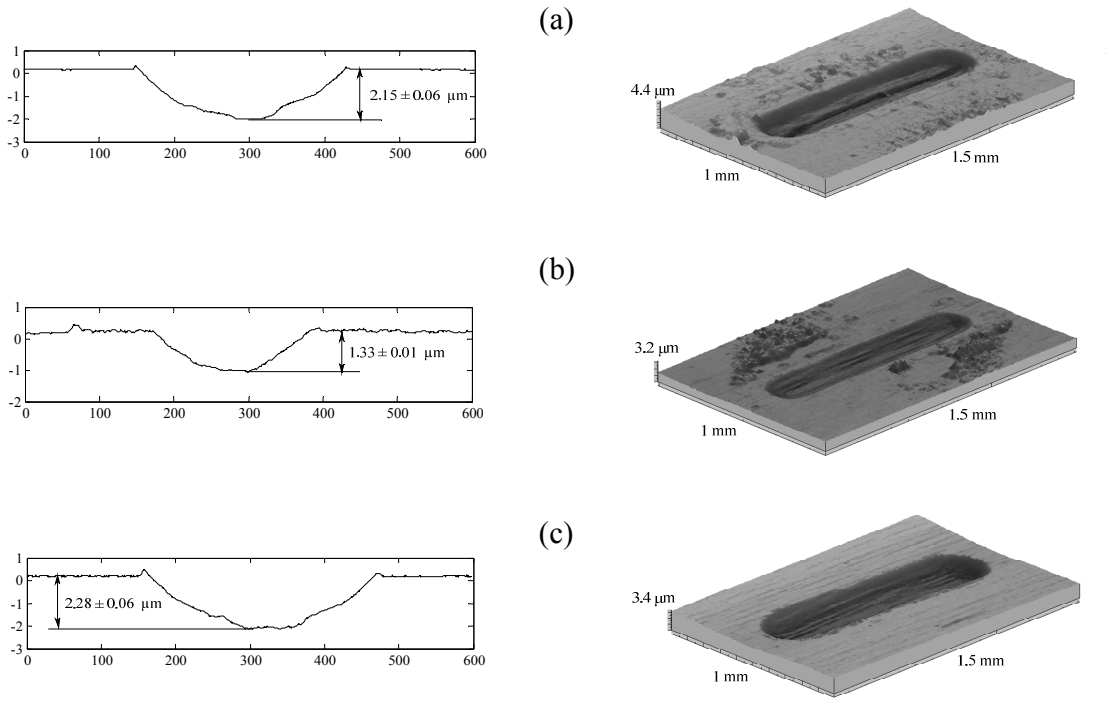

Figure 4.9: Wear scar profile perpendicular to sliding direction (left) and 3D worn surface (right): (a) ULSD, (b) RME and (c) GTL

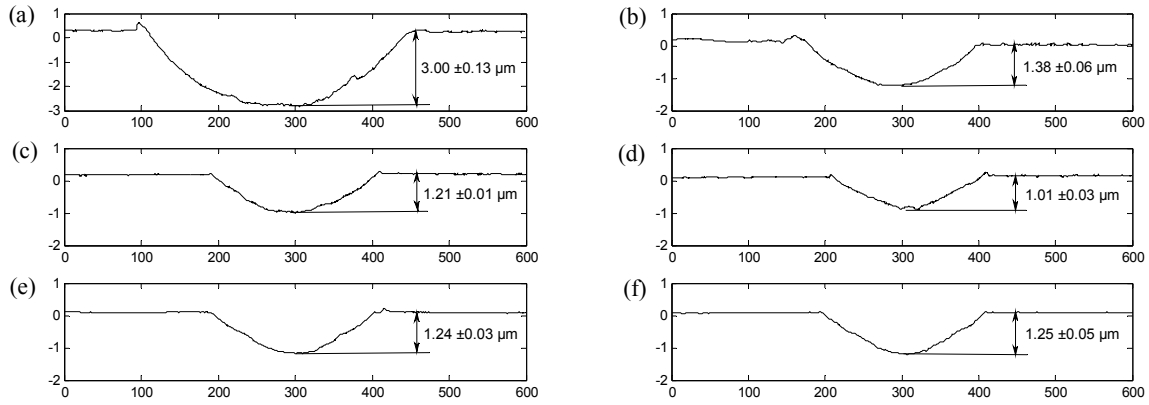

Figure 4.10: Wear scar profile perpendicular to sliding direction for 70% ULSD biased GTL/RME blends (a) D70G, (b) D70G25R, (c) D70G20R, (d) D70G15R, (e) D70G10R and (f) D70G5R.

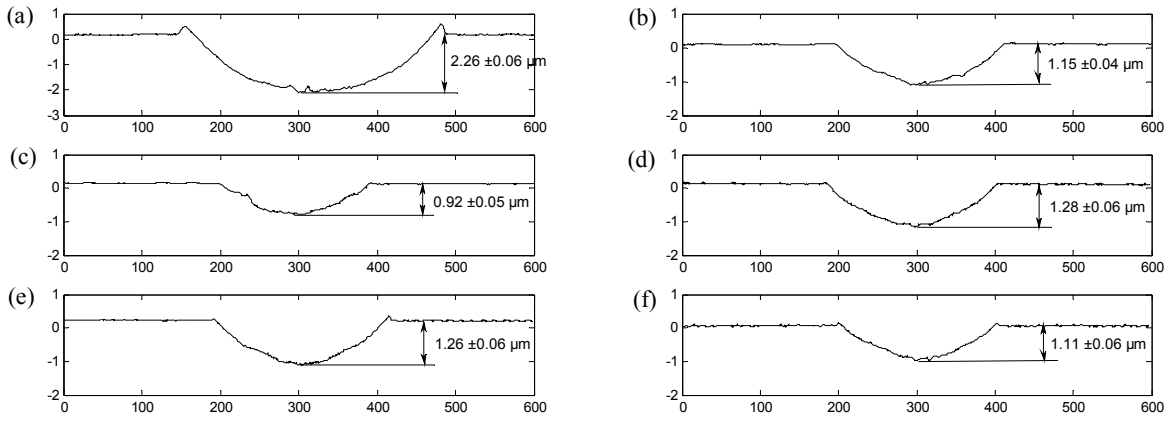

Figure 4.11: Wear scar profile perpendicular to sliding direction for 70% GTL biased ULSD/RME blends (a) G70D, (b) G70D25R, (c) G70D20R, (d) G70D15R, (e) G70D10R and (f) G70D5R.

4.3 Microscopic topography

The microscopic images of the surface of the lower specimens from the base fuel tests are shown in Figure 4.12. These confirm the measurements shown in Figure 4.9, with heavy deposits found on the specimens from the ULSD and RME tests. The characteristics of the residue for each fuel however, are quite different and are likely to be a consequence of the chemical composition of each fuel, which in the case of the RME is dependent on the feedstock from which it is derived. The SEM images for the GTL specimen shows a smooth and residue free surface, despite GTL containing hydrocarbons in the very close volumetric percentage compared to ULSD. This result is in agreement with results in Lacey et al. (2010).

Fuel blends, particularly those containing RME displayed an increase in residue. For example, the D70G20R blend, shown in Figure 4.12d, increased deposits significantly when compared to base ULSD and RME. Furthermore, this increase in residue was also noted on the

specimen from the optimum proportion of the three-way blended fuel, shown in Figure 4.12e. Residues were reduced when ULSD was blended with GTL, shown in Figure 4.13, this despite there being no great effect overall on the lubricity of this blend.

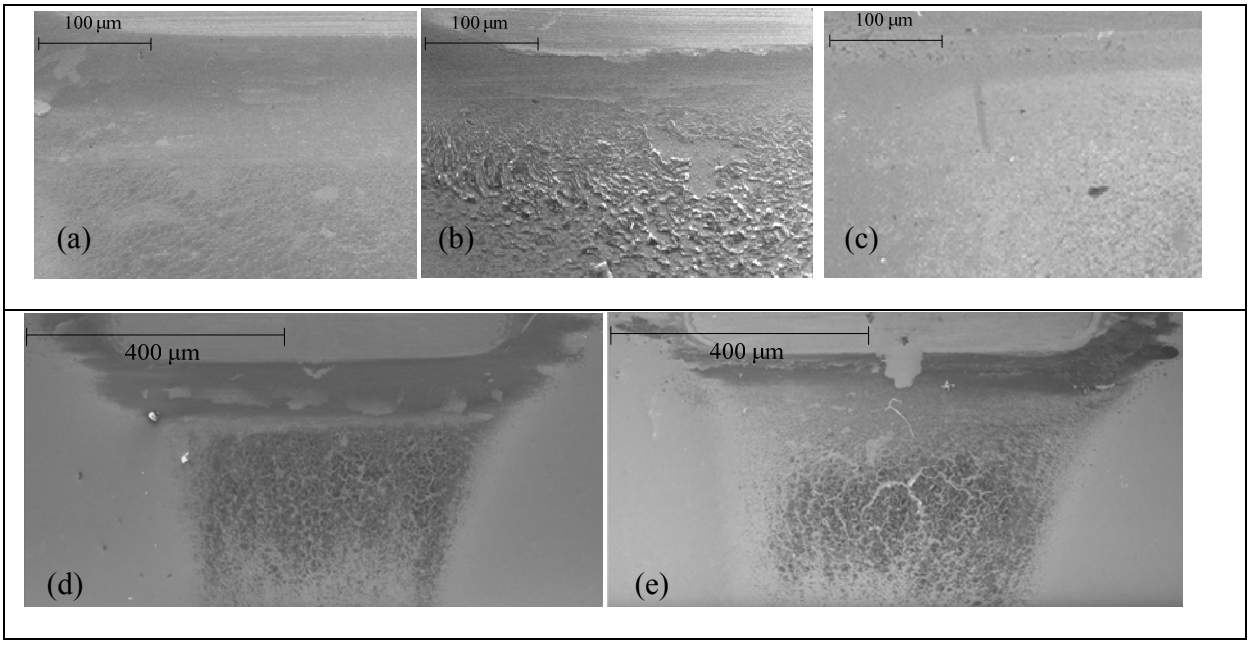

Figure 4.12: Microscopic images obtained from the SEM (a) ULSD, (b) RME, (c) GTL, (d) D70G20R and (e) G70D20R

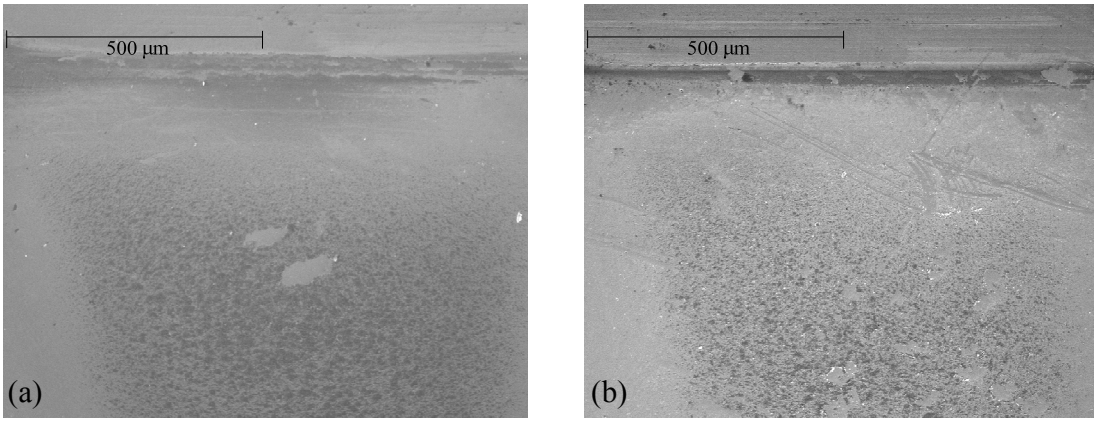

Figure 4.13: Microscopic images of GTL blended with ULSD (a) D90G and (b) D70G

To clarify the chemical composition of the residues on the specimen surfaces, energy dispersive spectroscopy was employed to analyse the area shown in Table 4.1 (an area encompassing the junction between worn and unworn areas). An unused lower specimen was analysed before studying the effect of fuel lubricity on the worn surface. The EDS reported that the main chemical composition of almost all the black residues on the test disc was carbon as shown in Table 4.1. The excessive carbon formation in the RME and ULSD tests is likely to be a result of the heat generated during the rubbing between the specimen surfaces. This is likely to accelerate the adsorption process from the hydrocarbon reaction resulting in the carbon formation. The formations of waxy carbon and dry carbon were found on the worn surfaces under the lubrication of RME and ULSD respectively. The maximum amount of carbon content on the surface was found in the ULSD test specimen. Conversely, GTL achieved the minimum amount with a mass percentage of carbon of less than half that of the ULSD test. Furthermore, a decrease in amount of carbonaceous deposits on the test specimen by 40% can be observed when 10% (v/v) of GTL was added to ULSD.

Table 4.1: Carbon content (% wt) on the worn surface

ULSD	RME	GTL	D90G	D70G	D70G20R	G70D20R
19.82	13.07	7.94	12.64	11.30	16.09	12.80

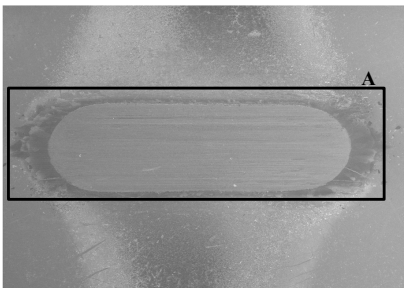

4.4 Summary

A comparative study on lubricating properties of current and future biofuels blended with ULSD has been conducted. The conclusions can be summarized as followed.

(1) The use of RME provides a very effective means of improving the lubricating properties of fuel blends. This is likely to be a consequence of the oxygen-containing compounds from the mixture of several fatty acids. This is further compounded by the adsorption of the compounds on to the friction surfaces, increasing the stability and thickness of the lubricating film. The optimum proportion of RME to restore the acceptable levels of lubricity for the duel blends was 10% (v/v).

(2) For tri-blend fuels the optimum combination for minimum effect on lubricity was G70D20R. The D70G15R blend, identified by Rounce et al. [23] as having combustion characteristics that closely match ULSD, also displayed very good lubricity.

(3) Despite having similar levels of percentage hydrocarbons and similar lubricity levels, GTL produced far less deposits than the ULSD. Carbonaceous deposits in tests based on ULSD decreased by approximately 40% when 10% of GTL was added. However this had very little effect on lubricity.

(4) The different feedstock used to produce the diesel fuel led to a difference in carbon deposit formation, observed in the character of carbon formation obtained from ULSD and RME tests.

(5) The trade-off between improved lubricating properties (from the use of RME) and a reduction in carbonaceous deposits (with blended GTL) may be important. This will be the case particularly if conventional diesel substitution targets are to be met with biofuels replacements.

CHAPTER 5

THE EFFECT OF THE ADDITION OF INDIVIDUAL METHYL ESTERS ON THE COMBUSTION AND EMISSIONS OF ETHANOL AND BUTANOL-DIESEL BLENDS

Biodiesel fuel is known to improve the properties of alcohol-diesel blends (e.g. stability, viscosity, lubricity) for use in compression ignition engines. In this work the effects on combustion characteristics and emissions of preselected methyl esters have been assessed. The most representative individual fatty acid methyl esters (methyl esters of lauric acid, myristic acid, palmitic acid, stearic acid, and oleic acid) were added to alcohol blends in order to understand the effect of carbon chain length and degree of unsaturation on combustion and emissions. The effects of alcohol addition on the properties of fuel blends were also investigated using ethanol and butanol. Relating to the physical properties, emphasis was given to both stability and lubricity of alcohol-diesel blends. The engine operating condition used in all the tests was 1500 rpm engine speed and 3 bar IMEP. In order to study the effect of EGR three different conditions were analysed (0%, 10 and 20% EGR).

5.1 Blend stability

Fuel blend stability tests were made in order to evaluate if phase separation of the fuel blends occurred. Ethanol-diesel (e-diesel) blends were mixed with methyl esters to establish levels of FAMEs at which phase separation occurred. The study was carried out using 0, 5, 10, 15, 20, 25 and 30% of ethanol and FAMEs by volume in diesel fuel. The blended fuels were

maintained in a temperature controlled atmosphere at 10 ºC and the stability was checked every two hours for the first 24 hours, and every day thereafter for one month. The results showed that a blend fraction of 15% methyl esters was enough to avoid phase separation of e-diesel blend at every percentage of ethanol used. In the case of 15% or higher (by volume) methyl palmitate (C16:0) and methyl stearate (C18:0) (i.e. with melting points that are higher than 30 ºC), solid phase separation was seen. The time required for the onset of the solid phase depended on the percentage of these methyl esters in the blends. However, butanol-diesel (but-diesel) blends were stable independently of butanol and methyl ester concentration. This behaviour is in agreement with that observed by other authors (Mehta et al., 2010). Two alcohol-diesel blends (10% of ethanol and 16% of butanol) were selected for the study of the lubrication properties, combustion and emissions.

5.2 Lubricity

Ethanol and butanol blends contained the same oxygen content and 15% of methyl esters was added to both to ensure their stability. The results of lubricity tests are shown in Figure 5.1. The corrected wear scar diameters of all fuels blended with FAMEs are below the limitation required by EN 590 and lower than those corresponding to e-diesel and but-diesel blends without the addition of FAMEs. The beneficial effect of FAMEs on lubricity is evident. In general, the longer the carbon chain length, the smaller the wear scar diameter (better lubricity). This trend is also seen in the incremental viscosity as the chain length increases. The mixture of several fatty acids contained in RME showed better lubricity in the fuel blends than the individual fatty acid esters. Regarding the unsaturation effect, FAMEs with double bonds have better lubricating properties than similar chain lengths without unsaturations.

The lubricity of pure alcohols increases with molecular weight (Lapuerta et al., 2010b), however the lubricating properties of the but-diesel blended with FAMEs decreased and were lower than the e-diesel blend. This is most likely due to the evaporation of ethanol from the e-diesel blends, which would allow more fatty acid moieties to be adsorbed onto rubbing surfaces (which are beneficial to the formation of boundary lubrication conditions).

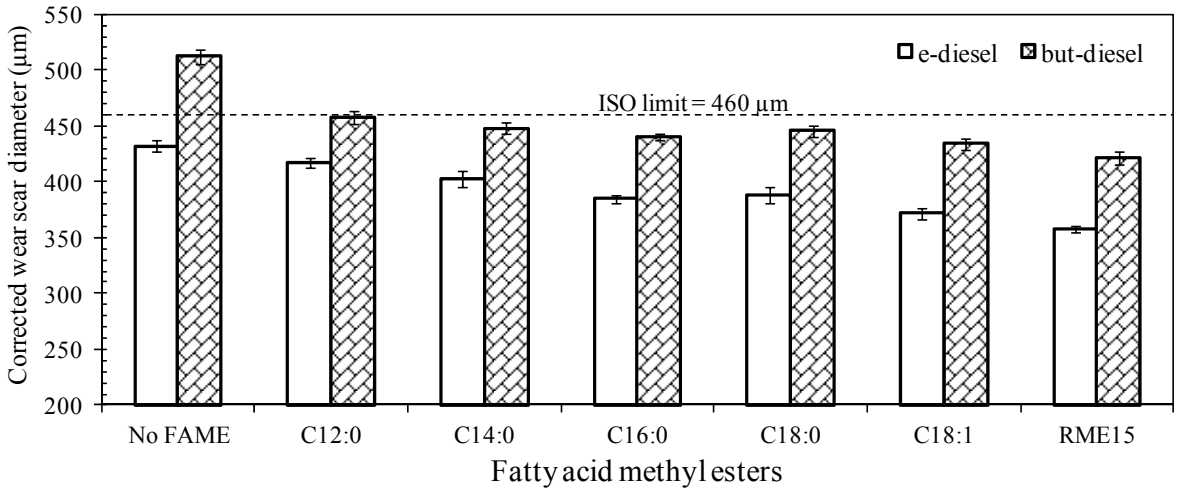

Figure 5.1: Corrected wear scar diameter of e-diesel and but-diesel blended with 15% of methyl esters

To clarify this hypothesis, a Philips XL-30 scanning electron microscope (SEM) was employed to investigate the microscopic topography of the worn surfaces. The microscopic images (Figure 5.2) show that the black residue found on the surface of the lower specimens under lubrication of 10% ethanol blended with diesel (E10D) is larger than that of 16% butanol blended with diesel (B16D). The main chemical composition of almost all the black residues on the test disc was carbon. Carbon formation is a result of the heat generated during fretting

between the specimen surfaces which leads to acceleration of the adsorption process from the chemical reactions of the hydrocarbons in the fuels. The evidence of larger carbonaceous deposits confirms that more molecules of fuel possessing good lubricating properties in the ethanol blends were adsorbed onto the worn surfaces compared to that of butanol blends. This results in the increase of lubricity due to stronger lubrication film formed (Sukjit and Dearn, 2011). This effect is clearer when RME containing polar- compounds was blended with alcohol-diesel blends. Much higher carbon formations were observed on the specimens lubricated with 15% RME with e-diesel (E10R15D) than those lubricated 15% RME and 16% butanol blended with diesel (B16R15D).

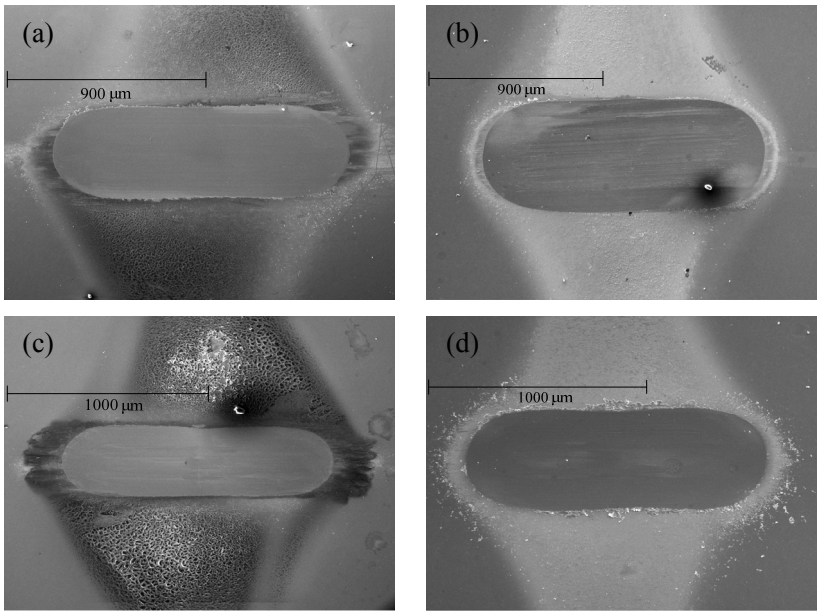

Figure 5.2: Microscopic images obtained from the SEM: (a) E10D, (b) B16D, (c) E10R15D and (d) B16R15D

5.3 Combustion

The in-cylinder pressure and rate of heat release (ROHR) versus crank angle degree (CAD) for base fuels and alcohol blends are shown in Figures 5.3-5.5. The use of RME resulted in an increased rate of the fuel burnt in the premixed phase with the combustion advanced to earlier crank angle positions and the peak pressure value increased over ULSD combustion. This is likely to be a consequence of the compressibility of biodiesel fuel which is lower than that of ULSD resulting in the advance of the start of injection, while cetane number of RME and ULSD are similar. In addition the oxygen content of RME may also contribute to improve fuel oxidation and reduce the ignition delay.

An increase of fatty acid chain length shows a slight increase in the peak cylinder pressure and an advance in the start of combustion (Figure 5.3). This is thought to be due to an increased cetane number as the chain length increases. The higher bulk modulus of longer chain methyl esters also increases the rate of injection pressure rise with respect to shorter chain length methyl esters (resulting in an advance of injection). A slight increase in the peak of the premixed combustion and an advance in the start of combustion were observed with an increase in unsaturation degree (Figure 5.4). This may be attributed to the higher bulk modulus of unsaturated methyl esters which show a stronger effect than an increase in ignition delay resulting from a decreased cetane number.

To study the effect of alcohol addition on combustion and emissions, the three fuel blends tested were R45D, E10R15D and B16R15D maintaining the same oxygen mass fraction (Figure 5.5). A significant delay in the start of combustion was found after the addition of alcohol. This

can be attributed to the lower cetane number of the fuel blends increasing the premixed combustion peak due to the longer ignition delay. This also led to a slightly higher peak pressure compared to that of the R45D blend. Butanol blends showed closer combustion characteristics with respect to R45D blend mainly as a consequence of the higher cetane number and bulk modulus with respect to ethanol blends. It can be observed that the recirculation of the engine exhaust (i.e. use of EGR) retarded the start of combustion because less air was used in the combustion process. This effect is clearer when ethanol was studied. Although the combustion of the alcohol fuel blends provoked an increase in brake specific fuel consumption as a result of their lower heating, both showed similar brake thermal efficiency with respect to biodiesel and diesel fuels.

5.4 THC emissions

The THC emissions are shown in Figure 5.6. It can be seen that THC of RME are lower than ULSD for both engine conditions at 0 and 20% EGR. This decrease is because of the oxygen content of biodiesel which makes the combustion more complete (Lapuerta et al., 2008b, Rakopoulos et al., 2004, Tsolakis et al., 2007). The advanced start of combustion with RME increases the available time for the hydrocarbon emissions oxidation. An increase in chain length leads to an increase in THC because of a reduction in the oxygen content and increase in viscosity. This increase in viscosity results in a worse atomisation and vaporisation of the fuel leading to more incomplete fuel combustion (Tzanetakis et al., 2011). An increase in unsaturation degree results in a decrease of THC, mainly due to the lower viscosity of unsaturated methyl esters. It is believed that the effect of viscosity is especially important in this type of engine which uses low boost and injection pressures.

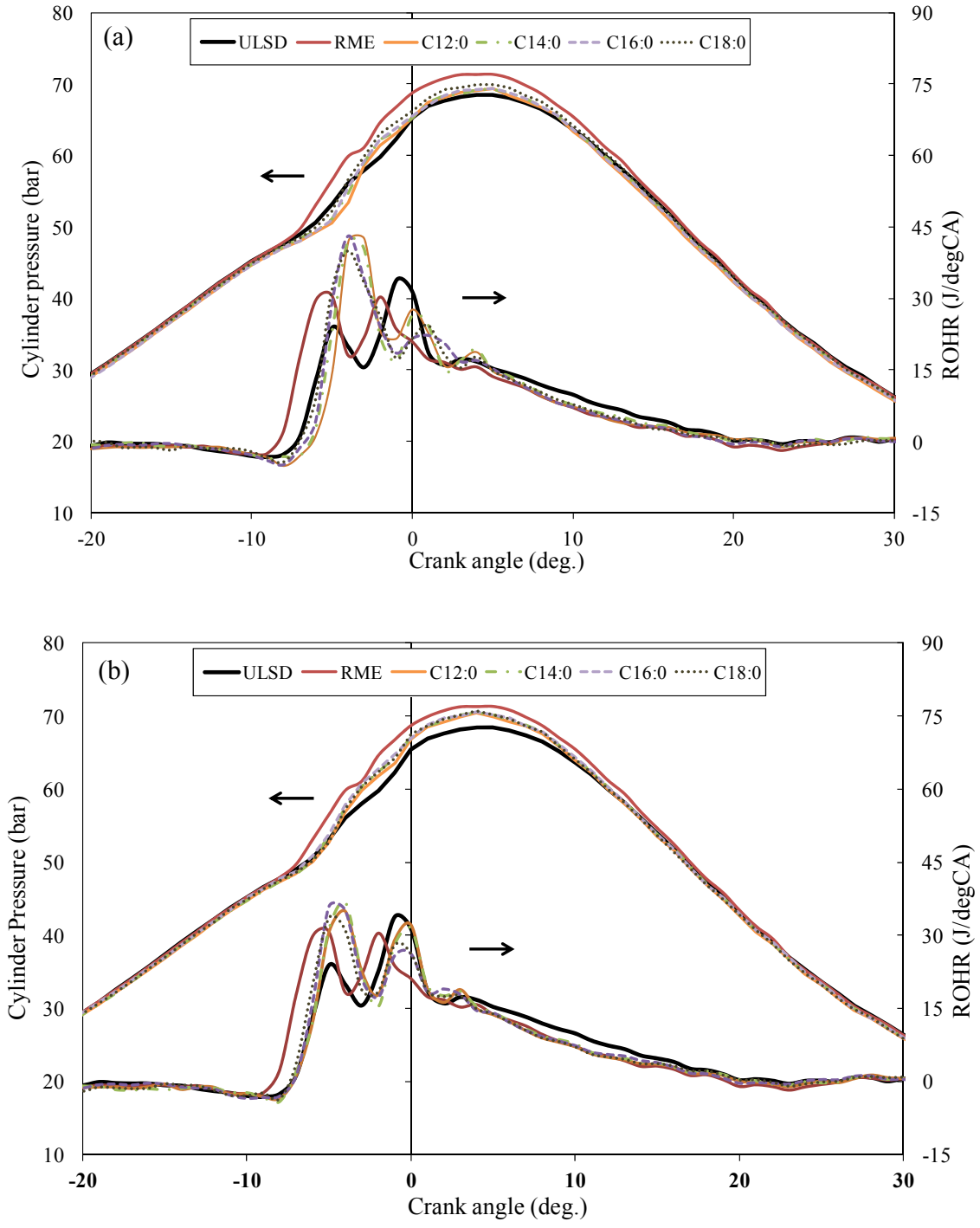

Figure 5.3: In-cylinder pressure and rate of heat release for methyl esters blended with alcohols (Chain length effect); (a) ethanol blends and (b) butanol blends

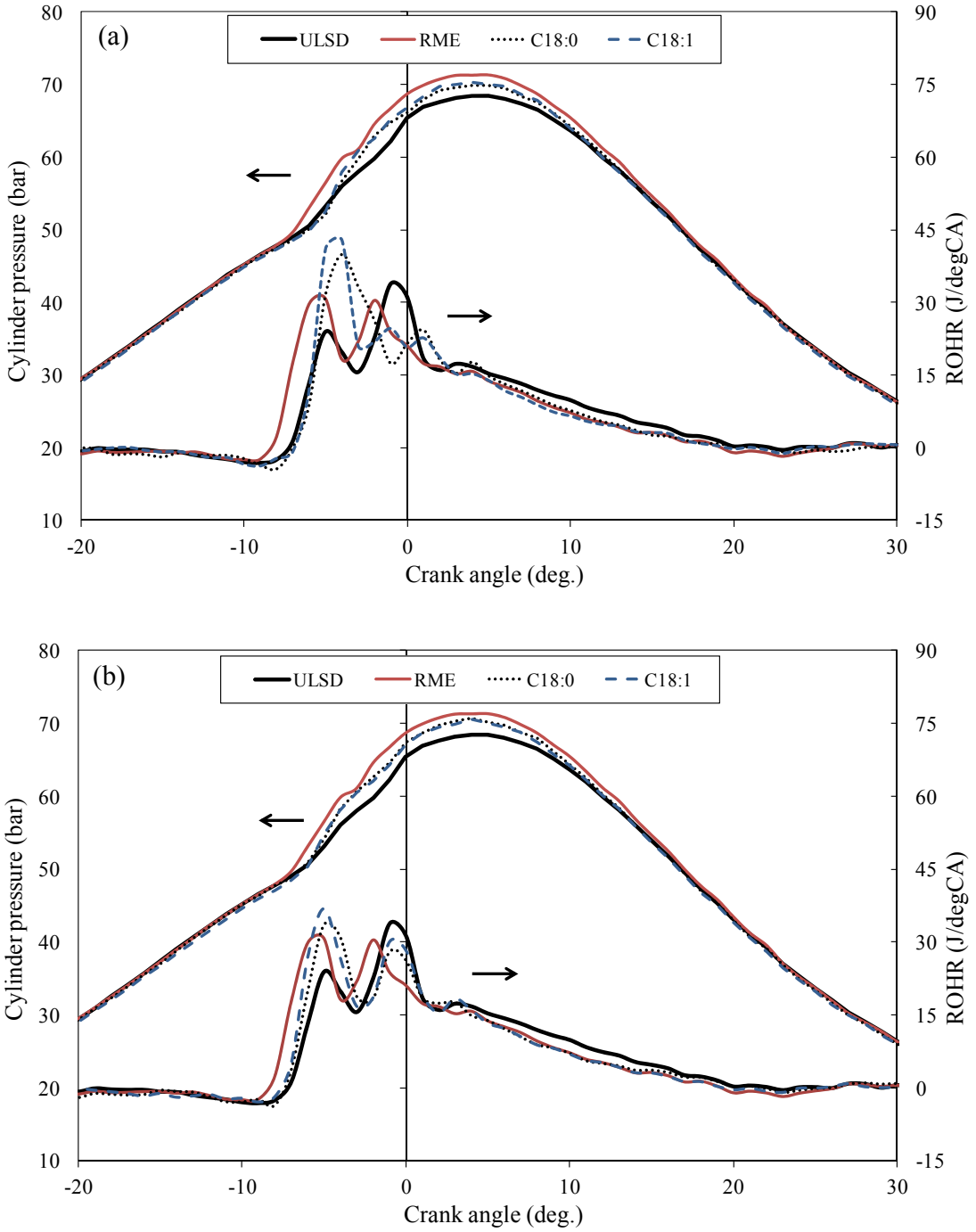

Figure 5.4: In-cylinder pressure and rate of heat release for methyl esters blended with alcohols (Unsaturation degree effect); (a) ethanol blends and (b) butanol blends

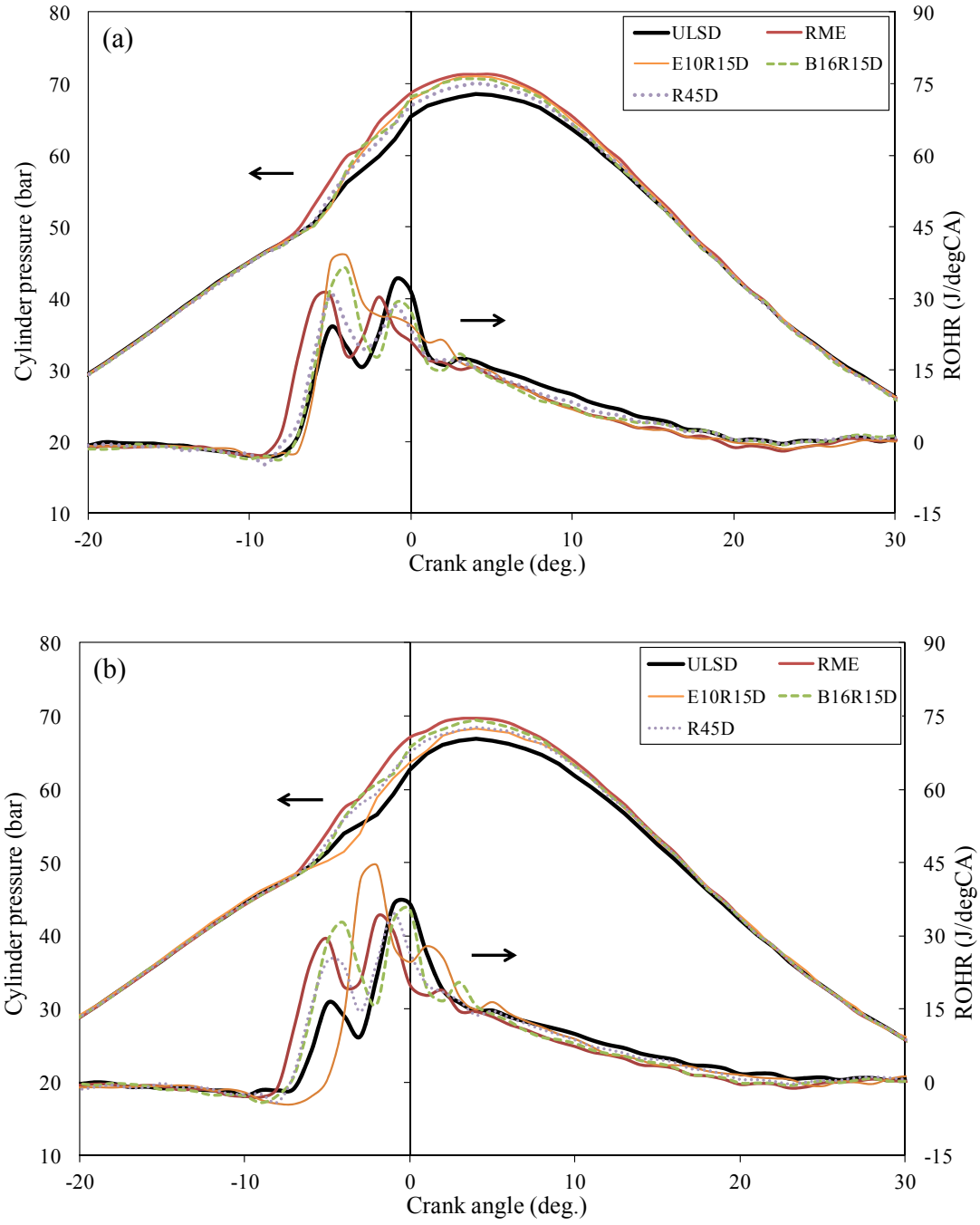

Figure 5.5: In-cylinder pressure and rate of heat release for alcohol addition to RME-ULSD blends; (a) 0% EGR and (b) 20% EGR

Comparing the alcohol blends to R45D, it is observed that THC emissions for both ethanol and butanol blends are higher than the R45D with the same oxygen content. This increase in THC emissions is also obtained for alcohols addition to the different methyl ester-ULSD blends. This means that alcohol addition produces higher THC emissions, mainly due to heat of vaporisation of alcohols, as it is obtained by others especially in low load engine conditions (Kass et al., 2001, Lapuerta et al., 2008a, Rakopoulos et al., 2010). The higher heat of vaporisation of alcohols results in incomplete combustion. This effect is more influential at low load conditions because the combustion temperature is itself lower than at high load. THC obtained with ethanol blends are higher than those obtained with butanol blends for the methyl ester addition. This result can be explained because of the higher heat of vaporisation of ethanol, which reduces the temperature more than in the case of butanol blends.

EGR addition produces higher THC emissions for all the blends, in agreement with previous study (Rounce et al., 2009), and the trends which have been previously discussed about chain length, unsaturation degree and alcohol effect can be also applied to the 20% EGR engine operating condition.

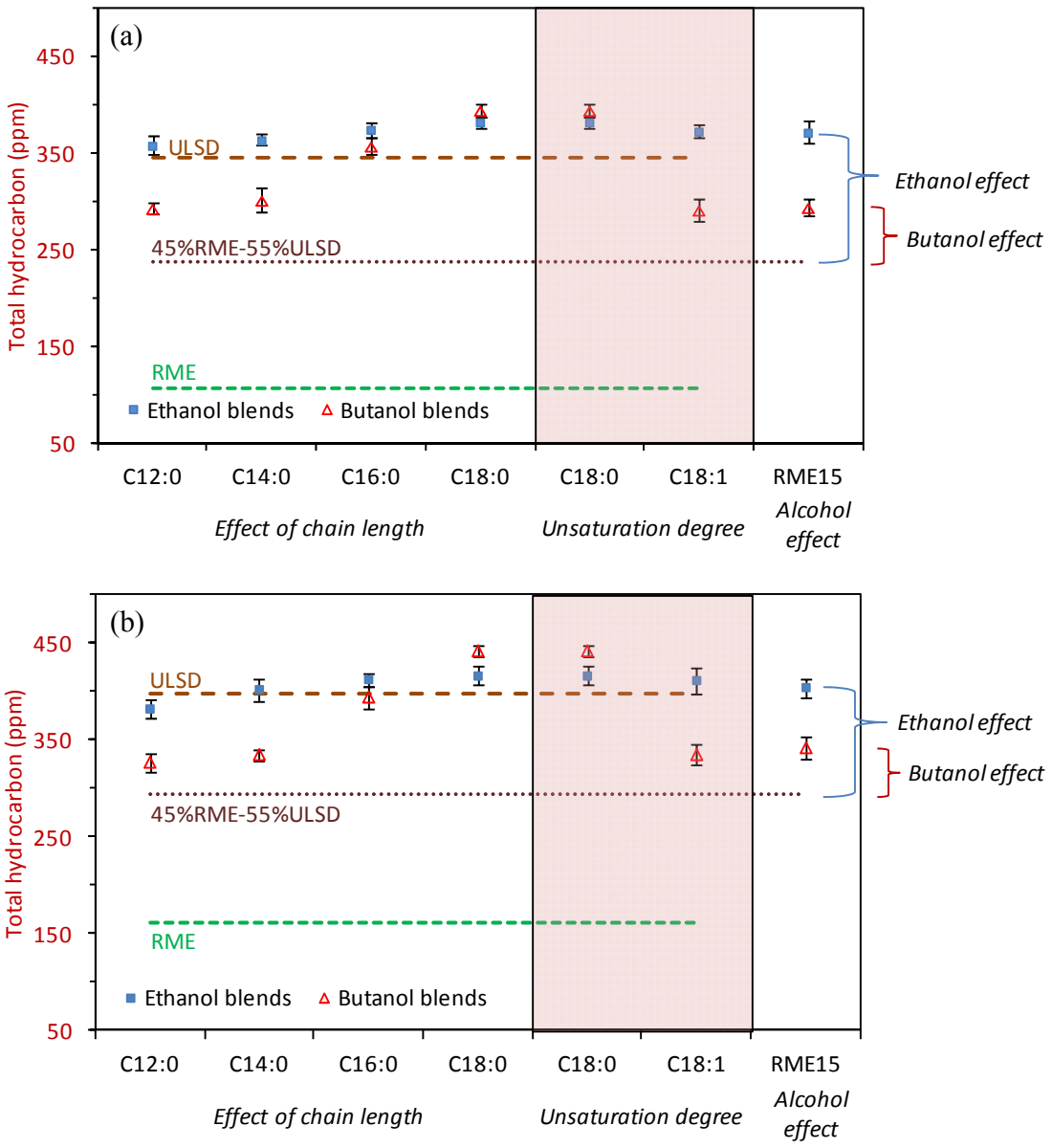

Figure 5.6: Effect of carbon chain length and unsaturation degree of methyl esters and alcohol addition on total hydrocarbons (THC); (a) 0% EGR and (b) 20% EGR

5.5 CO emissions

CO emissions of RME are lower than ULSD for both engine conditions (0 and 20% EGR), as it is shown in Figure 5.7. This decrease is mainly due to the oxygen content of biodiesel which makes the combustion more complete (Lapuerta et al., 2008b, Rakopoulos et al., 2004, Tsolakis et al., 2007). An increase in chain length leads to an increase in CO emissions as a result of the decrease in the blend oxygen content. On the other hand, an increase in unsaturation degree results in a decrease of CO. This is mainly due to the lower viscosity of unsaturated methyl esters which results in better atomisation and vaporisation of fuel leading to more complete fuel combustion. In contrast to THC for alcohol addition to RME-ULSD blend, CO emissions are lower for the alcohol blends at the same oxygen content. This benefit in CO emissions using alcohols blends could be due to the lower C/H ratio of alcohols compared to RME. It is suggested that this effect compensates for the potential increase in CO with alcohols blends due to the higher heat of vaporisation and as a consequence of reducing the in-cylinder temperatures. For the reference engine operating condition (0% EGR) this trend is obtained for all the methyl ester-ULSD blends. The alcohols, by comparison display higher CO emissions with ethanol than the butanol blend according to the higher heat of vaporisation of ethanol. When EGR is added, CO emissions increased for all the blends (Abu-Jrai et al., 2009). The trends related to methyl ester addition and alcohol effects are similar to those previously explained for the reference engine condition, except in the case of C18:0. CO emissions for the ethanol-C18:0-ULSD blend is higher than in the case of RME-ULSD blend, mainly due to the higher viscosity of this methyl ester which produces more incomplete combustion, as was explained previously.

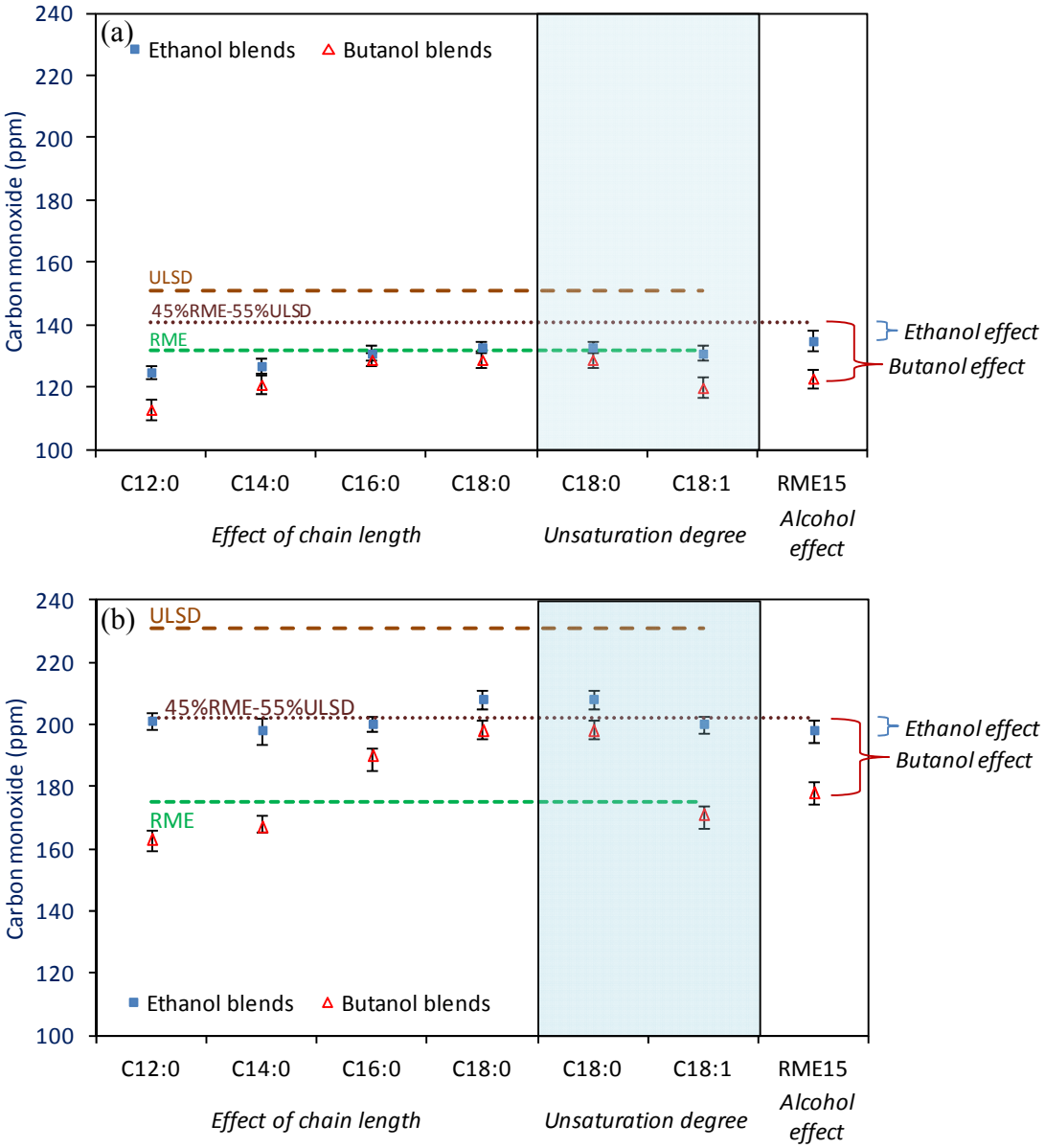

Figure 5.7: Effect of carbon chain length and unsaturation degree of methyl esters and alcohol addition on carbon monoxide (CO); (a) 0% EGR and (b) 20% EGR

5.6 NO_X emissions

NO_X emissions of RME are higher than ULSD for both engine conditions (0 and 20% EGR) as it is shown in Figure 5.8. This increase in NO_X emissions is due to several reasons. First

of all, the higher bulk modulus of biodiesel provokes an advance in injection timing and an advance in the start of combustion (see combustion plots), as a consequence NO_X emissions increases (Murillo et al., 2007). Also, the oxygen content of biodiesel can increase NO_x emissions (Bakeas et al., 2011). The increase in chain length does not produce a significant effect in NO_X emissions according to previous work (Pinzi et al., 2013). In this work, it is shown that there are different factors which result in similar NO_X emissions. The higher bulk modulus and higher adiabatic flame temperature tend to increase NO_X emissions, but these effects are compensated by the lower oxygen content and higher cetane number of the longer chain methyl esters. On the other hand, unsaturation degree produces a clear effect on NO_X emissions according to previous work (Knothe et al., 2006, Schönborn et al., 2009). This trend is mainly explained by the increase in bulk modulus and decrease in cetane number which provokes more premixed combustion and higher NO_X emissions when unsaturation degree increases. The alcohol effect in NO_X emissions is different for ethanol and butanol blends. Firstly, the low cetane number of alcohol blends tend to increase ignition delay and premixed combustion (see combustion plots) which results in higher local temperatures in the combustion chamber and higher NO_X emissions. On the other hand, the higher heat of vaporisation of alcohols compared to ULSD reduces the temperature in the cylinder, resulting in lower NO_X emissions (Ishida et al., 2010). In the case of ethanol, the heat of vaporization effect is more significant than that of the cetane number explaining the NO_X benefit with ethanol addition to ULSD-biodiesel blends. However, in the case of butanol, NO_X emissions are higher than in the case of RME-ULSD blends and higher than with ethanol blends with the same oxygen content. This difference is due to the lower heat of vaporisation of butanol which is not high enough to compensate for the cetane number effect. The effect of EGR addition produces lower NO_X emissions for all the blends (Lapuerta et al., 2008b). As in the rest of

gaseous emissions, the trends about the chain length, unsaturation degree and alcohol effect are similar with and without EGR.

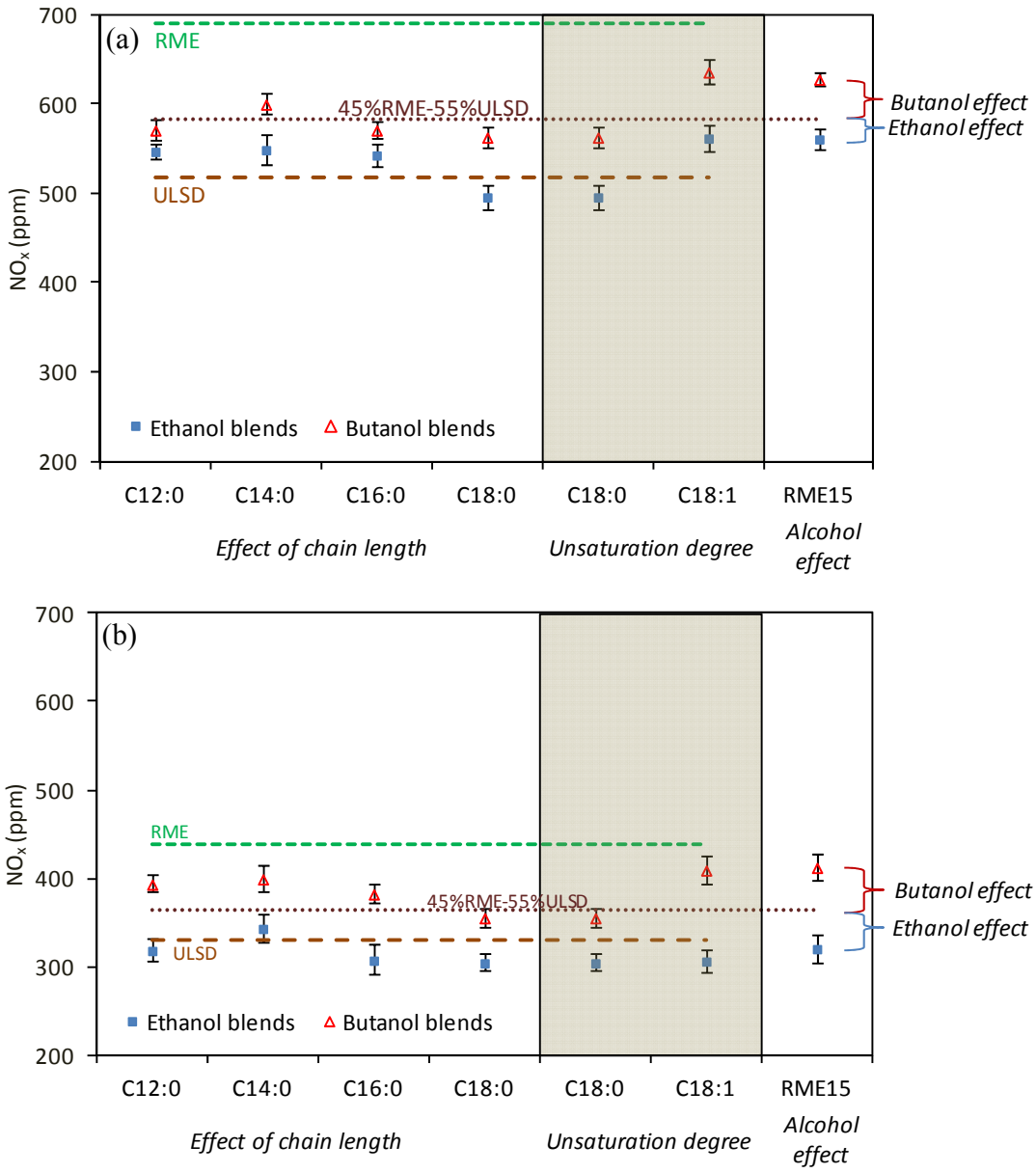

Figure 5.8: Effect of carbon chain length and unsaturation degree of methyl esters and alcohol addition on nitrogen oxide (NO_X); (a) 0% EGR and (b) 20% EGR

5.7 Soot emissions

Soot emissions of RME are significantly lower than ULSD for both engine conditions. This decrease in soot emissions is mainly due to the oxygen content and the absence of aromatic compounds (Lapuerta et al., 2008b) in biodiesel (Figure 5.9). The increase in chain length of the fuel produces an increase in soot emissions (Pinzi et al., 2013). This is due to the lower oxygen content of methyl esters when chain length increases. Additionally, the increase in viscosity and melting point, particularly for C16:0 and C18:0 makes fuel atomisation and evaporation in the cylinder more difficult favouring soot formation. The increase in the number of double bonds results in lower viscosity and lower melting point which favours the atomisation and evaporation processes, resulting in lower soot emissions. The soot emissions for the alcohol blends are significantly lower than those obtained with the RME-ULSD blend with the same oxygen content. This reflects the higher potential of alcohol fuels to reduce soot emissions with respect to the ester group, as it is reported by other authors (Lapuerta et al., 2009a). This is due to the different structure of the fuel molecules (Cheng et al., 2002, Pepiot-Desjardins et al., 2008). In the case of esters, one atom of carbon is attached to two atoms of oxygen, while in the case of alcohols one atom of oxygen is attached to one atom of carbon. Therefore, it is thought that the only atom of oxygen of alcohol is more effective to inhibit soot formation than the two atoms of oxygen of the esters (Westbrook et al., 2006). Regarding the comparison of alcohols to the baseline operating condition (0% EGR), soot reductions for both alcohols are similar or slightly higher in the case of butanol. The trends related to the effect of chain length and unsaturation degree are similar for both engine operating conditions, obtaining higher soot emissions in the

case of higher EGR. The influence of the alcohol fuels used on soot emissions is significant when EGR is applied; this reduction in soot emissions was more evidenced in the case of butanol.

Despite the lower viscosity and lower C/H and C/O ratios of pure ethanol with respect to pure butanol, soot emissions using butanol blends are lower than those using ethanol blends. This may be due to the following:

- The higher heat of vaporisation of ethanol blends lowers in-cylinder temperatures and diminishes soot oxidation. This effect is important in low load conditions and EGR application when heat is absorbed by CO_2, H_2O (main components of EGR). Ethanol in the vaporisation process is also enough to decrease in-cylinder temperatures to certain levels where soot oxidation is not favoured. (lower soot oxidation with ethanol).
- The poor cetane number of ethanol together with EGR addition retards the start of combustion (see combustion figures). This results in lower available time for soot oxidation, making soot emissions for ethanol higher than for butanol. (lower soot oxidation with ethanol).

5.8 Particle size distribution

It can be seen that the number concentration of particulate matter from biodiesel are significantly lower and these particles have a smaller mean diameter than in case of the particles emitted using ULSD (Figure 5.10). This is mainly due to the presence of oxygen in RME which produces more complete combustion resulting in a lower formation rate of particulate matter and therefore a lower possibility of collisions between carbon particles resulting in smaller carbon agglomerates (Lapuerta et al., 2008c). In addition, the fuel-born oxygen participates in the

oxidation of any newly formed particulate reducing its size. The effect of oxygen content on particle size distribution is more obvious when the carbon chain length effect in the methyl esters was investigated (Figure 5.10). As oxygen content decreases, chain length and the number of particles increases. Although the existence of oxygen in the fuel plays an important role in soot formation and oxidation, other fuel properties such as viscosity, boiling and melting point affecting spray properties can influence particulate matter formation. Considering the effect of unsaturation degree (Figure 5.11), only a slight change in oxygen content and boiling point can be found and the difference in viscosity and melting point explains the soot formation trend. Higher viscosity and melting point as the unsaturation degree decreases can increase the probability of soot or volatile matter formation through the hydrocarbons which are not able to vaporise resulting in an increased number of particles. Total and mean particle number diameters are shown in Figure 5.12. The short carbon chain and highly unsaturated degree methyl esters decrease the total number of particulate matter. On the other hand, there were no significant differences in mean particle diameter when the effects of chain length and unsaturation degree of methyl esters were studied.

Comparing the fuel blends with the same oxygen content, the use of alcohol is more effective in reducing the number of particulate matter than that of biodiesel blend, especially in the case of butanol. The same reasons previously explained in the soot section can be also applied to justify the trends found in particle size distributions. Besides that, the mean particle diameter of butanol blends was slightly smaller than that of ethanol blends (except C18:1 result). With no significant changes in the particle diameter the trend of total particle mass concentration (Figure 5.13) is similar to that of total particle number.

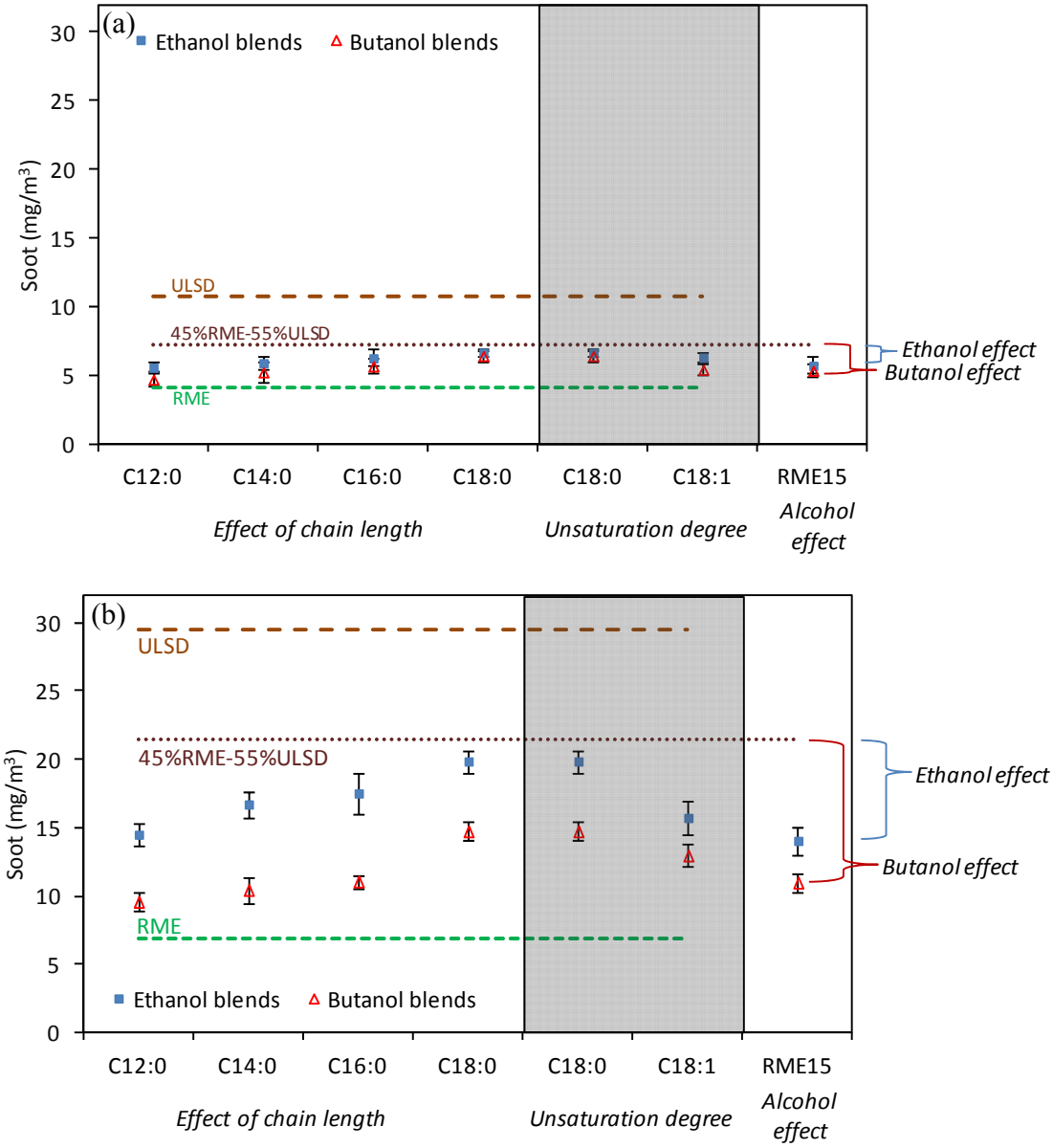

Figure 5.9: Effect of carbon chain length and unsaturation degree of methyl esters and alcohol addition on soot; (a) 0% EGR and (b) 20% EGR

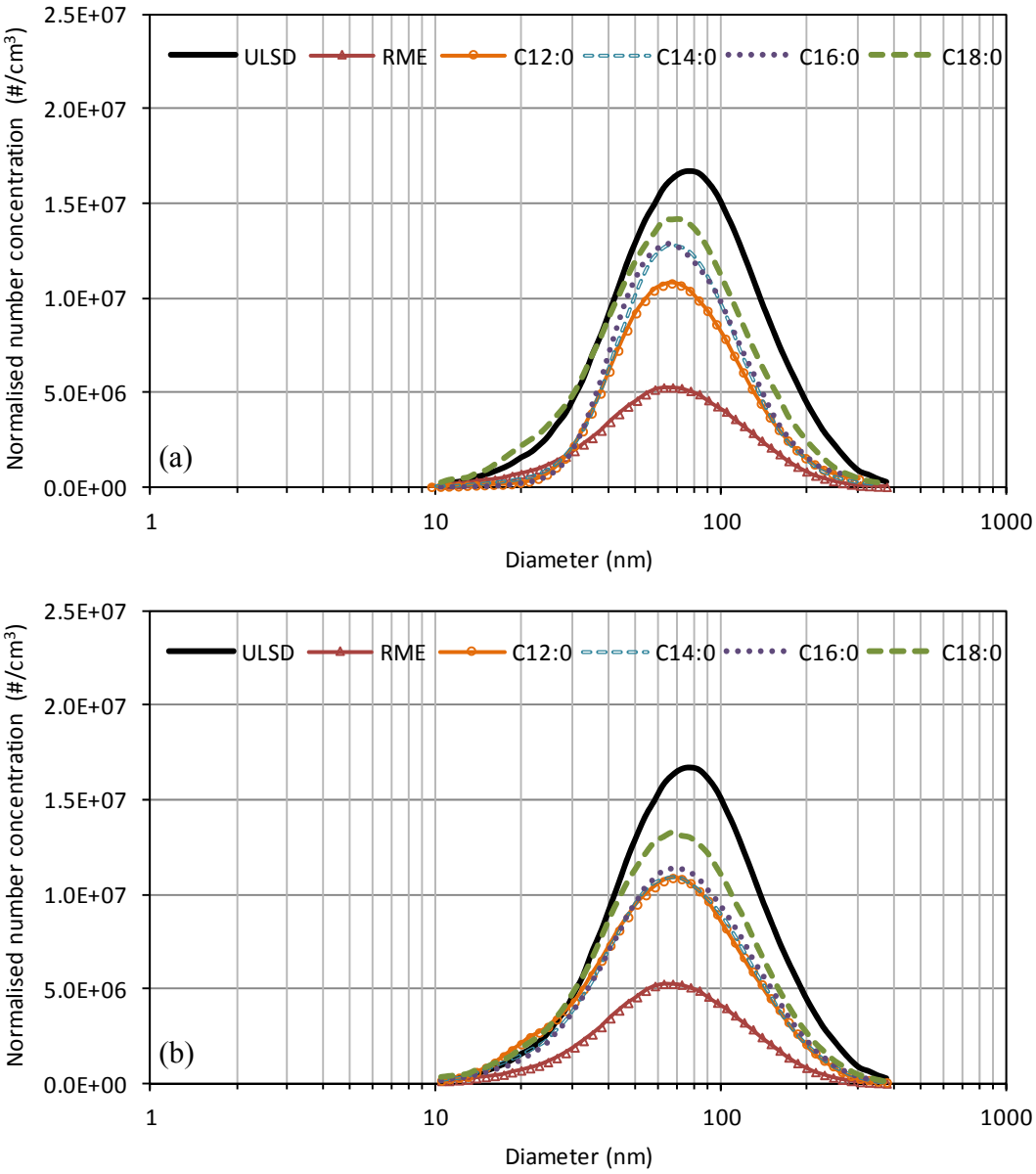

Figure 5.10: Effect of carbon chain length on particle number size distribution at baseline condition; (a) ethanol blends and (b) butanol blends

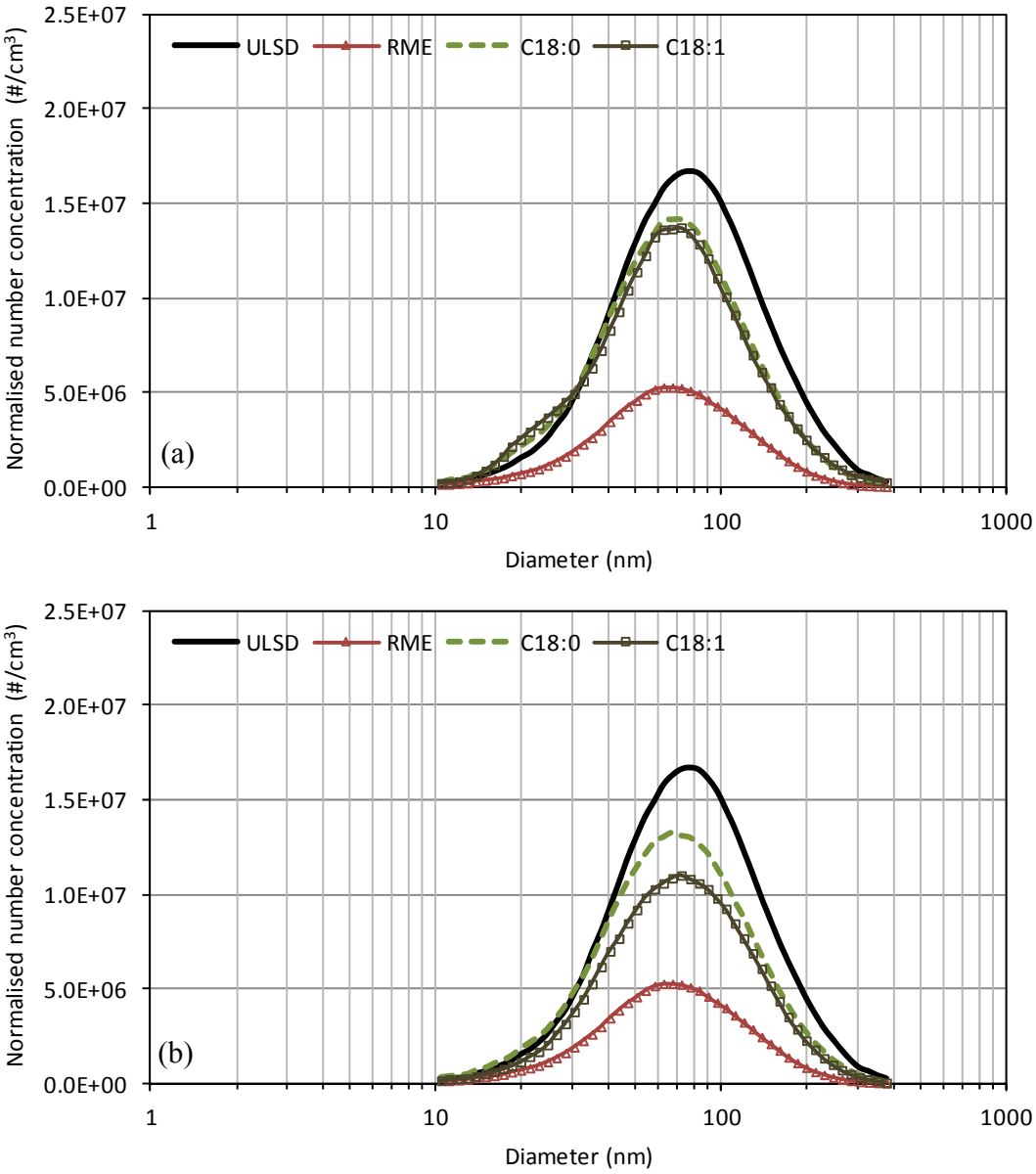

Figure 5.11: Effect of unsaturation degree on particle number size distribution at baseline condition; (a) ethanol blends and (b) butanol blends

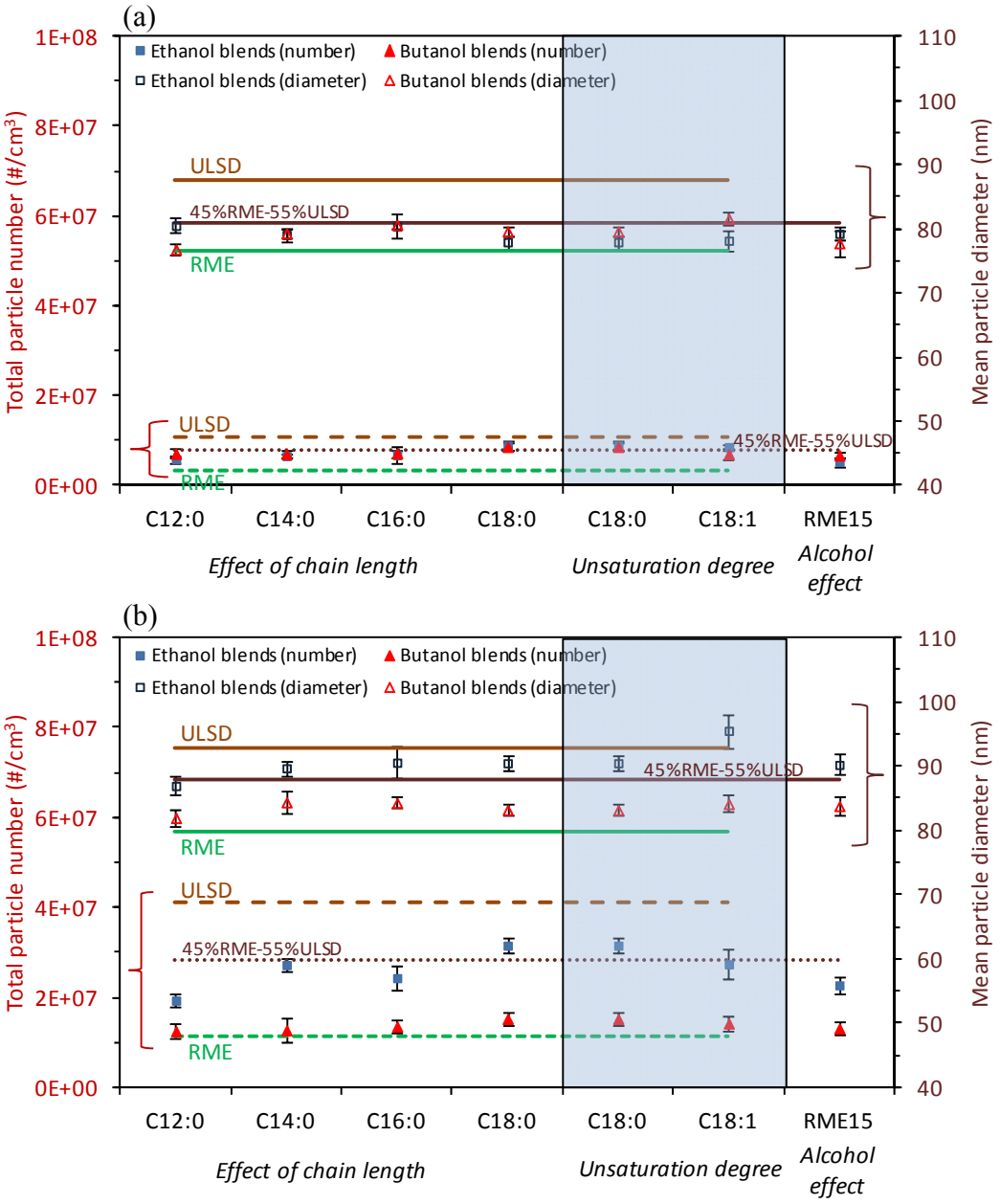

Figure 5.12: Effect of carbon chain length and unsaturation degree of methyl esters and alcohol addition on total particle number and mean particle diameter; (a) 0% EGR and (b) 20% EGR

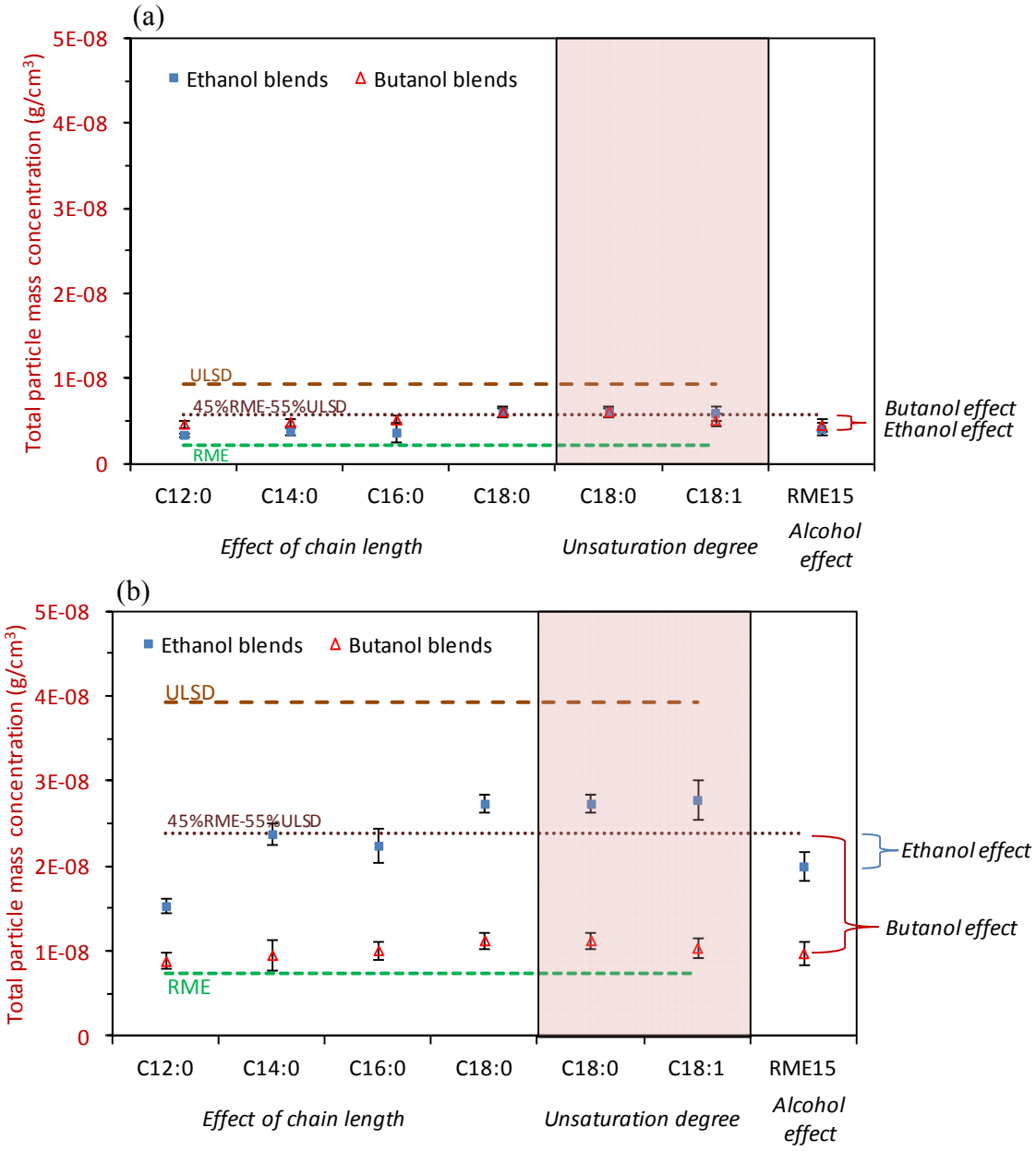

Figure 5.13: Effect of carbon chain length and unsaturation degree of methyl esters and alcohol addition on total particle mass concentration; (a) 0% EGR and (b) 20% EGR

It has to be noted that smaller particles are more difficult to trap, they have a longer residence time in the atmosphere and they are more reactive (higher surface by volume ratio). As a consequence, the emission of smaller particles provokes more harmful environmental and

health effects. Related to the results discussed here, it has to be clarified that the lower mean diameter corresponding to the particles emitted with the oxygenated fuels (R45D and alcohol blends) is not caused by an increase in the number of smaller particles but a significant reduction of the number of larger particles. Therefore, in Figure 5.10 and 5.11 it can be seen that the particle number concentration for the oxygenated blends are all reduced.

5.9 PM composition

Particulate matter is mainly composed of soot (analysed in previous section) and volatile or soluble organic material (VOM or SOM, depending on the method of characterisation). In the literature, instead of reporting the volatile or soluble organic material, the soluble or volatile organic fraction (SOF or VOF) is shown which represents the proportion of organic material which formed the particulate matter. In this case, data about soluble organic fraction are detailed (Figure 5.14) and analysed. SOF of RME is higher than in the case of the rest of fuels. This is a consequence of the lower volatility of biodiesel hydrocarbons which favours hydrocarbons adsorption and condensation onto soot particles, increasing the soluble organic material. Additionally, the reduction of soot with RME also increases the soluble organic fraction. It can be observed that SOF increases as carbon chain length is higher. This result is mainly due to an increase in soluble organic material, despite of the increase in soot. Higher soluble organic material can be justified by higher hydrocarbon concentration and lower volatility which make them easier to condense on the soot particles.

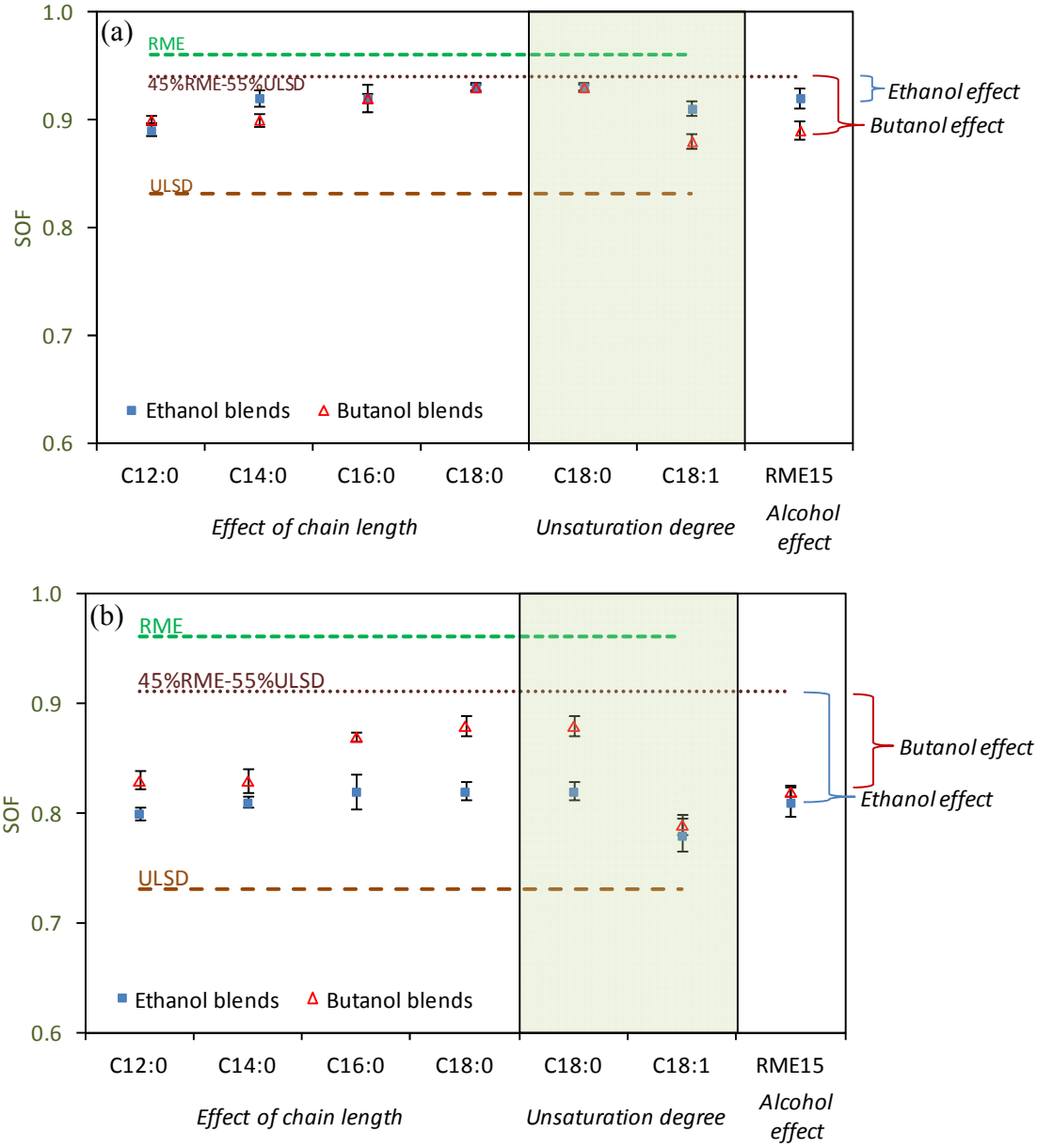

Figure 5.14: Effect of carbon chain length and unsaturation degree of methyl esters and alcohol addition on soluble organic fraction (SOF); (a) 0% EGR and (b) 20% EGR

The increase in unsaturation degree results in a reduction in SOF. The high melting point of C18:0 could be the reason to justify this trend. The soluble organic fraction of PM emitted using alcohol blends is lower than in the case of an RME-ULSD blend with the same oxygen content.

The reason to justify this trend is the lower volatility of the hydrocarbons emitted with the RME blend in comparison with the hydrocarbons emitted with alcohol blends. Therefore, the hydrocarbons in the case of RME blend are most likely to be adsorbed onto particulate matter, increasing the organic fraction of PM. As a summary, alcohol addition reduces soot (as is shown in previous section) and also reduces the soluble organic material adsorbed onto particulate matter. SOF differences with ethanol and butanol blends are not significant at the operating condition without EGR. However, when EGR is applied SOF emissions of butanol are significantly higher than those from ethanol blends, as there is no overlap in the confidence levels. The main reason to justify this trend is due to the higher soot reduction when butanol blends are used in comparison to ethanol blends (Figure 5.9). This soot reduction itself makes that the proportion of soluble organic material on particulate matter increases (SOF), even though the total organic material is similar. As it can be observed in Figure 5.14 these effects are clearer for the case of EGR.

5.10 NO_X–Soot trade-off

Soot and NO_X emissions are simultaneously shown for RME-ULSD blend, and ethanol and butanol blends with the same oxygen content for different EGR operating conditions (Figure 5.15). ULSD emissions with the different EGR rates are taken as the reference curve. As it can be seen, EGR addition decreases NO_X emissions, but increases soot (this is the well known NO_X-soot trade-off). In the case of R45D soot emissions are lower compared to ULSD, while NO_X emissions are higher at the same EGR rate, resulting in a curve which is slightly inside of the ULSD curve. This means that when soot emissions are equal to those obtained with ULSD, NO_X emissions are going to be lower for the RME blend or in other words, that when the same NO_X

emissions are obtained, soot emissions for the R45D blend are going to be lower than in the case of ULSD. Analysing the alcohols curves, it is clear that those are inside the R45D, which means that with the application of EGR it is possible to obtain further benefits in terms of soot and NO_X emissions with respect ULSD and R45D. Comparing between ethanol and butanol blends, the higher NO_X emissions in the case of butanol are compensated by the lower soot emissions at every EGR rate. This concludes that with the combination of butanol and low EGR rates can be obtained the same soot and NO_X benefits than in the case of ethanol. From Figure 5.15 it is also suggested that further EGR rates would result in a higher penalty in soot emissions than the benefit in NO_X emissions besides to higher CO and THC emissions.

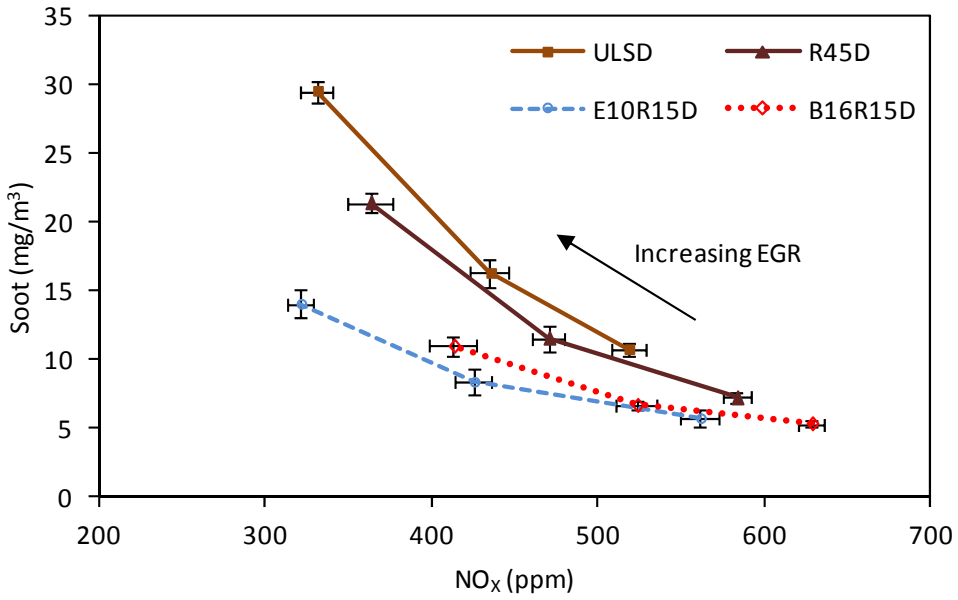

Figure 5.15: Trade-off between NO_X and soot emissions

5.11 Summary

The effect of molecular structure of the FAMEs on stability, lubricity, combustion characteristics and exhaust emissions of alcohol-diesel fuel blends was studied. The results show

that the presence of 15% of any methyl esters used in this study are enough to alleviate any stability and lubrication drawbacks that are associated with the blending of ethanol-diesel and butanol-diesel blends.

The study of carbon chain length recommends that the combustion of short chain length methyl esters reduce CO, THC and soot emissions. This is mainly due to lower viscosity and bulk modulus and higher oxygen content. Unsaturated compounds reduce THC, CO and soot emissions compared to C18:0 (same chain length), as a result of their lower viscosity and higher volatility. On the other hand, they clearly produce higher NO_X, soot, CO and THC emissions than short chain length saturated methyl esters. As a consequence, it is suggested the use of short chain length methyl esters in alcohols blends. Moreover, the addition in alcohol-diesel blends of small concentrations of long chain saturated methyl esters it is effective in improving lubricity, while the effect on engine performance, combustion characteristics and emissions of those small concentrations is negligible.

The alcohol-biodiesel-diesel fuel blends have more clear benefits in soot emissions reduction than conventional diesel with biodiesel blends with the same oxygen content. This is a consequence of the functional group of alcohol which is more effective in inhibiting soot formation than the ester group. Comparing the two alcohol fuels used in this study, butanol blends showed greater potential in reducing exhaust emissions compared to ethanol blends, except NO_X emissions as a consequence of its lower heat of vaporisation. The NO_X-soot trade-off diagram suggests that the butanol based blend with EGR has higher potential in reducing simultaneously both emissions.

CHAPTER 6

HYDROXYLATED BIODIESEL:

EFFECTS ON BUTANOL-DIESEL BLENDS

It has been discussed that economic factors, feedstock supply and availability are an obstruction for the use of first generation biodiesels derived from edible sources such as rapeseed, palm and soybean. And that this has led to an intensive search for additional sources of biodiesel. Non-edible oil crop and excellent lubricity are attractive factors for castor oil as an alternative feedstock of biodiesel. Its major constituent is hydroxylated fatty acid or ricinoleic acid (12-hydroxyoctadec-9-enoic acid according to the international union of pure and applied chemistry nomenclature). There are few studies on the effect of individual methyl esters on emissions of diesel fuel blends (Schönborn et al., 2009). However, more research regarding hydroxylated methyl ester is needed especially in alcohol blends. The European biodiesel standard (EN-14214, 2003) prohibits the use of methyl esters of castor oil (COME) as a biodiesel fuel, due to the properties (i.e. the extremely high viscosity) of methyl ricinoleate (C18:1 OH). Consequently, the substantial reduction in viscosity of alcohols blended with diesel fuel can be balanced with the addition of biodiesel derived from castor oil.

In this chapter the physical and chemical properties of tri-blended biodiesel (derived from COME)-butanol-diesel fuels are studied along with combustion and engine-out emissions. Rapeseed methyl ester was used as a base line test and which consists mainly of methyl oleate (C18:1) with the same number of carbon and unsaturation degree compared to methyl ricinoleate. Therefore the performance of the hydroxyl group in COME is assessed. The basic fuel properties

of fuels are listed in Table 6.1. The density, kinematic viscosity, gross calorific value and lubricity were measured according to ISO 12185, ISO 3105, ISO 1928 and ISO 12156 respectively, whereas other properties were calculated or obtained from suppliers or publications. The 16% butanol was selected to perform fuel based on previous investigations (Sukjit et al., 2012, Sukjit et al., 2013). All tests were performed at a constant engine speed of 1500 rpm and variable engine loads of 3 and 5 bar IMEP. These engine loads can be specified as low and high load for the tested engine. Three EGR rates (0%, 10% and 20%) were also introduced at each engine condition.

6.1 Fuel properties

The most critical property of castor oil methyl ester is viscosity which does not meet fuel specifications prescribed by EN 14214 (3.5-5.0 mm^2/s). The main reason is the high viscosity of methyl ricinolate (15.44 mm^2/s (Knothe and Steidley, 2005)) which is the main component of COME. Conversely, the viscosity of biodiesel derived from rapeseed fulfils the standard because it consists mainly of methyl oleate which has a lower viscosity than methyl ricinolate (4.51 mm^2/s (Knothe and Steidley, 2005)). Blending castor oil-based biodiesel with other fuels such as conventional diesel is an approach to fulfil the blend fuel specifications defined in EN 590. The results in Table 1 show that for a blend with approximately 30% by volume of COME in ULSD, the density is higher than the maximum limit which is given in EN 590 (820-845 kg/m^3) and its viscosity is close to the maximum defined acceptable value (4.5 mm^2/s). The effect of increasing COME concentration on the fuel properties of butanol-ULSD blend was also studied. The 16% butanol was fixed while the percentage of biodiesel was varied between 0% and 60% by volume

in the blends. The limit to keep the density and viscosity of the blend under the standard fuel specification is shown to be 15% and 35% of hydroxylated, respectively (Figure 6.1).

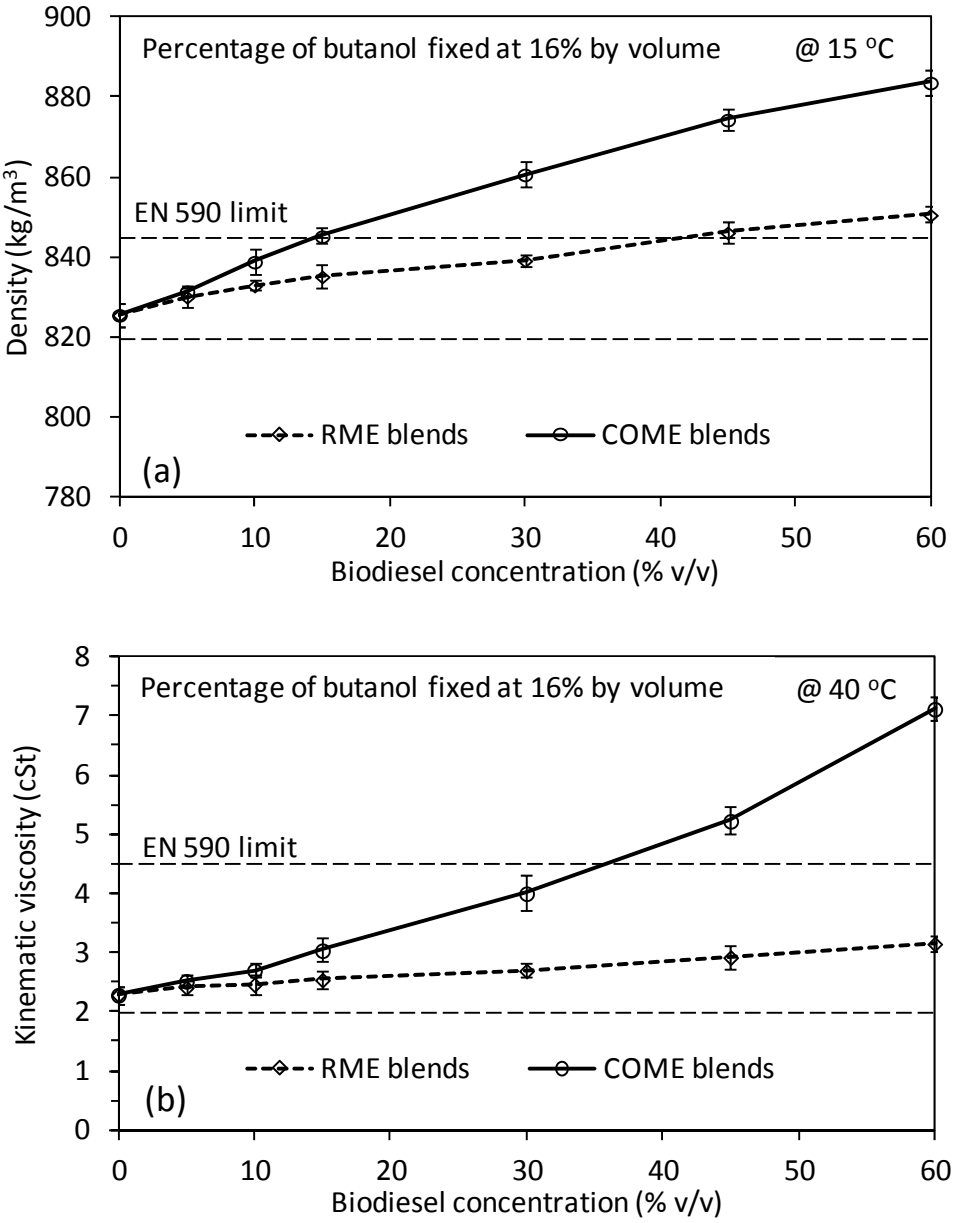

Figure 6.1: Fuel properties of selected butanol blends: (a) density and (b) viscosity

Table 6.1: Physical and chemical properties of tested fuels

Abbreviation	% Volumetric make-up
ULSD	100 Ultra low sulphur diesel
RME	100 Rapeseed methyl ester
COME	100 Castor oil methyl ester
R45D	55 ULSD + 45 RME
C31D	69 ULSD + 31 COME
B16R15D	69 ULSD + 15 RME + 16 Butanol
B16C10D	74 ULSD + 10 COME + 16 Butanol

Properties	ULSD	RME	COME	Butanol	R45D	C31D	B16R15D	B16C10D
Chemical formula	$C_{14}H_{26.1}$	$C_{19}H_{35.3}O_2$	$C_{19}H_{35.9}O_{2.9}$	C_4H_9OH	$C_{15.8}H_{29.5}O_{0.7}$	$C_{15.2}H_{28.4}O_{0.7}$	$C_{11}H_{21.4}O_{0.5}$	$C_{11}H_{21.2}O_{0.5}$
Cetane number	53.9	54.7	48.9	17	-	-	-	-
Latent heat of vaporisation (kJ/kg)	243	216	-	585	-	-	-	-
Bulk modulus (MPa)	1410	1553	-	1500	-	-	-	-
Density at 15 ^oC (kg/m^3)	827.1	883.7	928.7	809.5	852.3	864.4	835.2	838.9
Kinematic viscosity at 40 ^oC (cSt)	2.70	4.53	16.67	2.23	3.45	4.38	2.54	2.70
Lower calorific value (MJ/kg)	43.11	37.80	37.63	33.12	39.94	40.85	39.97	41.05
Lubricity at 60 ^oC (μm)	312	205	190	620	213	198	405	301
C (wt %)	86.44	77.09	73.48	64.78	82.08	82.09	81.58	81.64
H (wt %)	13.56	12.07	11.69	13.63	12.87	12.93	13.34	13.36
O (wt %)	0	10.84	14.83	21.59	5.05	4.98	5.08	5.00
O from OH group (wt %)	0	0	4.94	21.59	0	1.66	3.36	3.91

The lower calorific values of the alcohol blends are shown in Figure 6.2. The blends with COME resulted in lower calorific value with respect to blended RME in term of mass. However, similar results of calorific value based on volume were obtained for biodiesel blended with butanol-ULSD due to the higher density of castor oil.

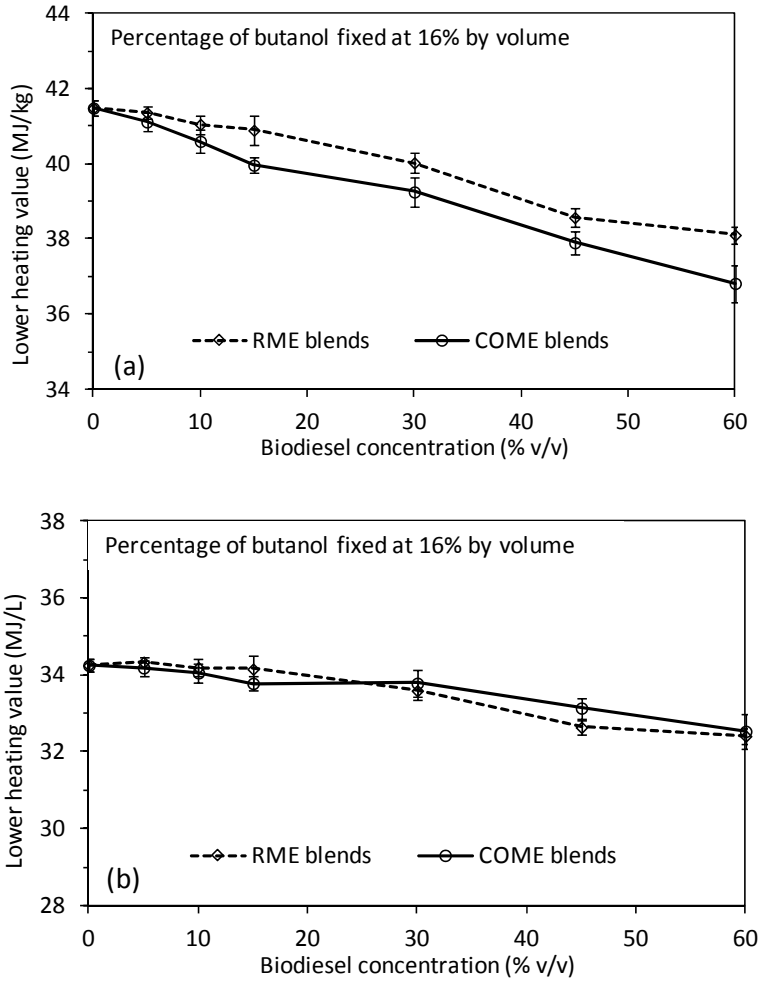

Figure 6.2: Calorific value of selected butanol blends: (a) mass and (b) volume

Figure 6.3 shows the lubricity of the blended fuels at 25 °C and 60° C. The decrease in lubricity between 25 °C and 60 °C is a result of the lack of boundary film formation. At 60 °C minor polar compounds within the biodiesel are, as a result of poor mixing, prevented from being

adsorbed on to the metal surface of the specimens by the predominant nonpolar and less lubricating components of the test fuels (Wadumesthrige et al., 2009). However, the addition of COME is more effective at restoring the lubricity of the alcohol blend compared to that of RME. This can be attributed to the high concentration of hydroxyl fatty acids which are responsible for enhancing lubricity (Geller and Goodrum, 2004). It can be seen that less than 3% COME is needed to keep the lubricity of 16% butanol blended with ULSD under the wear scar limit given in diesel fuel lubricity standard.

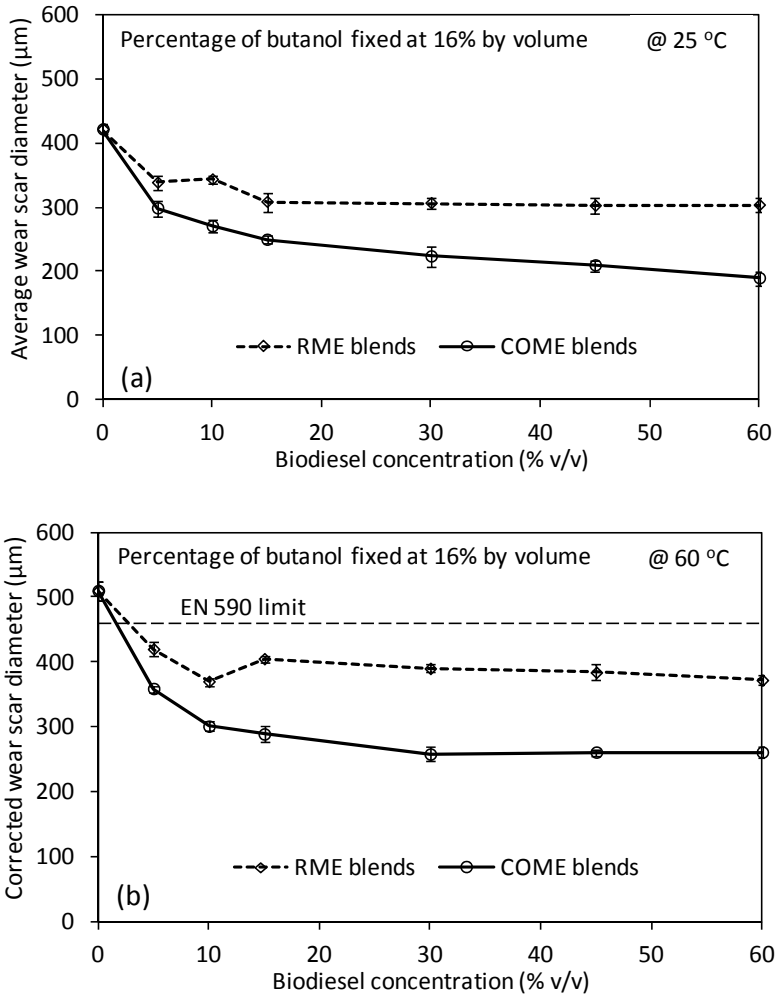

Figure 6.3: Lubricity of selected butanol blends: (a) 25 °C and (b) 60 °C

6.2 Combustion and performance

Regarding the selection of fuels investigated here, the blend containing 10% COME was selected for engine testing as it has similar properties (in terms of lubricity, viscosity, density and calorific value) when compared with ULSD. To assess the effect of hydroxylated biodiesel and the combination between biodiesel and butanol, four distinct fuel blends with the same oxygen content were selected in the engine test. The blends comprise of R45D, C31D, B16R15D and B16C10D. Biodiesel has an inherent oxygen availability with high density and viscosity that affects the injection process and combustion patterns e.g. it advances the start of combustion and increases the premixed combustion phase with respect to diesel fuel (Lapuerta et al., 2008b, Tsolakis, 2006). Combustion phasing and the heat release rate are also strongly influenced by the cetane number of fuel. A reduction in ignition delay is obtained as the cetane number increases. The start of combustion in the blend with COME was slightly retarded compared to the RME blend (Figure 6.4a). This was likely to be a consequence of the low cetane number of COME. As butanol was added to the blend an increase in the premixed combustion peak was obtained. The main reason for this was the low cetane number of butanol which increased ignition delay compared to the biodiesel-ULSD blends. The addition of biodiesel and alcohol to diesel fuel tended to increase the indicated specific fuel consumption as a result of their low calorific values, resulting in an increased fuel mass needed to obtain the same power output. Nevertheless, the indicated engine thermal efficiency for all fuel blends was similar with respect to the reference fuels (Figure 6.4b). The lambda ratio (i.e. the actual air/fuel ratio over the stoichiometric air/fuel ratio) was found to be similar for the fuels tested at each operating condition. This is an indication that the difference between the fuels was the direct result of the fuel composition.

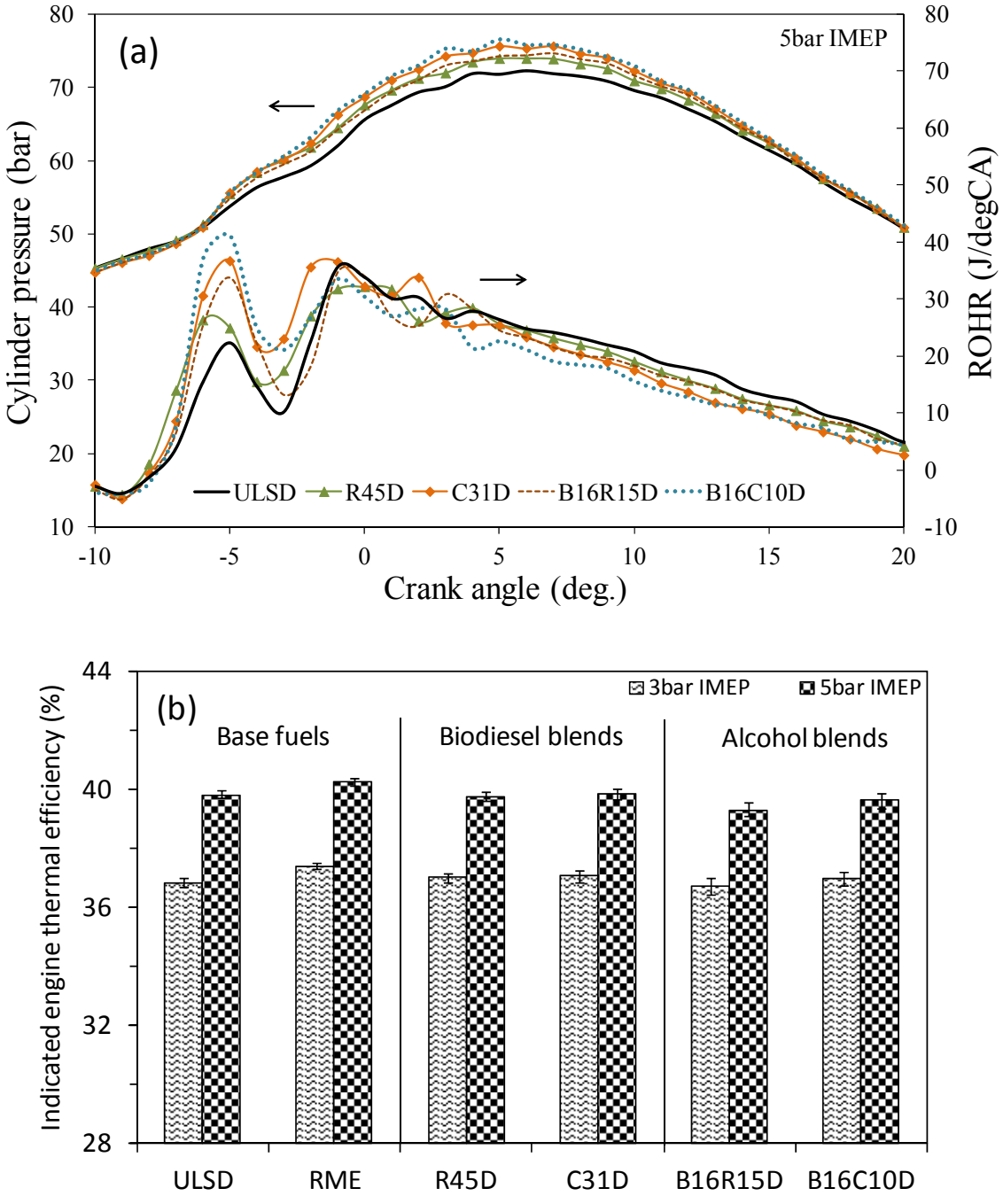

Figure 6.4: Combustion characteristics: (a) in-cylinder pressure and rate of heat release and (b) indicated engine thermal efficiency

6.3 Carbonaceous gas emissions

Biodiesel combustion produced lower unburnt total hydrocarbon emissions (THC) than that of diesel fuel (Figure 6.5). This is thought to be a result of more complete combustion brought about from the inherent oxygen availability of the biodiesel. In addition to this, the advanced start of combustion with biodiesel increases the available time for hydrocarbon emissions oxidation. Both biodiesels, RME and COME, blended with ULSD showed similar THC emissions at low and high engine loads. A slight increase in THC emissions was obtained when butanol was added to the fuel blends. This increase was mainly due to the high heat of vaporisation of alcohol fuel, resulting in incomplete combustion as the combustion chamber was cooled (Kass et al., 2001, Lapuerta et al., 2008a, Rakopoulos et al., 2010). This effect is more influential when the combustion temperature is lower, i.e. at low load rather than high load conditions.

CO emissions of biodiesel were lower than diesel fuel for both engine conditions. This reduction is mainly due to the oxygen content of biodiesel which leads to more efficient combustion. A slight decrease in CO emissions was obtained when COME was used instead of RME in the blends. Comparing the alcohol to biodiesel blends, adding butanol to the blends decreased CO emissions. This benefit could be due to the lower C/H ratio of butanol compared to biodiesel. This effect may compensate for an increase in CO with alcohol blends due to the higher heat of vaporisation and as a consequence of reducing the in-cylinder temperature. As the engine load was increased, the oxidation of the intermediates species was improved, resulting in a reduction in THC and CO emissions (Ren et al., 2008, Song et al., 2002).

6.4 NO_X emissions

It is well-known that the advanced fuel injection and combustion timing with biodiesel can cause an increase in NO_X emissions in diesel engines. Also, the adiabatic flame temperature and the oxygen content of biodiesel can promote NO formation reactions (Tsolakis et al., 2007). Consequently, NO_X emissions of RME were higher than that of conventional diesel fuel (Figure 6.5). At high load engine conditions NO_X emissions were higher than at low load as a result of the higher in-cylinder temperature.

Adding COME to the fuel blend resulted in higher NO_X emissions than those when RME was added. This is likely to be a consequence of the lower cetane number of the hydroxylated biodiesel. It was evident in the rate of heat release that a delay in ignition timing and an increase in premixed combustion peak were obtained by the addition of COME. These combustion characteristics resulted in higher in-cylinder pressures and temperatures, favouring NO_X formation. Also, the hydroxyl group of castor oil was expected to reduce soot emissions which results in higher temperatures in the combustion chamber because less heat is absorbed by soot.

In case of the alcohol blends, the poor cetane number of butanol increased ignition delay and the rate of premixed combustion as was previously shown in combustion phase plots, resulting in an increase in NO_X emissions (Armas et al., 2012). Conversely, the high enthalpy of vaporisation of alcohol fuel locally cooled the combustion chamber reducing NO_X formation (Ishida et al., 2010). The increase in NO_X emissions due to the low cetane number of butanol outweighs its reduction caused by the high heat of vaporisation. Therefore a slight increase in

NO_X emissions was found with the butanol blends compared to biodiesel-diesel blends with the same oxygen content.

6.5 Soot emissions

The soot emissions from the RME blends were much lower than those of the conventional diesel fuel (Figure 6.5). This is a result of the oxygen content and the absence of aromatic compounds in biodiesel (Lapuerta et al., 2008b). At high load, the overall equivalence ratio and the number of fuel rich regions in the combustion chamber were higher than at low load. As a consequence, the high load represents critical conditions for soot formation and hence the increase in soot emissions.

Again, adding COME to the fuel blend results in lower soot emissions when compared to those obtained with RME. This difference is likely to be a consequence of the different structure of the fuel molecules. The main functional group of RME is an ester group, where one carbon atom is bonded with two oxygen atoms, whereas COME contains a unique fatty acid methyl ester which consists of three oxygen atoms. Two of the oxygen atoms correspond to an ester group while the other oxygen atom belongs to a hydroxyl group. It has been previously reported that the hydroxyl group has higher potential to inhibit soot formation than the ester group (Cheng et al., 2002, Lapuerta et al., 2009a, Pepiot-Desjardins et al., 2008, Westbrook et al., 2006). This variation can be used to justify the lower soot emissions for COME blends with the same oxygen content compared to RME blends.

For the alcohol blends, soot emissions were lower than those obtained for biodiesel. This is due to the oxygen in the alcohol group which is more effective for oxidising soot emissions than

the oxygen in an ester group. Also, incorporating alcohol into the fuel blends reduces carbon content and the diffusion combustion phase, decreasing the possibility of soot formation. Additionally, the higher viscosity and boiling point of the biodiesel blends makes fuel atomisation and evaporation in the cylinder more difficult, favouring soot formation. It is notable that the blend composed of diesel, butanol and RME has a higher potential to reduce soot emissions than the COME-diesel blend for the same oxygen content. According to the oxygen content belonging to hydroxyl group, an order of effectiveness of oxygenated blends enhancing soot oxidation (B16C10D > B16R15D > C31D > R45D) was obtained.

6.6 NO_X/soot trade-off

A simultaneous variation of NO_X and soot emissions for fuel blends containing the same oxygen content at three different EGR operating conditions is shown in Figure 6.6. The ULSD emissions are taken as a benchmark to evaluate the effect of the use of biodiesel and alcohol blends. It can be seen that using EGR produced a significant reduction in NO_X emissions (Ladommatos et al., 2000), however soot emissions increased. When EGR is applied, the recirculation of less soot emissions into the combustion chamber with oxygenated fuels limits particle nucleation and surface growth in the combustion chamber reducing the soot recirculation penalty (Gill et al., 2012b). It can be seen that the application of EGR with oxygenated blends resulted in a better trade-off between NO_X and soot emissions compared to conventional diesel.

A better improvement in such a trade-off is obtained by the COME-diesel blends compared to the RME- blends. This is likely to be a consequence of the more effective oxygen corresponding to the hydroxyl group in COME, considerably reducing soot emissions without a

high NO_X penalty. The addition of alcohol to the biodiesel blends also improves the NO_X/soot trade-off. This is not only a consequence of the higher heat vaporisation of alcohol which tends to reduce NO_X emissions caused by biodiesel, but is also a result of the highly effective soot oxidation caused by the functional group of alcohol with respect to that of the esters. Similar trends are observed at both engine operating conditions tested.

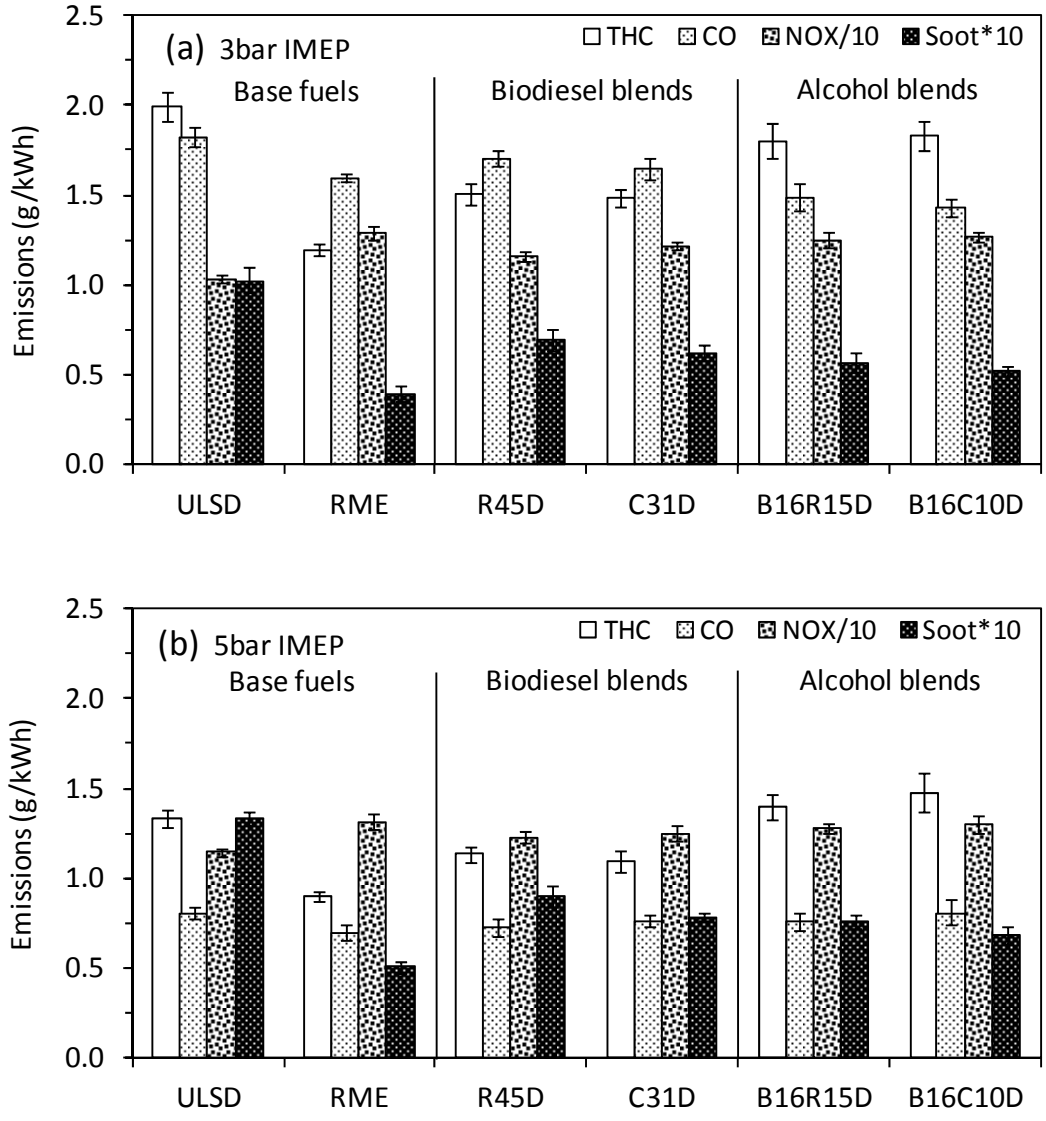

Figure 6.5: Engine-out emissions: (a) 3 bar IMEP and (b) 5 bar IMEP

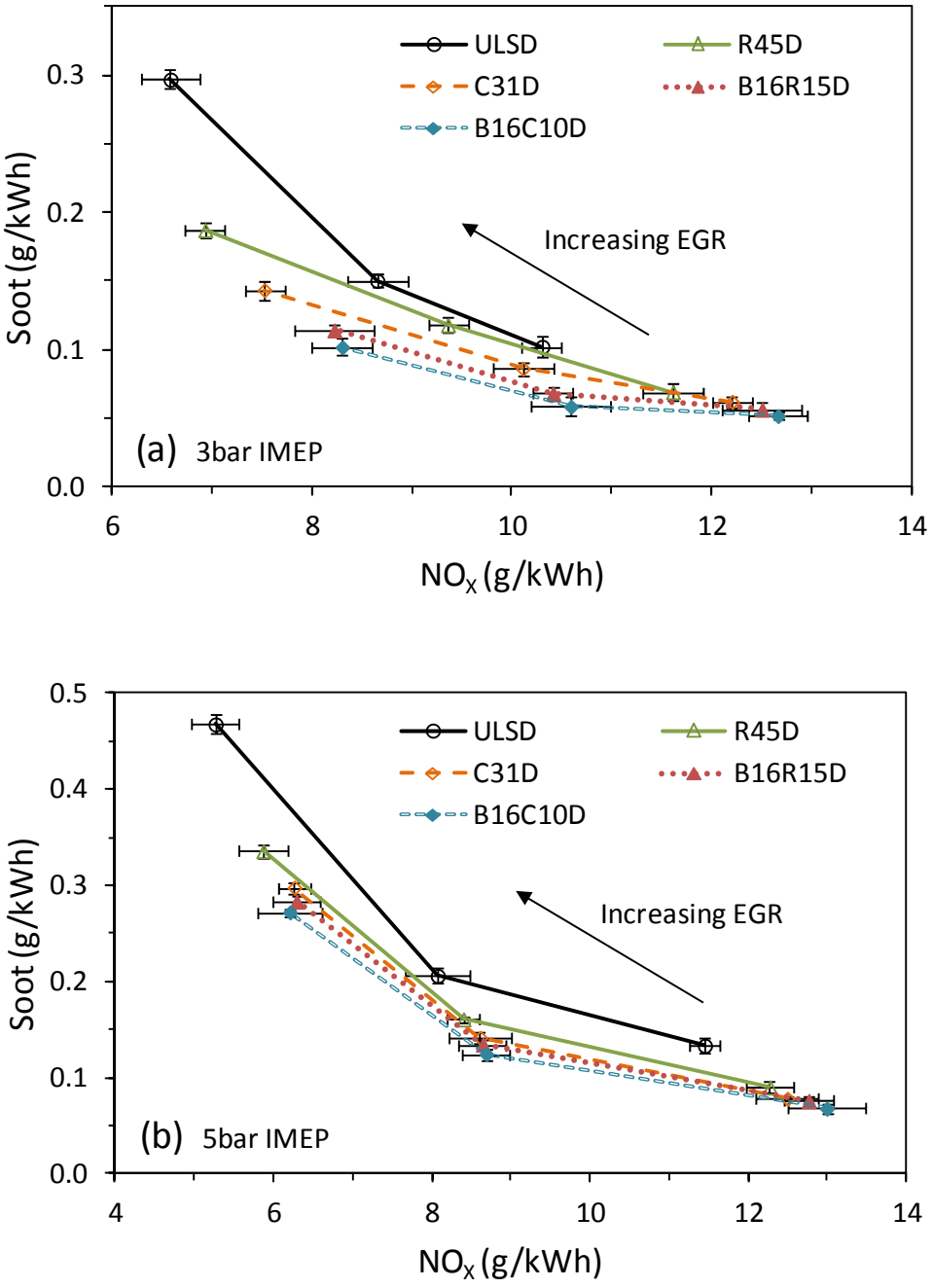

Figure 6.6: Trade-off between NO_X and soot emissions: (a) 3 bar IMEP and (b) 5 bar IMEP

6.7 Particle size distribution

It can be seen that the concentration number of particulate matter from oxygenated fuels were significantly lower than those obtained with ULSD (Figure 6.7a). The oxygen content, increased premixed combustion and reduced diffusion combustion are the main reasons for the reduction in the number of particles. The presence of oxygen in fuel molecules reduces the number of rich regions in the combustion chamber diminishing particle precursors and formation, and also enhancing the process of particle oxidation. Moreover, the number concentration with a shift in the size distribution to smaller diameter particles was obtained with the use of oxygenated fuels leading to a reduction in the mean particle diameter. The reduced average particle size is not only a result of the reduction in the soot formation but also due to a reduction in the likelihood of collisions between particles (preventing the formation of larger particles through agglomeration). It should be noted that the smaller mean diameter corresponding to the particles emitted with the oxygenated fuels is not caused by an increase in the number of smaller particles but is a result of a significant reduction in the number of larger particles. Comparing alcohol blends to biodiesel blends, the use of alcohol reduces the number of particulate matter. This can be explained by the arguments given in the soot section above.

The total particle mass concentration was estimated from the particle number size distributions using an agglomerate density function which decreased as agglomerate size increases (Lapuerta et al., 2003). The results can be used to confirm that the alcohol blended with hydroxylated biodiesel is most beneficial for reducing particulate matter emissions compared to the other tested fuels (Figure 6.7b).

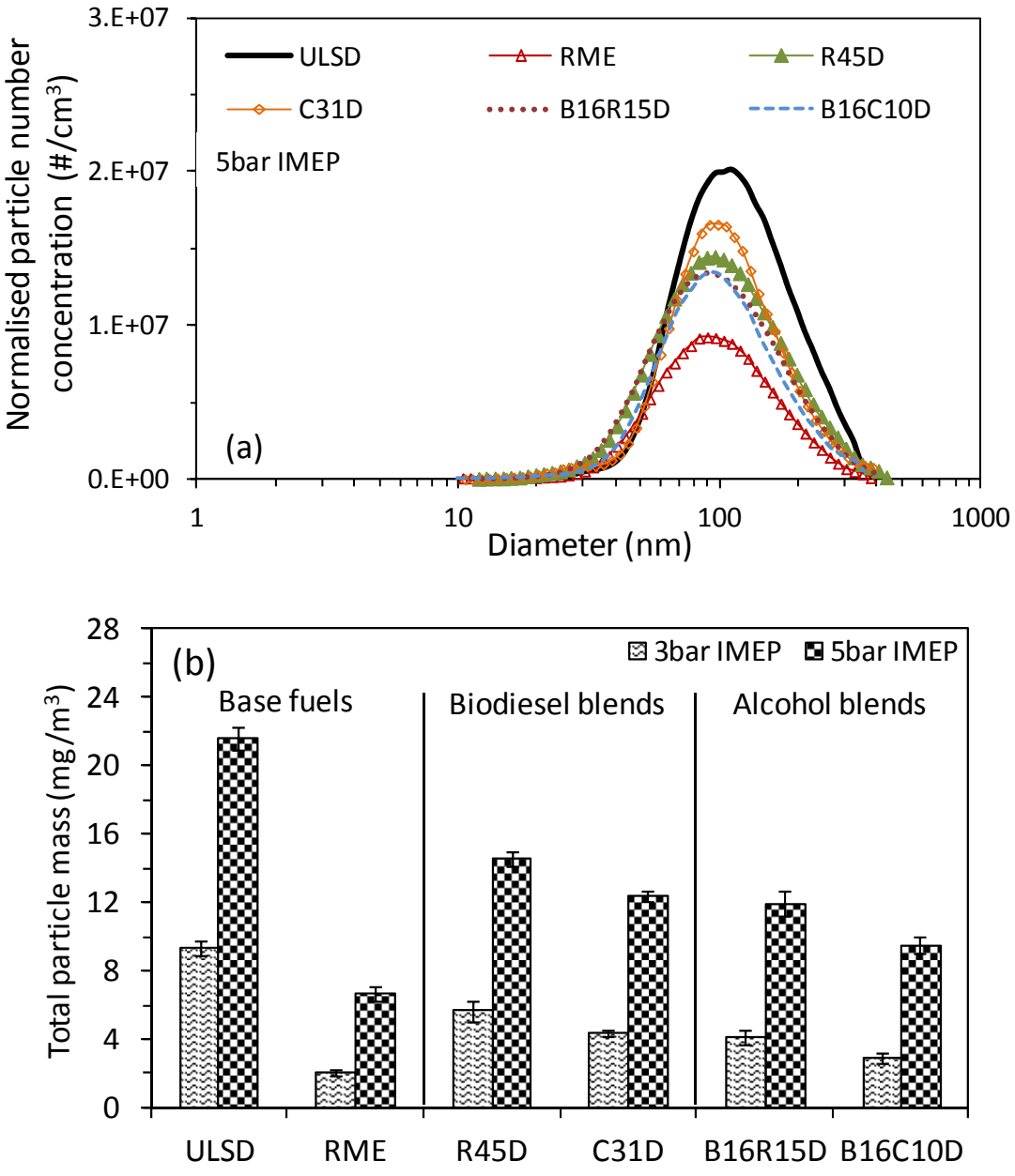

Figure 6.7: Particulate matter emissions: (a) number and size distribution and (b) total mass concentration

6.8 Particulate composition and soot oxidation

Particulate matter composition was also analysed using thermogravimetric analyser (TGA). This analysis has been carried out only for 5 bar IMEP load (i.e. high load conditions). The TGA heating program is shown in the Chapter 3. Volatile organic fraction (VOF) is obtained by comparing the mass of particulate matter which is lost in the inert atmosphere (volatile organic material) with the mass of total particulate matter (volatile organic material and soot). The comparison between the volatile organic fraction and soluble organic fraction (SOF) obtained from real time measurement is shown in Figure 6.8. It can be seen that both show a good correlations. The organic fraction of biodiesel is larger than in the case of conventional diesel fuel. This increase is derived from the lower soot and the heavier organic material obtained when using biodiesel. The organic fraction from RME is lower than the organic fraction from COME. This is due to the lower soot emissions from COME. This same trend is also observed when the butanol blends are compared. However, the addition of butanol reduced organic material with respect to pure biodiesel and the biodiesel blends with the same oxygen content. This is a consequence of the lower soot emissions from the butanol blends and, as a result of the higher volatility of butanol and its combustion products, the reduction in the organic material.

The derivative of soot oxidation for the different fuel blends at high load is shown in Figure 6.9a. From this curve, the temperature at which maximum soot oxidation is obtained and the activation energy are calculated and shown in Figure 6.9b. The temperature at which the maximum rate of soot is oxidised for the biodiesel blends is lower compared to ULSD. This has already been observed for biodiesels that contain both an ester group and dyglime (i.e. which contains an ether group and that can be justified by the oxygen content in the fuel molecules)

(Gill et al., 2012a, Lapuerta et al., 2012, Song et al., 2006). In the case of the butanol blends, compared to ULSD, a lower temperature for maximum soot oxidation was obtained as well as being slightly lower than the biodiesel blends with the same oxygen content. The maximum temperature for soot oxidation for COME is lower than in the case of RME, with and without butanol. Therefore, the hydroxyl group present in the butanol and COME lowers the temperature at which maximum rate of soot oxidation is obtained. In general, a similar trend compared to the case of the temperature at the maximum rate of soot oxidation is obtained for the activation energy. From the results, it is concluded that oxygenated fuel blends containing the hydroxyl radical such as butanol and COME reduce the energy needed to start soot oxidation and lower the temperature at which soot is oxidised. This results in a double benefit in the diesel particle filter, as these fuels produce lower engine output soot and this soot is easier to oxidise.

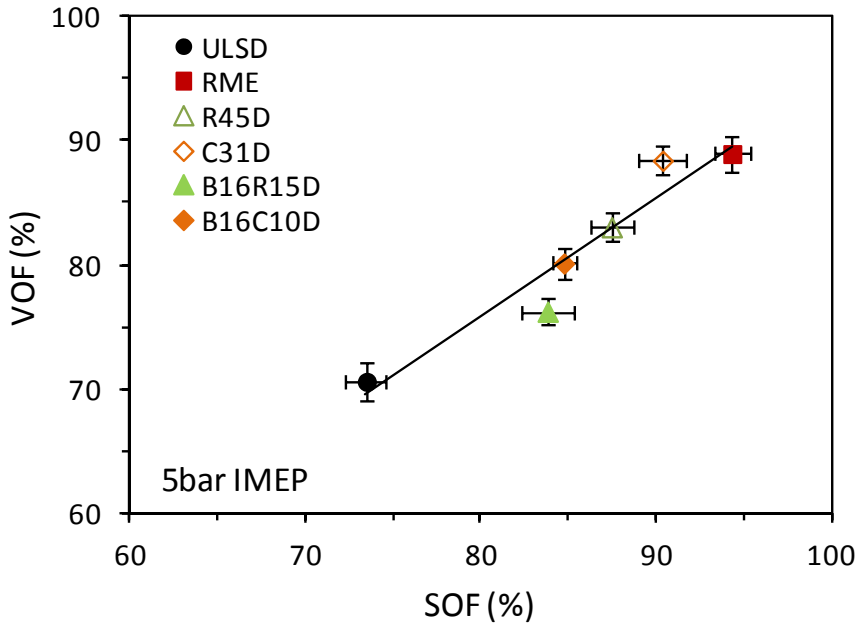

Figure 6.8: Volatile organic material versus soluble organic material at 5 bar IMEP

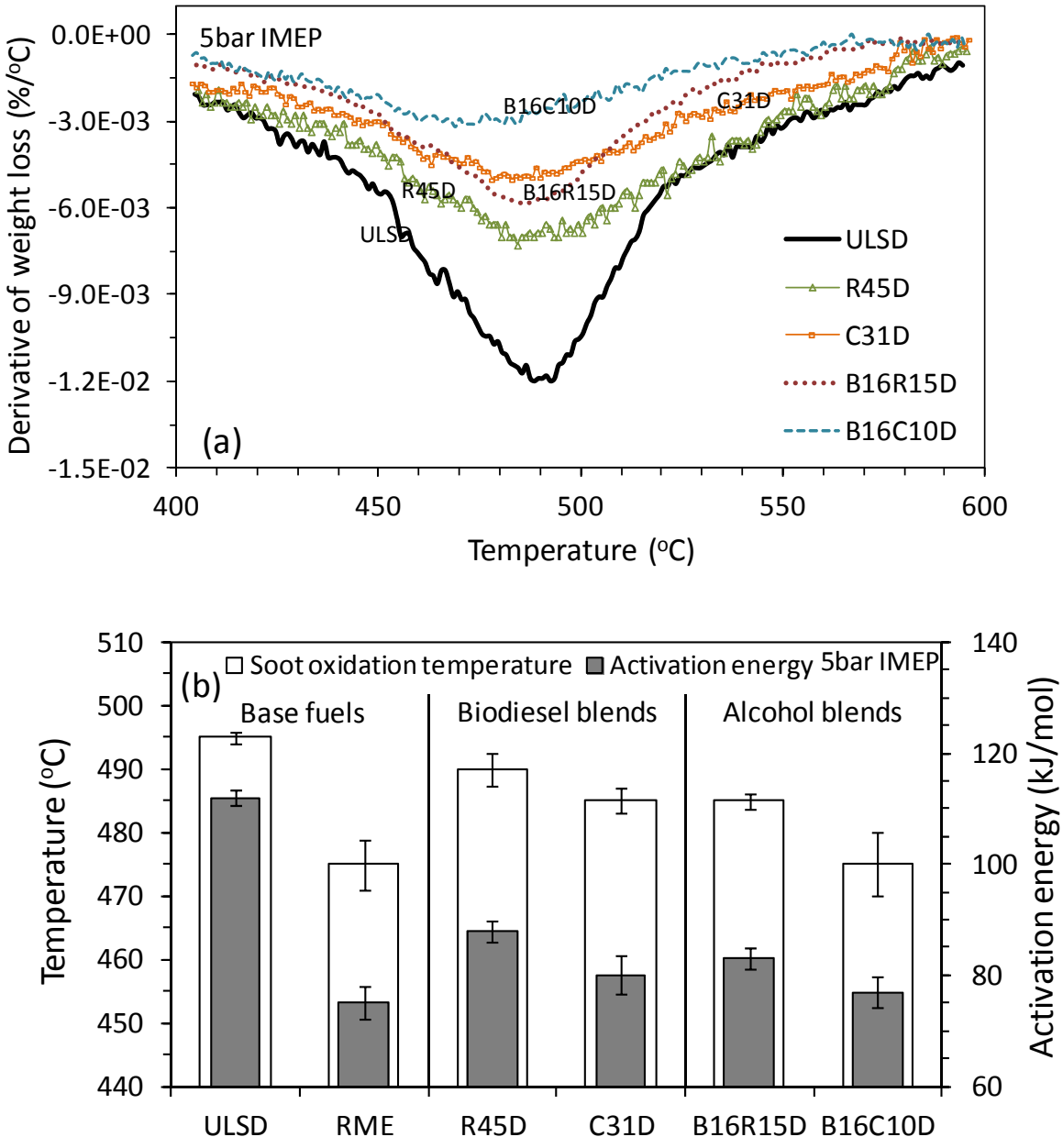

Figure 6.9: Soot oxidation: (a) derivative of weight loss and (b) temperature and activation energy

6.9 Summary

The presence of COME less than 30% by volume can keep the density and viscosity of the fuel blends under the European standard for automotive diesel. The addition of COME with higher viscosity brought about from methyl ricinoleate (hydroxyl fatty acid methyl ester) performs better as lubricity with respect to RME.

Comparing the biodiesels blended with diesel fuel, the order of improvement of the NO_X/soot trade-off was butanol-COME > butanol-RME > COME > RME. The existence of the hydroxyl group enhanced soot oxidation, reduced soot formation and diminished the temperature and energy needed to oxidise the formed soot. It is envisaged that these soot emissions benefits will favour the function of the aftertreatment system (e.g. it may enhance passive regeneration in diesel particulate filter, and has the potential to decrease the number of active regeneration cycles and increase the lifetime of the filter).

The combination of butanol with COME has been shown to be a feasible alternative for next generation fuels. This is due to the most relevant fuel properties of the blends (e.g. viscosity, lower heating value etc.) which influence combustion are closer to ULSD. The presence of the hydroxyl group has been shown to be beneficial in terms of engine-out emissions.

CHAPTER 7

EFFECT OF HYDROGEN ON BUTANOL-BIODIESEL BLENDS IN COMPRESSION IGNITION ENGINES

In this chapter a totally renewable binary liquid fuel blend composed of biodiesel and butanol was studied in order to reduce NO_X emissions with respect to pure biodiesel (heat of vaporisation of butanol), while maintaining similar particulate matter emissions benefits (oxygen content in butanol). However, CO and THC emissions could increase with respect to pure biodiesel due to the high heat of vaporisation of butanol. To counteract the likely increase in gaseous carbonaceous emissions with butanol, the addition of hydrogen to replace part of the carbon within the liquid fuel was investigated and presented here.

The experimental apparatus was set up as detailed in Figure 7.1 and the basic properties of tested fuels are given in Table 7.1. Experiments were performed at a constant engine speed of 1500 rpm and variable engine loads of 3 and 5 bar IMEP. The tests were carried out initially using diesel and biodiesel fuels as a benchmark. B8R and B16R blends were prepared and tested under same conditions for comparison. Hydrogen, when added was introduced and mixed with the air before the intake manifold valve. The effect of hydrogen concentration (0.5, 1, 2 and 3% of volumetric air flow rate) was investigated with the aim of determining the optimal hydrogen concentration. Three different conditions of cooled EGR rate (0%, 10% and 20%) were analysed to overcome the penalty of NO_X emissions.

Table 7.1: Specification of tested fuels

Abbreviation	% Volumetric make-up
ULSD	100 Ultra low sulphur diesel
RME	100 Rapeseed methyl ester
B8R	8 Butanol + 92 RME
B16R	16 Butanol + 84 RME

Properties	ULSD	RME	Butanol	Hydrogen	B8R	B16R
Chemical formula	$C_{14}H_{26.09}$	$C_{18.96}H_{35.29}O_2$	C_4H_9OH	H_2	$C_{15.36}H_{29.2}O_{1.76}$	$C_{12.83}H_{24.92}O_{1.59}$
Cetane number	53.9	54.7	17	-	-	-
Density at 15 ^oC (kg/m^3)	827.1	883.7	809.5	0.08	878.3	870.5
Kinematic viscosity at 40 ^oC (cSt)	2.70	4.53	2.23	-	3.95	3.78
Lower heating value (MJ/kg)	43.11	37.80	33.12	120	37.12	36.91
Latent heat of vaporisation (kJ/kg)	243	216	585	-	-	-
Bulk modulus (MPa)	1410	1553	1500	-	-	-
Lubricity at 60 ^oC (μm)	312	205	620	-	257	293
Stoichiometric A/F mass ratio	14.53	12.49	11.14	34.07	12.39	12.29
Sulphur (mg/kg)	46	5	-	-	-	-
Total aromatics (wt%)	24.4	-	-	-	-	-
C (wt %)	86.44	77.09	64.78	0	76.18	75.26
H (wt %)	13.56	12.07	13.63	100	12.19	12.30
O (wt %)	0	10.84	21.59	0	11.63	12.44

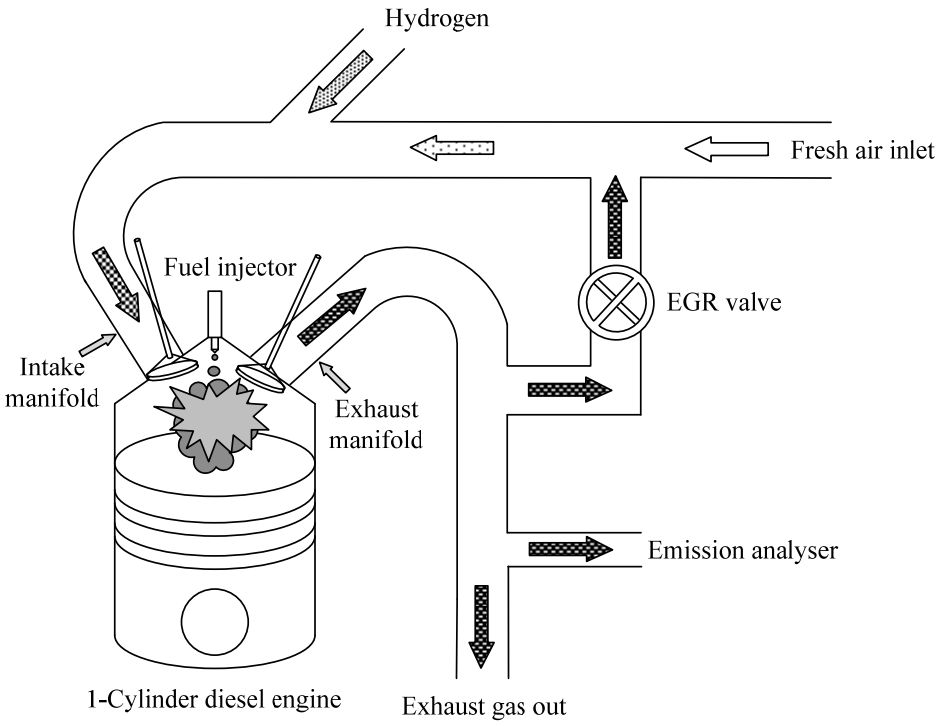

Figure 7.1: A simplified schematic diagram of the test rig

7.1 Combustion studies and engine performance

The use of RME resulted in an increase of the rate of the fuel burnt in the premixed phase with the combustion advanced to an earlier crank angle positions, leading to higher peak in-cylinder pressures compared to ULSD combustion (Figure 7.2 and Table 7.2). This is likely to be a consequence of the compressibility of biodiesel fuel which is lower than that of ULSD resulting in the advance of the start of injection (Szybist et al., 2005a).

Table 7.2: Summarised results of combustion parameters

Abbreviation	
SOC	Start of combustion (CAD)
MICP	Maximum in-cylinder pressure (bar)
MHRR	Maximum of heat release rate in premixed combustion (J/CAD)

	ULSD					RME					B8R					B16R				
	Hydrogen addition					Hydrogen addition					Hydrogen addition					Hydrogen addition				
	0%	0.5%	1%	2%	3%	0%	0.5%	1%	2%	3%	0%	0.5%	1%	2%	3%	0%	0.5%	1%	2%	3%
3bar IMEP																				
SOC	-7	-7	-7	-7	-7	-8	-8	-8	-8	-8	-8	-8	-8	-9	-8	-8	-8	-8	-8	-8
MICP	68.2	68.4	68.0	68.1	68.6	70.3	70.6	70.8	70.8	70.9	71.4	72.3	72.4	72.8	72.7	72.2	72.2	73.2	73.3	72.9
MHRR	21.7	23.2	24.9	26.9	31.3	24.4	27.9	28.3	33.6	32.2	33.2	35.8	35.7	37.4	37.8	33.6	35.7	35.4	35.8	36.2
5bar IMEP																				
SOC	-7	-8	-8	-8	-8	-8	-8	-8	-8	-8	-8	-9	-9	-9	-9	-8	-8	-8	-8	-8
MICP	73.6	74.0	73.7	74.2	75.8	75.1	75.0	75.4	77.4	78.3	76.0	77.4	77.1	78.3	80.0	77.9	77.6	77.5	78.6	79.7
MHRR	24.9	26.2	24.5	26.0	26.6	23.2	23.4	24.5	25.3	27.6	28.2	28.9	29.2	29.4	31.2	33.0	38.0	39.1	39.9	41.5

The addition of butanol increased the rate of heat release in premixed combustion (Table 7.2) and resulted in a longer ignition delay due to the lower cetane number of the fuel and higher heat of vaporisation compared with ULSD and RME (Armas et al., 2012). The addition of hydrogen led to an increase in the premixed combustion at both operating conditions (3 and 5 bar IMEP) (Figure 7.3) due to the faster flame speed of hydrogen compared with liquid fuels. This trend for hydrogen and its effect on RME can be also applied to the combustion characteristics of the other tested fuels (Table 7.2).

The equivalence ratio (i.e the stoichiometric air/fuel ratio over the actual air/(fuel ratio) was calculated to be similar for the different liquid fuels tested in this study at each operating condition (Figure 7.4a). This indicates that the difference between the fuels was the direct result of the fuel composition. The combustion of the butanol fuel blends produced an increase in the indicated specific fuel consumption as a result of their lower heating value (Figure 7.4b), while the indicated thermal efficiency was similar with both biodiesel and diesel fuels. The addition of hydrogen reduced the engine thermal efficiency by a small amount. This is most likely to be a consequence of a decrease in the volumetric efficiency because of the replacement of air with hydrogen into the engine. The energy substitution of the liquid fuel (not shown) by hydrogen at 3 bar IMEP is higher than at 5 bar IMEP, i.e. as the same amount of hydrogen was delivered and the total power at 5 bar is higher than at 3 bar. For instance, when 3% of hydrogen was used, it replaced 20% and 15% of liquid fuel at low and high load respectively.

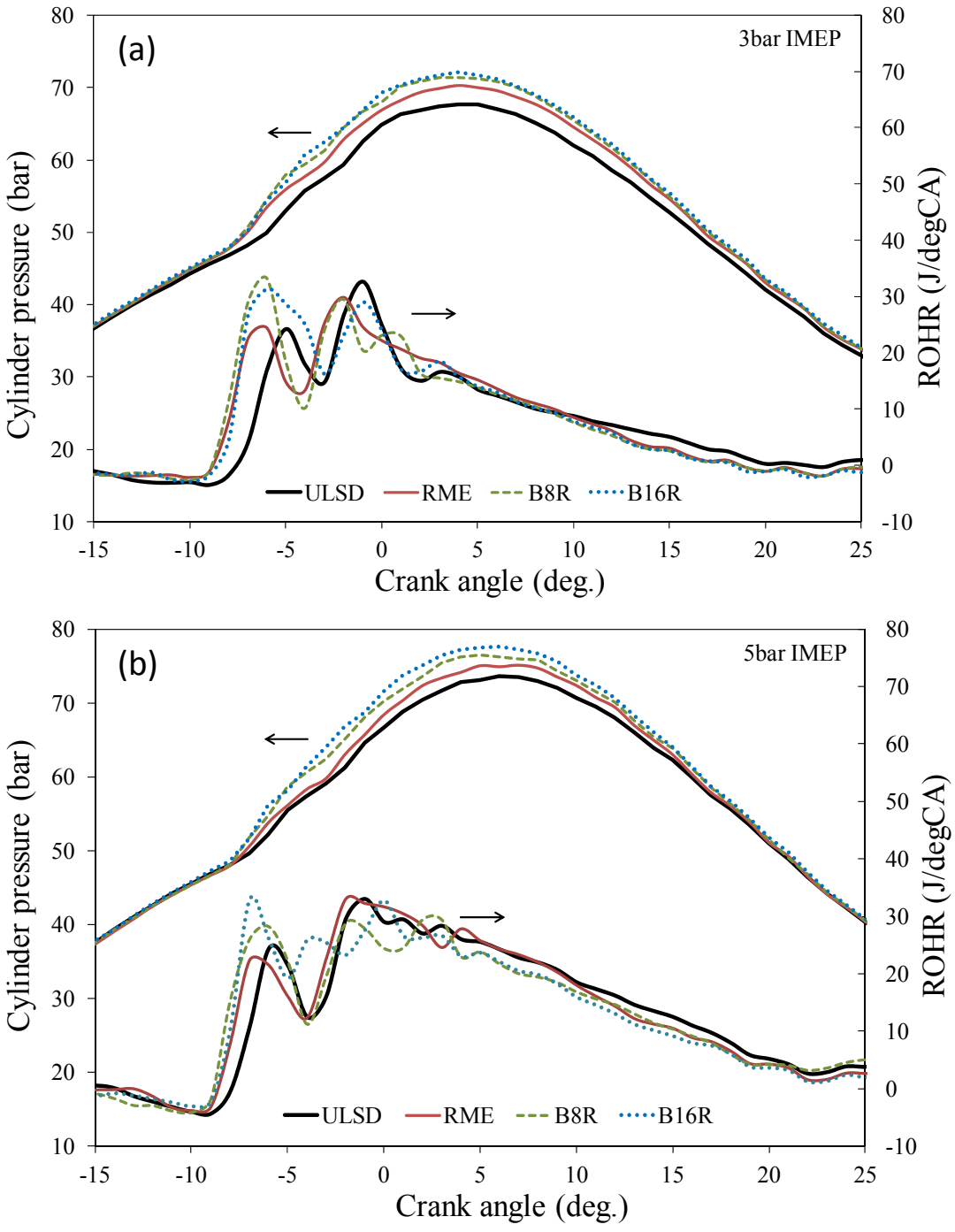

Figure 7.2: In-cylinder pressure and rate of heat release for the tested liquid fuels: (a) 3 bar IMEP and (b) 5 bar IMEP

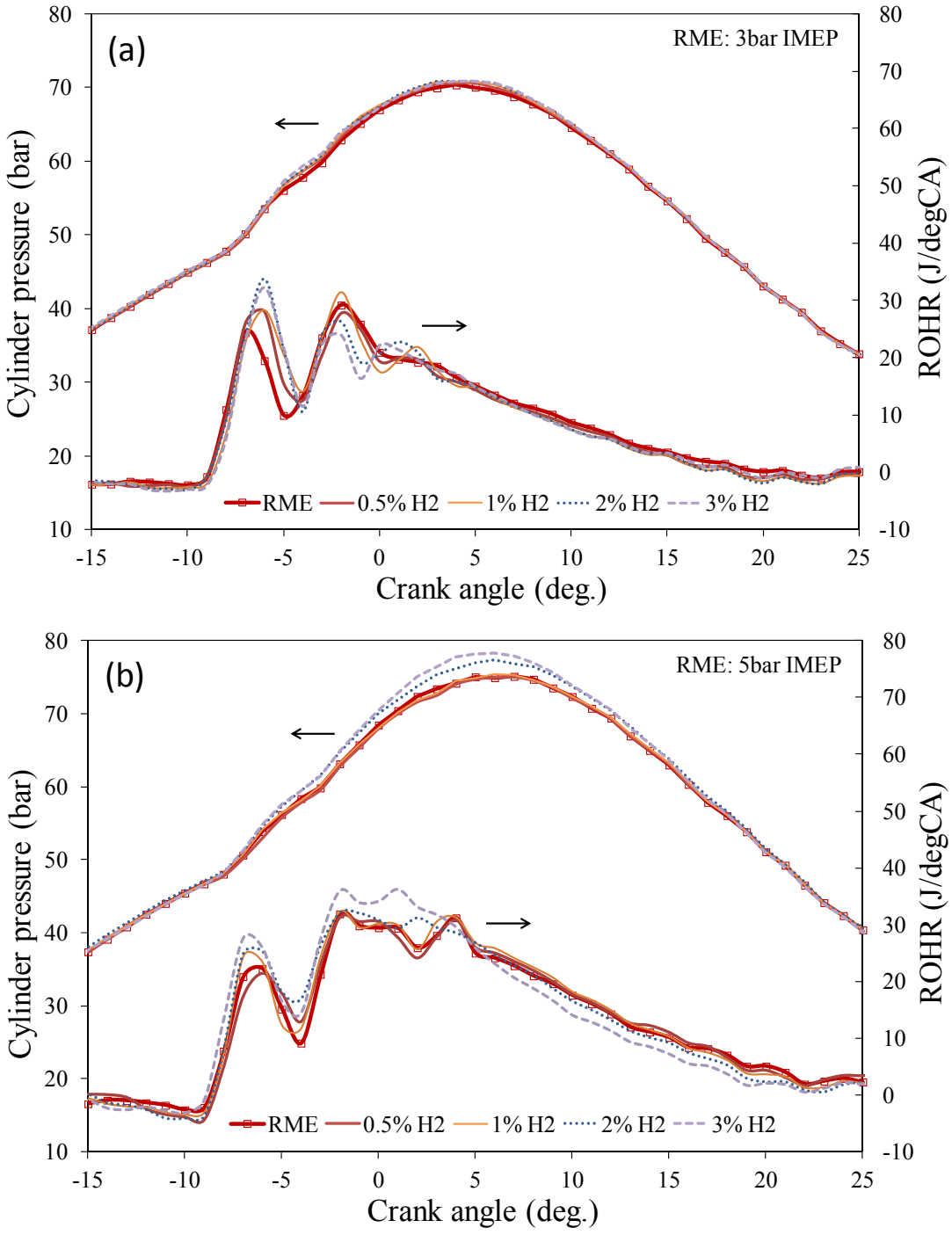

Figure 7.3: The effect of hydrogen on the combustion characteristics of RME: (a) 3 bar IMEP and (b) 5 bar IMEP

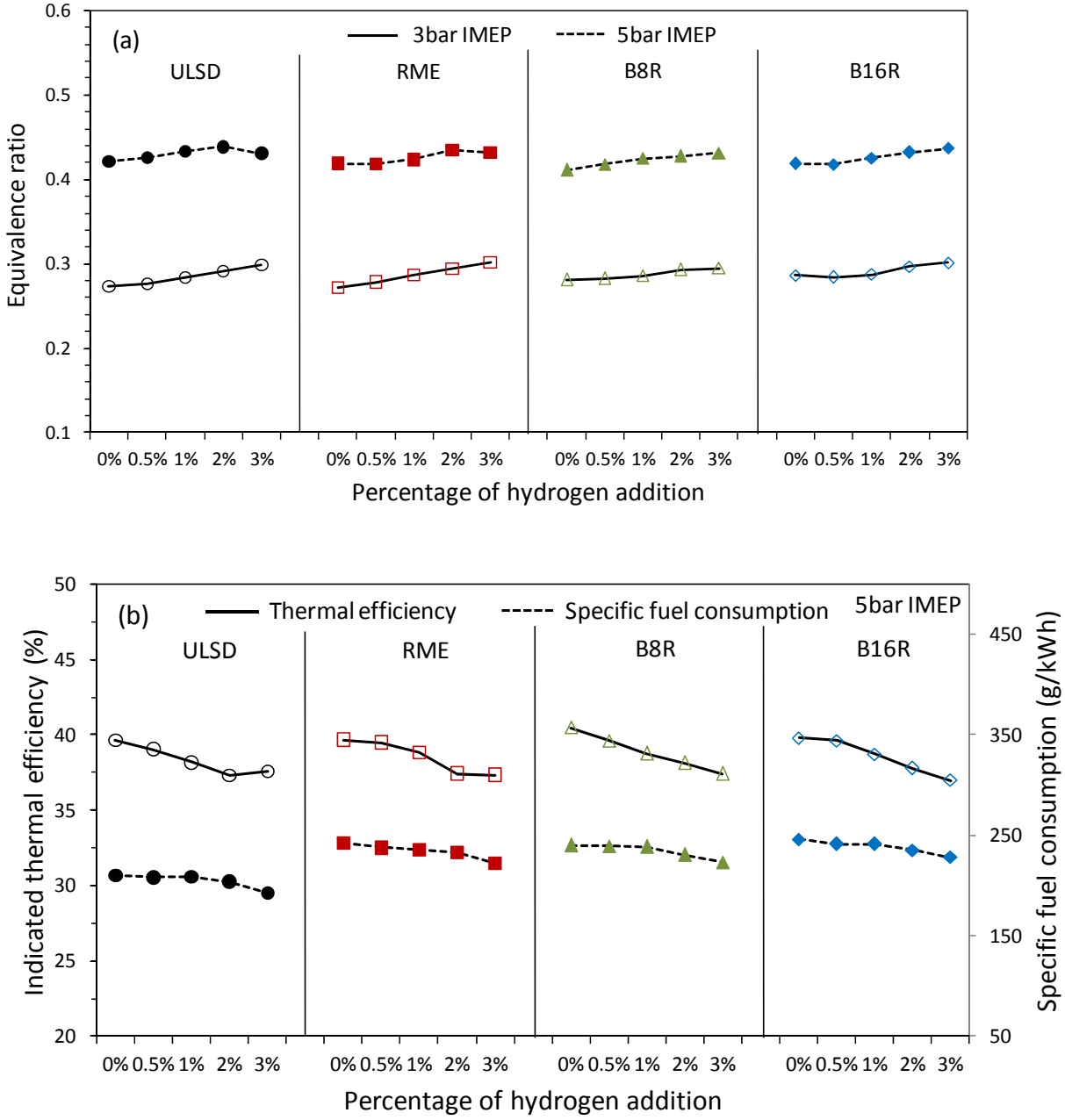

Figure 7.4: Engine operating performance at high load: (a) equivalence ratio and (b) indicated specific fuel consumption and indicated thermal efficiency

7.2 Carbonaceous gas emissions

The THC emissions are shown in Figure 7.5a. It can be seen that THC of RME was lower than ULSD for both engine loads, due to the oxygen content of biodiesel which makes the combustion more complete (Lapuerta et al., 2008b). Also, the advanced start of combustion with RME increased the available time for the oxidation of the hydrocarbon emissions. An increase in THC emissions was obtained when butanol was substituted for RME in B8R and B16R. This increase was mainly due to the high heat of vaporisation of alcohol fuels, as is explained in other work (Rakopoulos et al., 2010, Valentino et al., 2012). It is suggested that the higher heat of vaporisation of butanol cooled the combustion chamber resulting in incomplete combustion. This effect is more influential at low load conditions because the combustion temperature is lower than at high load. The addition of hydrogen to the tested fuels tended to decrease THC emissions due to the hydrogen replacing some of the liquid fuels in the combustion process. It is notable that incomplete combustion can occur due to the lack of oxygen leading to an increase in THC emissions when a high fraction of hydrogen was applied at high load (Miyamoto et al., 2011).

CO emissions of RME are lower than ULSD for both engine conditions (Figure 7.5b) and this is again the result of complete combustion due to the oxygen content of the biodiesel. The addition of butanol resulted in a decrease in CO emissions, potentially a result of the lower C/H ratio of butanol compared to RME. This effect compensated for the increase in CO with alcohol blends due to the higher heat of vaporisation and as a consequence of reduced in-cylinder temperatures. Further reductions in CO were found when hydrogen was added to the fuel blends.

The CO emissions decreased as the hydrogen content increased. As in the case of unburnt hydrocarbons emissions, this decrease is mainly due to the reduction in liquid fuel.

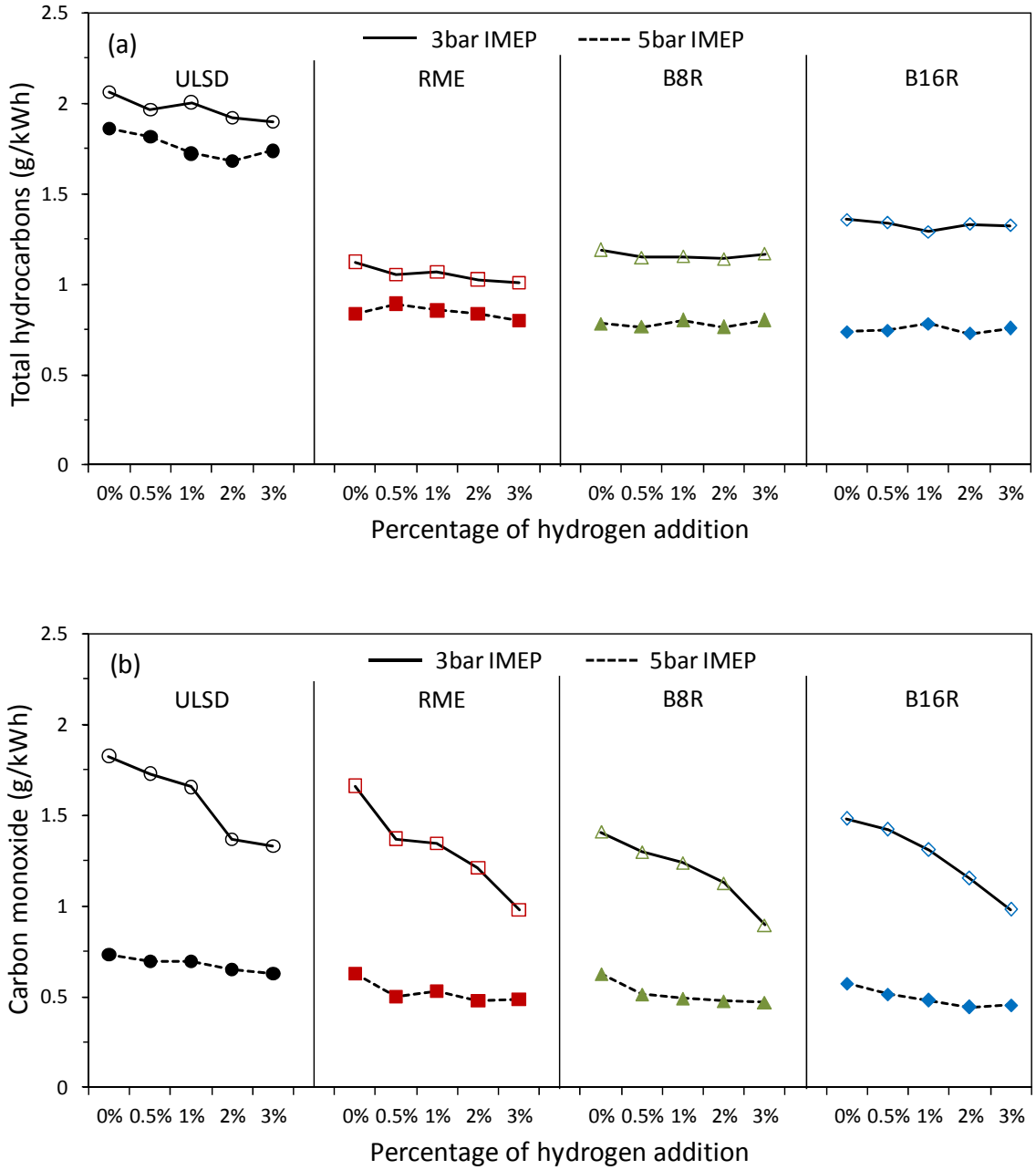

Figure 7.5: Carbonaceous gas emissions: (a) THC and (b) CO

7.3 NO_X emissions

The effect of hydrogen addition on NO_X emissions for all the tested fuels at low and high load is shown in Figure 7.6. Comparing the liquid fuels, NO emissions (Figure 7.6a) for RME and butanol blends are higher than in the case of ULSD. The reason for this is the higher bulk modulus of RME which advances injection (especially in mechanical injection systems) and as a result the start of combustion is advanced. Additionally, the oxygen content of RME can also favour NO emissions. In the case of butanol blends the poor cetane number of butanol increases the ignition delay and the rate of premixed combustion favouring NO formation. Conversely, the high heat of vaporisation of butanol cools the combustion chamber reducing NO emission. In the case of B8R (8% butanol in RME v/v) these two main effects compensate for each other resulting in similar NO emissions when butanol replaced RME. As NO_2 emissions are similar for all the tested fuels (Figure 7.6b), this resulted in similar level of total NO_X for all the fuels. However, when a higher percentage of butanol is used (B16R), the effect of the heat of vaporisation tends to be more influential and as a consequence NO_X emissions are reduced.

The addition of hydrogen significantly reduced NO emissions at low loads for all the tested fuels. As shown by Bade Shrestha et al (2000), a small addition of hydrogen reduces the NO_X due to its combustion characteristics. Also, Masood et al. (2007) and Shin et al. (2011) showed that hydrogen addition into the engine increases the fraction of H_2O, which decreases the cylinder peak temperature and NO_X emissions. However, at high load when more than 1% of hydrogen was inducted, NO emissions increased as a result of faster hydrogen combustion due to high diffusivity and the high flame speed of hydrogen (White et al., 2006).

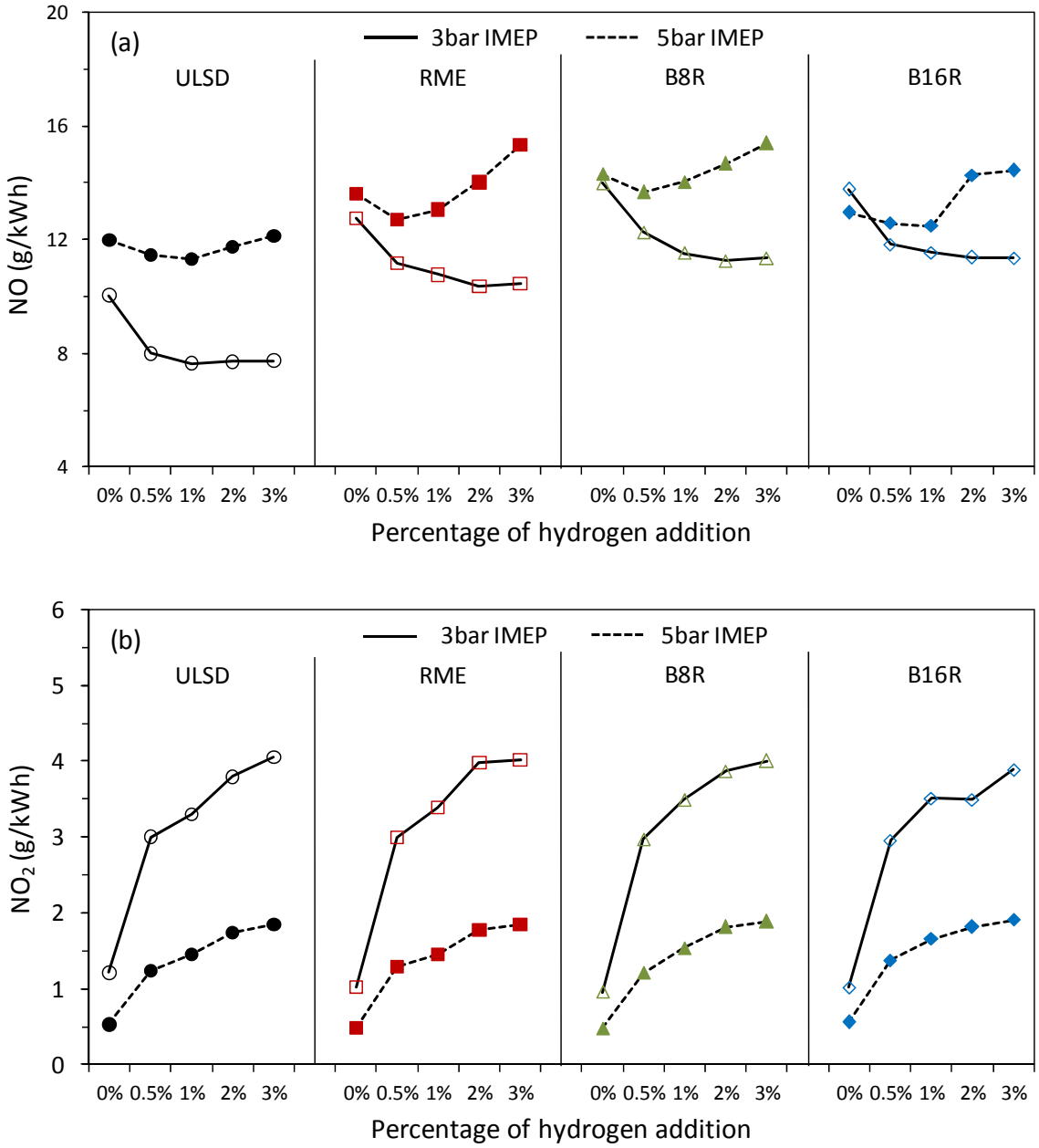

Figure 7.6: Nitrogen oxide emissions: (a) NO and (b) NO_2

These results are confirmed by the combustion traces shown in Figure 7.3. At low load the addition of hydrogen did not increase the combustion pressure, while at high load the hydrogen

addition clearly produces an increase in combustion pressure and as a consequence an increase in local combustion temperature favouring NO_X emissions.

In terms of nitrogen dioxide (NO_2), it can be seen from Figure 7.6b that the addition of hydrogen significantly increased NO_2 emissions compared to only liquid fuel combustion. The main route in the production of NO_2 is via the oxidation of NO to NO_2 with the hydroperoxyl (HO_2) radical. Therefore, the introduction of hydrogen increased the HO_2 level, as shown experimentally by Bika et al. (2008) and numerically by Lilik et al. (2010) which in turn resulted in the increase of NO_2 emissions.

At low loads the reduction in NO emissions with hydrogen was balanced by the increase in NO_2 emissions resulting in similar NO_X emissions. However, in the case of high load the increase in both NO and NO_2 emissions with hydrogen addition resulted in a larger increase in total NO_X emissions, especially when more than 1% hydrogen was used.

7.4 Particle size distribution

Particle size distributions expressed in particle number concentration are shown in Figures 7.7 and 7.8. The particle number concentrations for every particle diameter are significantly lower in the case of RME and butanol blends than ULSD at both engine loads (Figure 7.7). The reduction in the number of particles was mainly a result of the oxygen content and absence of aromatics in RME and butanol. The presence of oxygen in fuel molecules reduces the number of rich regions in the combustion chamber diminishing particle precursors and particle formation. The higher oxygen content also enhances particle and precursors oxidation. Comparing the

renewable blends, when butanol replaces RME (B8R and B16R) further reductions in particle number concentrations are obtained. This is a result of the higher oxygen content when RME is replaced by butanol and also because of the higher effectiveness of the oxygen within the alcohol group with respect to the oxygen in an ester group as it has been previously reported (Cheng et al., 2002, Lapuerta et al., 2009a, Pepiot-Desjardins et al., 2008, Westbrook et al., 2006).

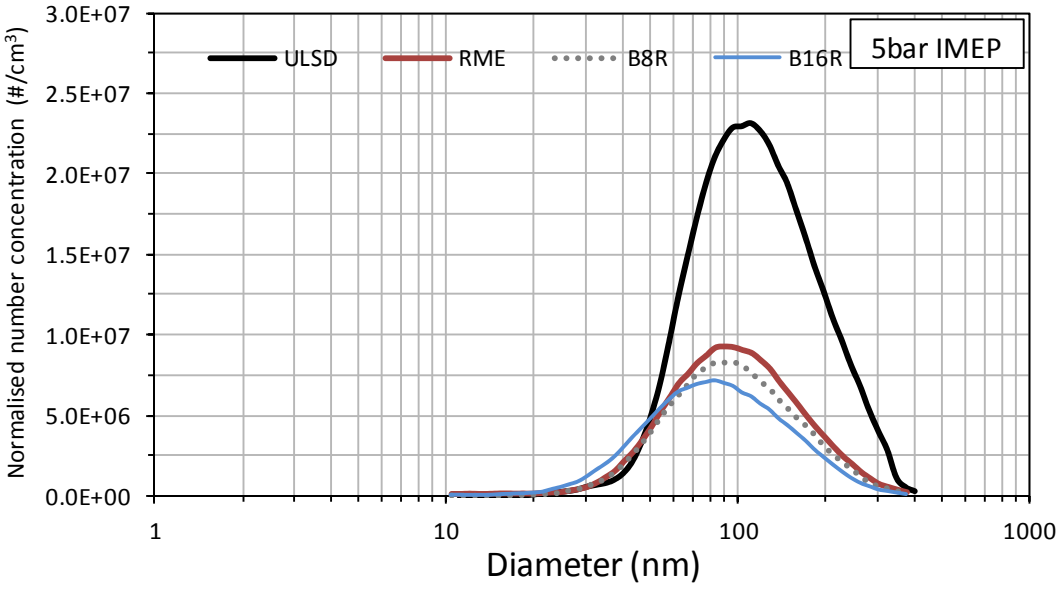

Figure 7.7: Effect of oxygenated fuels on particle size distributions at high load

Hydrogen addition produced a decrease in the particle number concentration between 30 and 300 nm at low and high engine loads, a range corresponding to where most of the particles are emitted. This reduction in particle number concentration is obtained for all the tested fuels as can be seen in Figure 7.8. Firstly, this decrease is based on the replacement of liquid fuel by hydrogen, avoids particle precursors and formation (in the absence of carbon). As part of the liquid fuel is replaced, the number of locally fuel rich zones (where particles are formed) in the

combustion chamber are reduced inhibiting soot formation. Some of hydrogen in the hydrogen-air mixture promoted the formation of OH radicals during compression and combustion, where the temperature and pressure are high enough for the reaction between oxygen and hydrogen to occur (Saxena and Williams, 2006). As the OH radical is efficient in soot and precursor oxidation, this can lead to a reduction in the particle surface area and the number of soot nuclei (Pandey et al., 2007).

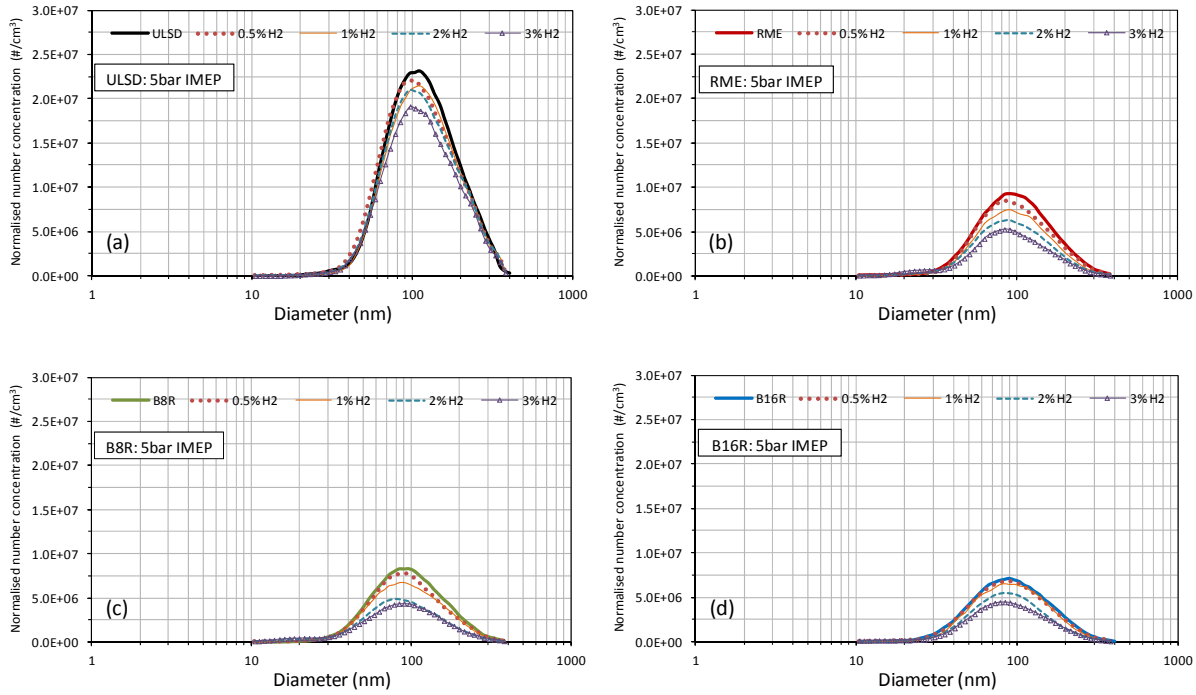

Figure 7.8: Particle size distributions at high load: (a) ULSD, (b) RME, (c) B8R and (d) B16R

Total particle number (statistical parameter derived from the particle number size distribution) is shown in Figure 7.9a. The total particle number concentration for the RME and butanol blends is notably lower than ULSD at both engine loads, due to the oxygen content and absence of aromatics in RME and butanol. The particle mass concentration was estimated from the particle number concentration using an agglomerate density function which decreases as agglomerate size increases (Lapuerta et al., 2003) (Figure 7.9b). The same trend for different liquid fuels was obtained than in the case of total particle number concentration.

The addition of hydrogen linearly decreased the total number and mass of particles for all liquid fuels at both engine loads. At high load, the overall equivalence ratio, the number of fuel rich regions in the combustion chamber and the total particle concentration are higher than at low load. The high load represents a critical condition in terms of PM formation compared to the low load and for this reason the addition of hydrogen is more effective than at low load, even though the liquid fuel replacement is lower. Comparing different fuels, at high load, hydrogen addition is equally efficient for all the tested blends, while at low load it seems to be slightly more efficient for ULSD because PM emissions are already low compared to when oxygenated blends are used.

As the number of particles is lower in the case of oxygenated fuels and with hydrogen addition, the probability of collisions between particles is reduced resulting in smaller mean diameter agglomerates overall. Smaller particles are more difficult to trap, they have a longer residence time in the atmosphere and they are more reactive (higher surface by volume ratio). As a consequence, the emission of smaller particles provokes more harmful environmental and health effects. It has to be clarified that the lower mean diameter corresponding to the particles

emitted with the oxygenated fuels and hydrogen is not caused by an increase in the number of smaller particles but a significant reduction of the number of larger particles (Kittelson, 1998).

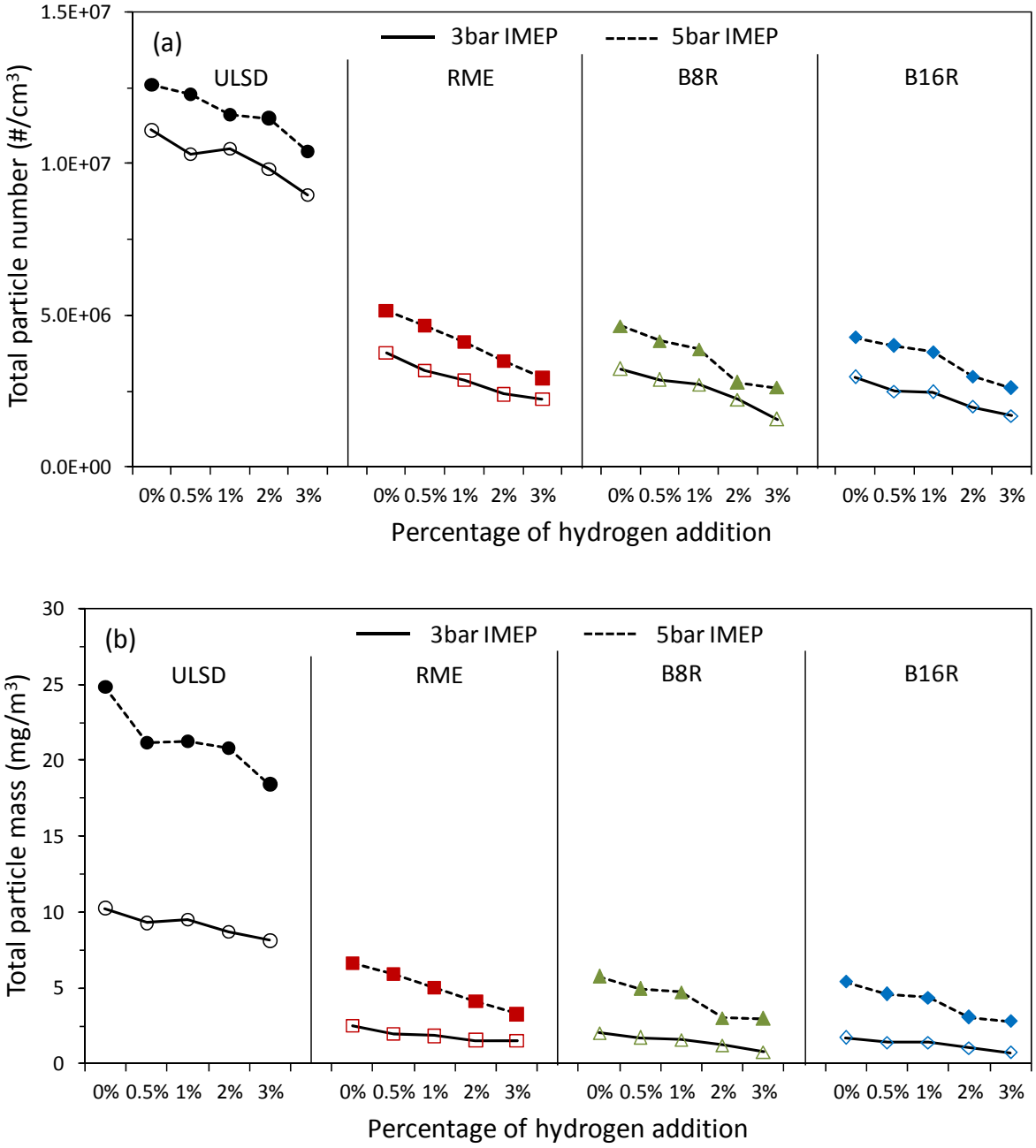

Figure 7.9: Total particle concentration: (a) number and (b) mass

7.5 Effect of oxygenated fuels, hydrogen and EGR on NO_X-PM trade-off

NO_X and PM emissions are simultaneously shown in Figure 7.10a for RME and butanol blends at different percentage of hydrogen addition. The RME emissions are used as reference curve to study the effect of butanol and hydrogen addition. The incorporation of the hydroxyl group and the increase in the oxygen content in the blended fuel when butanol replaced RME led to further reduction in PM emissions at both engine loads. This gives a double benefit of a reduction in PM obtained by the combination of butanol and hydrogen. Although in this work the hydrogen addition tends to increases NO_X emissions because of the faster combustion of hydrogen especially at high load, the use of hydrogen less than 2% of volumetric air flow rate does not show a significant penalty in NO_X emissions. In the case of B16R even though hydrogen addition slightly increases NO_X, it is concluded that the addition of hydrogen and butanol to RME results in lower PM and NO_X emissions compared to pure RME breaking the NO_X-PM trade-off.

To improve the NO_X emissions caused by the addition of hydrogen, three different conditions of EGR rate comprising of 0%, 10% and 20% were investigated and their effects on B16R blend with hydrogen addition are shown in Figure 7.10b. It can be seen that EGR showed a significant reduction in NO_X emissions. This is a well-known consequence of the dilution, chemical and thermal effects of EGR (Ladommatos et al., 2000). The recirculation of the inert gas, such as carbon dioxide and water vapour, resulted in a delay in the combustion process with the diluted air. Consequently the whole combustion process was shifted further to expansion stroke which led to lower in-cylinder temperatures, diminishing NO_X formation (SinghYadav et

al., 2012). The reduction in NO_X emissions by EGR was more distinguished than the increase caused by hydrogen addition. It is also well-established that an increase in PM emissions using EGR should be expected.

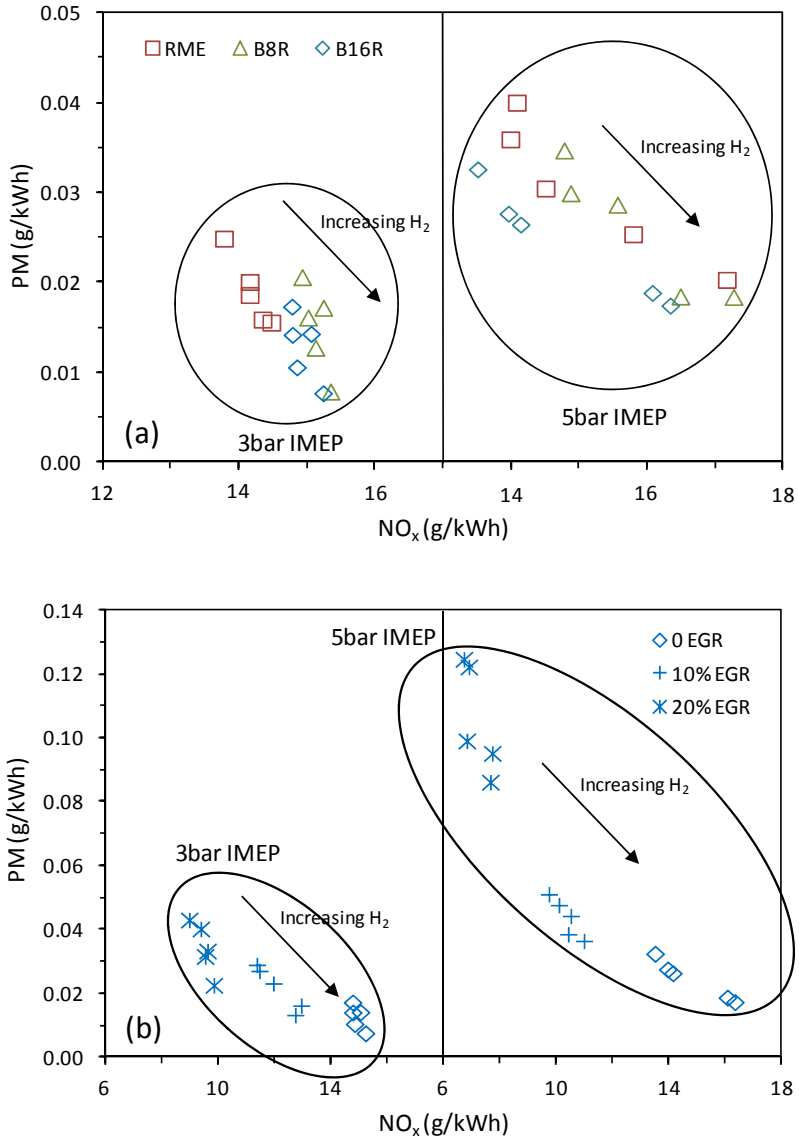

Figure 7.10: Trade-off between NO_X and PM emissions: (a) oxygenated fuels and hydrogen addition and (b) effect of EGR on B16R blend

However oxygenated fuels (such as biodiesel and alcohols) produce lower PM emissions with respect to ULSD reducing the recirculation of PM through EGR. The recirculation of less PM emissions in to the combustion chamber limited particle nucleation and surface growth reducing PM formation (Gill et al., 2012b). Therefore, for the biodiesel and alcohol blends the application of EGR resulted in a lower increase in PM emissions than in the case of ULSD, improving the trade-off between NO_X and PM emissions (Sukjit et al., 2012). Hydrogen can also assist in controlling PM emissions with EGR. For instance, when 10% EGR was applied at low load, 1% of hydrogen shows similar PM emissions compared to the engine operating without hydrogen addition and without EGR. Higher PM emissions produced by higher EGR rates may need more hydrogen to limit the PM penalty. However, it needs to be considered carefully because of the reduction in oxygen from the addition of hydrogen which could result in deficient combustion and a reduction in PM oxidation leading to no further benefits.

7.3 Summary

A study of the effect of butanol and hydrogen addition on combustion characteristics and emissions of biodiesel fuel has been conducted. This research has shown favourable synergetic effects in terms of combustion characteristics and engine-out emissions when butanol and RME are blended. Therefore, it is envisaged that a combination of renewable fuels rather than the use of one single fuel is more feasible alternative for next generation fuels. This approach will exclude the dependence on a single component as well as better emission benefits can be obtained.

The potential to combine hydrogen as a combustion enhancer with biodiesel-butanol blends has been demonstrated. The addition of hydrogen represents an ideal alternative to counteract some of the combustion and emissions penalties (e.g. THC) due to the presence of butanol in the blended fuel. Further beneficial emission effects (e.g. CO, PM) are found through the interaction of hydrogen with these blends. However, it is suggested a limit in the hydrogen induction at high load as further hydrogen significantly increases NO_X emissions.

The increase in NO_X emissions caused by the hydrogen addition can be effectively controlled through EGR system without an excessive PM penalty due to the existence of the PM concentration which is emitted from the combustion of alcohol-biodiesel blends is low in the exhaust gas. It is envisaged that this PM emissions benefit as well as the increase in the NO_2/NO_X ratio will have significant benefits in the function of aftertreatment systems (e.g. enhance passive regeneration in the diesel particulate filter).

CHAPTER 8

CONCLUSIONS

This thesis details the research conducted in an attempt to extend the use of bio-derived (or alternative) alcohol-diesel blends in compression ignition. Biodiesel has been shown to improve lubricating properties of blended diesel fuels. The results given offer an understanding of the effect of molecular structure of methyl esters on fuel properties and emissions of alcohol-diesel blends. This is information that can be applied to improve the penetration of alcohol use in diesel engines in conjunction with biodiesel. Further study has been performed on the incorporation of hydrogen and alcohol blends, hydrogen being used as a combustion enhancer whilst simultaneously reducing carbonaceous gas emissions. The overriding conclusions of this research programme are presented in this chapter and from these recommendations for future work are also proposed.

8.1 Concluding remarks

The use of biodiesel is a very effective way to enhance the lubricating properties of blended diesel fuels. The adsorption of the polar compounds derived from the methyl esters on to the friction surfaces increases the stability and thickness of developed lubricating film, resulting in a reduction in wear scar and an improvement of boundary lubrication. This will ultimately lead to an improvement in the performance and durability of fuel injection equipment. Recommendations on the optimum blend proportion of biodiesel (derived from rapeseed) have been made such that acceptable levels of lubricity are achieved. These were 10% - 15% by

volume. Topography measurements showed the formation of a residue when biodiesel was blended in the fuels and composition analysis indicated a predominately carbon formation (waxy carbon) on the worn surfaces that correlated with wear scar diameters.

The most representative individual fatty acid methyl esters including methyl esters of lauric acid, myristic acid, palmitic acid, stearic acid, and oleic acid were added to alcohol-diesel blends in order to understand the effect of carbon chain length and degree of unsaturation on lubricating properties, blend stability, combustion characteristics and emissions. The results showed that 15% of all methyl esters were enough to avoid phase separation of alcohol-diesel blends and keep the wear scar diameter of the blends below the limitation required by the European lubricity standard. The combustion of the blends containing short chain length methyl esters reduces CO, THC and soot emissions. This is mainly due to lower viscosity,bulk modulus and higher oxygen content. The blends with unsaturated compounds reduced THC, CO and soot emissions as a result of their lower viscosity and higher volatility. However, they clearly produced higher NO_X, soot, CO and THC emissions than short chain length saturated methyl esters. It is recommended that short carbon chain length and saturated methyl esters are a very effective means of improving alcohol blends. A comparison between two different alcohols used in the engine tests, where butanol blends showed more potential to reduce exhaust emissions compared to ethanol blends.

More studies on the effect of molecular structure of methyl esters were conducted to understand how the hydroxyl group existing in biodiesel influenced fuel properties and emissions of butnaol-diesel blends. Hydroxylated biodiesel (castor oil methyl esters) which, in its pure form, cannot be used as a biodiesel fuel due to its extremely high viscosity and density showed

favourable synergetic effects in terms of fuel blend properties, combustion characteristics and engine-out emissions when combined with butanol. An intensive investigation on PM emissions of tested fuels reported that the presence of the hydroxyl group in castor oil methyl esters was more effective in restraining soot precursors and soot formation than common biodiesels. The temperature needed to oxidise soot emissions also was lower in the case of hydroxylated biodiesel resulting in a potential decrease in the number of active regeneration cycles and an increase in the lifetime of the diesel particulate filter.

Further improvements were evident in the use of alcohol blends in diesel engines in term of exhaust emissions, especially carbonaceous gas emissions, were found when some of liquid fuel blends were replaced by the combustion of hydrogen. The addition of hydrogen showed an ideal alternative to counteract some emissions penalties (e.g. THC and CO) due to the presence of alcohol in the blended fuels. The penalty of using hydrogen was shown to be an increase in NO_X emissions due to the increase in NO_2 formation during combustion. The main route in the production of NO_2 was via the oxidation of NO to NO_2 with HO_2 radicals which increased with hydrogen combustion. It is suggested that the limit in hydrogen induction is 2% of volumetric air flow rate to avoid the penalty in NO_X emissions. This may be produced using an on-board fuel reforming process.

This thesis has described the design and use of multi-component renewable fuel blends in diesel engines, with the aim of improving combustion and reducing emissions when compared to diesel fuels. The research has shown favourable synergetic effects in terms of fuel blend properties, combustion characteristics and engine-out emissions when biodiesel and alcohols are blended with diesel fuels. The tri-blend fuels tested have also alleviated the potential drawback of

increased NO_X emissions, when biodiesels are used with the addition of alcohol (as a consequence of high enthalpy of vaporisation of alcohol). The use of biodiesel in the tri-blends has also improved some of the inferior properties such as lubricity of alcohol blended with diesel fuels. This is particularly the case when hydroxylated biodiesel is used as a result of the hydroxyl group. The implementation of EGR with oxygenated blends and hydrogen is an attractive approach to reduce NO_X emissions while reducing PM penalty associated with EGR through limiting the PM and hydrocarbon recirculation. The influence of molecular structure of methyl esters and hydrogen used to extend the use of alcohol-diesel blends on regulated emissions is summarised in Table 8.1.

8.2 Future work

The investigation into extending the use of alcohol-diesel blends in diesel engines has shown that the addition of methyl esters and hydrogen to the blends are a very effective means of improving fuel properties, combustion characteristics and exhaust emissions of alcohol-diesel blends. To further extend this research the following recommendations are suggested.

- The carbon deposit on mating specimens under the lubrication of difference fuel blends should be investigated to understand what kind of carbon structure deposits on the specimens to form more stable and stronger lubrication film resulting in an improvement of lubricating properties of the fuel blends.
- More details on the stability of alcohol-diesel blends with methyl esters should be studied to characterise liquid emulsions and aspect of different phase separations.

- Oxygenated fuel with high cetane number such as diethylene glycol dimethyl ether (DGM) and diethylene glycol diethyl ether (DGE) has potential as a blend component to extend the use of alcohol-diesel blends in compression ignition engines. The high cetane number of these oxygenated fuels can compensate for a reduction in alcohol induced cetane number. Moreover the ether functional group can be more beneficial to inhibit the soot precursors and soot formation compared to hydroxyl and ester group.

- Implementation of a measurement system to more accurately measure/control injection settings (e.g. start of injection) and EGR rate (e.g. based on CO_2 concentration).

- Currently commercial fuels may contain some additives to meet lubricity standard requirements therefore it is worth to know which additives are employed and how the additives affect the fuel properties and emissions of fuel blends.

Table 8.1: The influence of molecular structure of methyl esters and hydrogen on regulated emissions

An increase in parameter	THC	CO	NO_X	PM
Methyl esters				
Chain length	**Increase** - Decrease oxygen content (Increase THC) - Increase viscosity (Increase THC)	**Increase** - Decrease oxygen content (Increase CO) - Increase viscosity (Increase CO)	**No clear trend** - Decrease oxygen content (Reduce NO_X) - Increase bulk modulus (Increase NO_X) - Increase cetane number (Reduce NO_X) - Increase adiabatic flame temperature (Increase NO_X)	**Increase** - Decrease oxygen content (Increase PM) - Increase melting point (Increase PM) - Increase viscosity (Increase PM)
Unsaturation degree	**Decrease** - Decrease viscosity (Reduce THC)	**Decrease** - Decrease viscosity (Reduce CO)	**Increase** - Increase bulk modulus (Increase NO_X) - Decrease cetane number (Increase NO_X) - Increase adiabatic flame temperature (Increase NO_X)	**Decrease** - Decrease melting point (Reduce PM) - Decrease viscosity (Reduce PM)
Hydroxyl group	**Tend to Decrease** - Increase oxygen content (Reduce THC) - Increase viscosity (Increase THC)	**Tend to Decrease** - Increase oxygen content (Reduce CO) - Increase viscosity (Increase CO)	**Increase** - Decrease cetane number (Increase NO_X) - Less soot to absorb heat during combustion (Increase NO_X)	**Decrease** - Increase oxygen content (Reduce PM) - More potential of function group to inhibit soot formation (Reduce PM)
Hydrogen	**Decrease** - Liquid fuel replacement (Reduce THC)	**Decrease** - Liquid fuel replacement (Reduce CO)	**Increase** - Faster hydrogen combustion (Increase NO_X) - Increase HO_2 radicals (Increase NO_2)	**Decrease** - Liquid fuel replacement (Reduce PM) - Promote OH radicals (Reduce PM)

AUTHOR PUBLICATIONS

1. Sukjit, E, Dearn, KD. Enhancing the lubricity of an environmentally friendly Swedish diesel fuel MK1. Wear. 2011;271(9-10):1772-7.

2. Sukjit E, Dearn KD, Tsolakis A. Interrogating the surface: the effect of blended diesel fuels on lubricity. SAE International Journal of Fuels and Lubricants. 2012;5(1): 154-162. DOI: 10.4271/2011-01-1940.

3. Sukjit E, Herreros JM, Dearn KD, García-Contreras R, Tsolakis A. The effect of the addition of individual methyl esters on the combustion and emissions of ethanol and butanol -diesel blends. Energy. 2012;42(1):364-74.

4. Sukjit E, Herreros JM, Piaszyk J, Dearn KD, Tsolakis A. Finding synergies in fuels properties for the design of renewable fuels − hydroxylated biodiesel effects on butanol-diesel blends. Environmental Science & Technology. 2013;47:3535-42.

5. Sukjit E, Herreros JM, Dearn KD, Tsolakis A, Theinnoi K. Effect of hydrogen on butanol-biodiesel blends in compression ignition engines. International Journal of Hydrogen Energy. 2013;38(3):1624-35.

LIST OF REFFERENCES

ABD-ALLA, G. H., SOLIMAN, H. A., BADR, O. A. & ABD-RABBO, M. F. (2001) Effects of diluent admissions and intake air temperature in exhaust gas recirculation on the emissions of an indirect injection dual fuel engine. *Energy Conversion and Management,* 42**,** 1033-1045.

ABU-JRAI, A., RODRÍGUEZ-FERNÁNDEZ, J., TSOLAKIS, A., MEGARITIS, A., THEINNOI, K., CRACKNELL, R. F. & CLARK, R. H. (2009) Performance, combustion and emissions of a diesel engine operated with reformed EGR. Comparison of diesel and GTL fuelling. *Fuel,* 88**,** 1031-1041.

AGARWAL, A. K. (2007) Biofuels (alcohols and biodiesel) applications as fuels for internal combustion engines. *Progress in Energy and Combustion Science,* 33**,** 233-271.

ANASTOPOULOS, G., LOIS, E., SERDARI, A., ZANIKOS, F., STOURNAS, S. & KALLIGEROS, S. (2001) Lubrication properties of loe sulfur diesel fuels in the presence of specific types of fatty acid derivatives. *Energy & Fuels,* 15**,** 106-112.

ARMAS, O., GARCÍA-CONTRERAS, R. & RAMOS, Á. (2012) Pollutant emissions from engine starting with ethanol and butanol diesel blends. *Fuel Processing Technology,* 100**,** 63-72.

ARMAS, O., HERNÁNDEZ, J. J. & CÁRDENAS, M. D. (2006) Reduction of diesel smoke opacity from vegetable oil methyl esters during transient operation. *Fuel,* 85**,** 2427-2438.

ARMAS, O., MARTÍNEZ-MARTÍNEZ, S. & MATA, C. (2011) Effect of an ethanol-biodiesel-diesel blend on a common rail injection system. *Fuel Processing Technology,* 92**,** 2145-2153.

BADE SHRESTHA, S. O., LEBLANC, G., BALAN, G. & DE SOUZA, M. (2000) A before treatment method for reduction of emissions in diesel engines. *SAE Paper*.

BAKEAS, E., KARAVALAKIS, G. & STOURNAS, S. (2011) Biodiesel emissions profile in modern diesel vehicles. Part 1: Effect of biodiesel origin on the criteria emissions. *Science of the Total Environment,* 409**,** 1670-1676.

BARABÁS, I. & TODORUȚ, A. I. (2009) Key fuel properties of biodiesel-diesel fuel-ethanol blends. *SAE Paper*.

BERMAN, P., NIZRI, S. & WIESMAN, Z. (2011) Castor oil biodiesel and its blends as alternative fuel. *Biomass and Bioenergy,* 35**,** 2861-2866.

BHATNAGAR, A. K., KAUL, S., CHHIBBER, V. K. & GUPTA, A. K. (2006) HFRR studies on methyl esters of nonedible vegetable oils. *Energy & Fuels,* 20**,** 1341-1344.

BIKA, A. S., FRANKLIN, L. M. & KITTELSON, D. B. (2008) Emissions effects of hydrogen as a supplemental fuel with diesel and biodiesel. *SAE Paper*.

BOWMAN, C. T. (1975) Kinetics of pollutant formation and destruction in combustion. *Progress in Energy and Combustion Science,* 1**,** 33-45.

BURTSCHER, H., STEFAN, S. & HUGLIN, C. (1998) Characterization of particles in combustion engine exhaust. *Journal of Aerosol Science,* 29**,** 389-396.

CAN, Ö., ÇELIKTEN, İ. & USTA, N. (2004) Effects of ethanol addition on performance and emissions of a turbocharged indirect injection Diesel engine running at different injection pressures. *Energy Conversion Management,* 45**,** 2429-2440.

CANAKCI, M. (2007) Combustion characteristics of a turbocharged DI compression ignition engine fueled with petroleum diesel fuels and biodiesel. *Bioresource Technology,* 98**,** 1167-1175.

CARDONE, M., PRATI, M. V., ROCCO, V., SEGGIANI, M., SENATORE, A. & VITOLO, S. (2002) Brassica carinata as an alternative oil crop for the production of biodiesel in italy: Engine Performance and Regulated and Unregulated Exhaust Emissions. *Environmental Science & Technology,* 36**,** 4656-4662.

CHAE, J. O., HAN, D. S., LEE, S. M., JEONG, Y. S., CHUN, Y. N. & CHUNG, S. C. (1994) A study on the performance and particulate emission characteristics for the hydrogen-premixed diesel engine. *XXV FISITA Congress.*

CHENG, A. S., DIBBLE, R. W. & BUCHHOLZ, B. A. (2002) The effect of oxygenates on diesel engine particulate matter. *SAE Paper.*

COHEN, A. J., ANDERSON, H. R., OSTRO, B., PANDEY, K. D., KRZYZANOWSKI, M., KÜNZLI, N., GUTSCHMIDT, K., POPE, A., ROMIEU, I., SAMET, J. M. & SMITH, K. R. (2005) The global burden of disease due to outdoor air pollution. *Journal of Toxicology and Environmental Health: Part A,* 68**,** 1-7.

CORKWELL, K. C. & JACKSON, M. M. (2002) Lubricity and injector pump wear issues with E diesel fuel blends. *SAE Paper*.

DEC, J. E. (1997) A conceptual model of DI diesel combustion based on laser-sheet imaging. *SAE Paper*.

DI, Y., CHEUNG, C. S. & HUANG, Z. (2009) Experimental investigation on regulated and unregulated emissions of a diesel engine fueled with ultra-low sulfur diesel fuel blended with biodiesel from waste cooking oil. *Science of the Total Environment,* 407**,** 835-846.

DOĞAN, O. (2011) The influence of n-butanol/diesel fuel blends utilization on a small diesel engine performance and emissions. *Fuel,* 90**,** 2467-2472.

DORADO, M. P., BALLESTEROS, E., ARNAL, J. M., GÓMEZ, J. & LÓPEZ, F. J. (2003) Exhaust emissions from a Diesel engine fueled with transesterified waste olive oil. *Fuel,* 82**,** 1311-1315.

EN-590 (2009) Automotive fuels-diesel requirements and test methods.

EN-14214 (2003) Automotive fuels-diesel-fatty acid methyl ester (FAMEs) - requirements and test methods.

FERGUSON, C. R. (1986) *Internal Combustion Engines: Applied Thermosciences,* New York, Wiley.

FERNANDO, S., HALL, C. & JHA, S. (2006) NO_X reduction from biodiesel fuels. *Energy & Fuels,* 20**,** 376-382.

FUKUMOTO, M., OGUMA, M. & GOTO, S. (2003) Experimental investigation of lubricity improvement of gas to liquid (GTL) fuels with additives for low sulphur diesel fuel. *SAE Paper*.

FUKUSHIMA, H., ASANO, I., NAKAMURA, S., ISHIDA, K. & GREGORY, D. (2000) Signal processing and practical performance of a real-time PM analyzer using fast FIDs. *SAE Paper*.

GELLER, D. P. & GOODRUM, J. W. (2004) Effects of specific fatty acid methyl esters on diesel fuel lubricity. *Fuel,* 83**,** 2351-2356.

GILL, S. S., TSOLAKIS, A., HERREROS, J. M. & YORK, A. P. E. (2012a) Diesel emissions improvements through the use of biodiesel or oxygenated blending components. *Fuel,* 95**,** 578-586.

GILL, S. S., TURNER, D., TSOLAKIS, A. & YORK, A. P. E. (2012b) Controlling soot formation with filtered EGR for diesel and biodiesel fuelled engines. *Environment Science & Technology,* 46**,** 4215-4222.

GOODGER, E. M. (2000) *Transport Fuels Technology: Mobility for the Millennium,* Norwich, Landfall Press.

GOODRUM, J. W. & GELLER, D. P. (2005) Influence of fatty acid methyl esters from hydroxylated vegetable oils on diesel fuel lubricity. *Bioresource Technology,* 96**,** 851-855.

GOSWAMI, D. Y., MIRABAL, S. T., GOEL, N. & INGLEY, H. A. (2003) A review of hydrogen production technologies. *First International Conference on Fuel Cell Science.* Engineering and Technology.

GOUW, T. H. & VLUGTER, J. C. (1964a) Physical properties of fatty acid methyl esters I. Density and molar volume. *Journal of the Americal Oil Chemists Society,* 41**,** 142-145.

GOUW, T. H. & VLUGTER, J. C. (1964b) Physical propertiesof fatty acid methyl esters IV: Ultrasonic sound velocity. *Journal of the Americal Oil Chemists Society,* 41**,** 524-526.

GRABOSKI, M. S. & MCCORMICK, R. L. (1998) Combustion of fat and vegetable oil derived fuels in diesel engines. *Progress in Energy and Combustion Science,* 24**,** 125-164.

GRABOSKI, M. S., MCCORMICK, R. L., ALLEMAN, T. L. & HERRING, A. M. (2003) *The Effect of Biodiesel Composition on Engine Emissions from a DDC Series60 Diesel Engine,* Colorado, National Renewable Energy Laboratory.

GRABOSKI, M. S., ROSS, J. D. & MCCORMICK, R. L. (1996) Transient emissions from No.2 diesel and biodiesel blends in a DDC series 60 engine *SAE Paper*.

HAAS, M. J., SCOTT, K. M., ALLEMAN, T. L. & MCCORMICK, R. L. (2001) Engine performance of biodiesel fuel prepared from soybean soapstock: A high quality renewable fuel produced from a waste feedstock *Energy & Fuels,* 15**,** 1207-1212.

HANSEN, K. F. & JENSEN, M. G. (1997) Chemical and biological characteristics of exhaust emissions from a DI diesel engine fuelled with rapeseed oil methyl ester (RME). *SAE Paper*.

HE, B.-Q., SHUAI, S.-J., WANG, J.-X. & HE, H. (2003) The effect of ethanol blended diesel fuels on emissions from a diesel engine. *Atmospheric Environment,* 37**,** 4965-4971.

HERREROS, J. M. (2010) Framework to optimize the use of alternative fuels in motorsport. Case study: emission benefits in compression ignition engines. *School of applied sciences motorsport engineering and management.* Cranfield university.

HEYWOOD, J. B. (1988) *Internal Combustion Engine Fundamentals,* New York, McGraw-Hill.

ISHIDA, M., YAMAMOTO, S., UEKI, H. & SAKAGUCHI, D. (2010) Remarkable improvement of NOx-PM trade-off in a diesel engine by means of bioethanol and EGR. *Energy,* 35**,** 4572-4581.

ISO12156-1 (2006) Diesel fuel: Assessment of lubricity using the high frequency reciprocating rig (HFRR). *Part 1: Test Method.*

KARABEKTAS, M. & HOSOZ, M. (2009) Performance and emission characteristics of a diesel engine using isobutanol-diesel fuel blends. *Renewable Energy,* 34**,** 1554-1559.

KASS, M. D., THOMAS, J. F., STOREY, J. M., DOMINGO, N., WADE, J. & KENRECK, G. (2001) Emissions from a 5.9 liter diesel engine fueled with ethanol diesel blends. *SAE Paper.*

KITTELSON, D. B. (1998) Engines and nanoparticles: a review. *Journal of Aerosol Science,* 29**,** 575-588.

KNOTHE, G. (2005) Dependence of biodiesel fuel properties on the structure of fatty acid alkyl esters. *Fuel Processing Technology,* 86**,** 1059-1070.

KNOTHE, G., SHARP, C. A. & RYAN, T. W. (2006) Exhaust emissions of biodiesel, petrodiesel, neat methyl esters, and alkanes in a new technology engine. *Energy & Fuels,* 20**,** 403-408.

KNOTHE, G. & STEIDLEY, K. R. (2005) Kinematic viscosity of biodiesel fuel components and related compounds. Influence of compound structure and comparison to petrodiesel fuel components. *Fuel,* 84**,** 1059-1065.

KORAKIANITIS, T., NAMASIVAYAM, A. M. & CROOKES, R. J. (2010) Hydrogen dual-fuelling of compression ignition engines with emulsified biodiesel as pilot fuel. *International Journal of Hydrogen Energy,* 35**,** 13329-13344.

KRAHL, J., MUNACK, A., SCHRODER, O., STEIN, H. & BUNGER, J. (2003) Influence of biodiesel and different designed diesel fuels on the exhaust gas emissions and health effects. *SAE Paper*.

KWANCHAREON, P., LUENGNARUEMITCHAI, A. & JAI-IN, S. (2007) Solubility of a diesel-biodiesel-ethanol blend, its fuel properties, and its emission characteristics from diesel engine. *Fuel,* 86**,** 1053-1061.

LABECKAS, G. & SLAVINSKAS, S. (2006) The effect of rapeseed oil methyl ester on direct injection diesel engine performance and exhaust emissions. *Energy Conversion and Management,* 47**,** 1954-1967.

LACEY, P., KOENTZ, J. M., GAIL, S., MILOVANOIC, N., STEVENSON, P., STRANDLING, R., CLARK, R. H. & BOONWATSAKUL, R. (2010) Evaluation of Fischer-Tropsch fuel performance in advanced diesel rail FIE. *SAE Paper*.

LADOMMATOS, N., ABDELHALIM, S. & ZHAO, H. (2000) The effects of exhaust gas recirculation on diesel combustion and emissions. *International Journal of Engine Research,* 1**,** 107-126.

LAKKIREDDY, R. V., MOHAMMED, H. & JOHNSON, H. J. (2006) The effect of a diesel oxidation catalyst and a catalyzed particulate filter on particle size distribution from a heavy duty diesel engine. *SAE Paper*.

LAMBE, S. M. & WATSON, H. C. (1992) Low polluting energy efficient C.I. hydrogen engine. *International Journal of Hydrogen Energy,* 17**,** 513-525.

LAPUERTA, M., ARMAS, O., BALLESTEROS, R. & FERNÁNDEZ, J. (2005) Diesel emissions from biofuels derived from Spanish potential vegetable oils. *Fuel,* 84**,** 773-780.

LAPUERTA, M., ARMAS, O. & GARCÍA-CONTRERAS, R. (2009a) Effect of ethanol on blending stability and diesel engine emissions. *Energy & Fuels,* 23**,** 4343-4354.

LAPUERTA, M., ARMAS, O. & GÓMEZ, A. (2003) Diesel particle size distribution estimation from digital image analysis. *Aerosol Science and Technology,* 37**,** 369-381.

LAPUERTA, M., ARMAS, O. & HERREROS, J. M. (2008a) Emissions from a diesel-bioethanol blend in an automotive diesel engine. *Fuel,* 87**,** 25-31.

LAPUERTA, M., ARMAS, O. & RODRÍGUEZ-FERNÁNDEZ, J. (2008b) Effect of biodiesel fuels on diesel engine emissions. *Progress in Energy and Combustion Science,* 34**,** 198-223.

LAPUERTA, M., BALLESTEROS, R. & RODRÍGUEZ-FERNÁNDEZ, J. (2007) Thermogravimetric analysis of diesel particulate matter. *Measurement Science and Technology,* 18**,** 650-658.

LAPUERTA, M., GARCIA-CONTRERAS, R. & AGUDELO, J. R. (2010a) Lubricity of ethanol-biodiesel-diesel fuel blends. *Energy & Fuels,* 24**,** 1374-1379.

LAPUERTA, M., GARCÍA-CONTRERAS, R., CAMPOS-FERNÁNDEZ, J. & DORADO, M. P. (2010b) Stability, lubricity, viscosity, and cold-flow properties of alcohol-diesel blends. *Energy & Fuels,* 24**,** 4497-4502.

LAPUERTA, M., HERREROS, J. M., LYONS, L. L., GARCÍA-CONTRERAS, R. & BRICEÑO, Y. (2008c) Effect of the alcohol type used in the production of waste cooking oil biodiesel on diesel performance and emissions. *Fuel,* 87**,** 3161-3169.

LAPUERTA, M., OLIVA, F., AGUDELO, J. R. & BOEHMAN, A. L. (2012) Effect of fuel on the soot nanostructure and consequences on loading and regeneration of diesel particulate filters. *Combustion and Flame,* 159**,** 844-853.

LAPUERTA, M., RODRÍGUEZ-FERNÁNDEZ, J., OLIVA, F. & CANOIRA, L. (2009b) Biodiesel from low-grade animal fats: Diesel engine performance and emissions. *Energy & Fuels,* 23**,** 121-129.

LATA, D. B. & MISRA, A. (2010) Theoretical and experimental investigations on the performance of dual fuel diesel engine with hydrogen and LPG as secondary fuels. *International Journal of Hydrogen Energy,* 35**,** 11918-11931.

LAVOIE, G. A., HEYWOOD, J. B. & KECK, J. C. (1970) Experimental and theoretical study of nitric oxide formation in internal combustion engines. *Combustion Science and Technology,* 1**,** 313-326.

LI, D.-G., ZHEN, H., XINGCAI, L., WU-GAO, Z. & JIAN-GUANG, Y. (2005) Physico-chemical properties of ethanol-diesel blend fuel and its effect on performance and emissions of diesel engines. *Renewable Energy,* 30**,** 967-976.

LILIK, G. K., ZHANG, H., HERREROS, J. M., HAWORTH, D. C. & BOEHMAN, A. L. (2010) Hydrogen assisted diesel combustion. *International Journal of Hydrogen Energy,* 35**,** 4382-4398.

LUJAJI, F., KRISTOF, L., BERECZKY, A. & MBARAWA, M. (2011) Experimental investigation of fuel properties, engine performance, combustion and emissions of blends containing croton oil, butanol, and diesel on a CI engine. *Fuel,* 90**,** 505-510.

MAJEWSKI, W. A. & KHAIR, M. K. (2006) *Diesel Emissions and Their Control,* Warrendale, SAE International.

MASOOD, M., ISHRAT, M. M. & REDDY, A. S. (2007) Computational combustion and emission analysis of hydrogen-diesel blends with experimental verification. *International Journal of Hydrogen Energy,* 32**,** 2539-2547.

MEHTA, R. N., CHAKRABORTY, M., MAHANTA, P. & PARIKH, P. A. (2010) Evaluation of fuel properties of butanol-biodiesel-diesel blends and their impact on engine performance and emissions. *Industrial & Engineering Chemistry Research,* 49**,** 7660-7665.

MIERS, S. A., CARLSON, R. W., MCCONNELL, S. S., NG, H. K., WALLNER, T. & ESPER, J. L. (2008) Drive cycle analysis of butanol/diesel blends in a light-duty vehicle. *SAE Paper*.

MIYAMOTO, T., HASEGAWA, H., MIKAMI, M. & KOJIMA, N. (2011) Effect of hydrogen addition to intake gas on combustion and exhaust emission characteristics of a diesel engine. *International Journal of Hydrogen Energy,* 36**,** 13138-13149.

MONYEM, A., VAN GERPEN, J. H. & CANAKCI, M. (2001) The effect of timing and oxidation on emissions from biodiesel-fueled engines. *Transactions of the ASAE,* 44**,** 35-42.

MUELLER, C. J., PITZ, W. J., PICKETT, L. M., MARTIN, G. C., SIEBERS, D. L. & WESTBROOK, C. K. (2003) Effects of oxygenates on soot processes in DI diesel engines: Experiments and numerical simulations. *SAE Paper*.

MUNACK, A., SCHRÖDER, O., KRAHL, J. & BÜNGER, J. (2001) Comparison of relevant gas emissions from biodiesel and fossil diesel fuel. *Agricultural Engineering International: the CIGR Journal of Scientific Research and Development* Manuscript EE 01 001. Vol. III

MURILLO, S., MÍGUEZ, J. L., PORTEIRO, J., GRANADA, E. & MORÁN, J. C. (2007) Performance and exhaust emissions in the use of biodiesel in outboard diesel engines. *Fuel,* 86**,** 1765-1771.

NABI, M. N., AKHTER, M. S. & ZAGLUL SHAHADAT, M. M. (2006) Improvement of engine emissions with conventional diesel fuel and diesel-biodiesel blends. *Bioresource Technology,* 97**,** 372-378.

NIKANJAM, M. & RUTHERFORD, J. (2006) Improving the precision of the HFRR lubricity test. *SAE Paper.*

OGUMA, M., GOTO, S. & CHEN, Z. (2004) Fuel characteristics evaluation of GTL for DI diesel engine. *SAE Paper*.

OSMONT, A., CATOIRE, L. & GÖKALP, I. (2007) Thermochemistry of methyl and ethyl esters from vegetable oils, International Journal of Chemical Kinetics. *International Journal of Chemical Kinetics* 39**,** 481-491.

PANDEY, P., PUNDIR, B. P. & PANIGRAHI, P. K. (2007) Hydrogen addition to acetylene: air laminar diffusion flames: Studies on soot formation under different flow arrangements. *Combustion and Flame,* 148**,** 249-262.

PANUCCIO, G. J. & SCHMIDT, L. D. (2007) Species and temperature profiles in a differential sphere bed reactor for the catalytic partial oxidation of n-octane. *Applied Catalysis A: General,* 332**,** 171-182.

PEPIOT-DESJARDINS, P., PITSCH, H., MALHOTRA, R., KIRBY, S. R. & BOEHMAN, A. L. (2008) Structural group analysis for soot reduction tendency of oxygenated fuels. *Combustion and Flame,* 154**,** 191-205.

PINTO, A. C., GUARIEIRO, L. L. N., REZENDE, M. J. C., RIBEIRO, N. M., TORRES, E. A., LOPES, W. A., DE P. PEREIRA, P. A. & DE ANDRADE, J. B. (2005) Biodiesel: an overview. *Journal of the Brazilian Chemical Society,* 16**,** 1313-1330.

PINZI, S., ROUNCE, P., HERREROS, J. M., TSOLAKIS, A. & PILAR DORADO, M. (2013) The effect of biodiesel fatty acid composition on combustion and diesel engine exhaust emissions. *Fuel,* 104**,** 170-182.

PRADEEP, V. & SHARMA, R. P. (2007) Use of HOT EGR for NOx control in a compression ignition engine fuelled with bio-diesel from Jatropha oil. *Renewable Energy,* 32**,** 1136-1154.

RAKOPOULOS, C. D., ANTONOPOULOS, K. A. & RAKOPOULOS, D. C. (2007) Experimental heat release analysis and emissions of a HSDI diesel engine fueled with ethanol-diesel fuel blends. *Energy,* 32**,** 1791-1808.

RAKOPOULOS, C. D., HOUNTALAS, D. T., ZANNIS, T. C. & LEVENDIS, Y. A. (2004) Operational and environmental evaluation of diesel engines burning oxygen-enriched intake air or oxygen-enriched fuels: a review. *SAE Paper*.

RAKOPOULOS, C. D., RAKOPOULOS, D. C., HOUNTALAS, D. T., GIAKOUMIS, E. G. & ANDRITSAKIS, E. C. (2008) Performance and emissions of bus engine using blends of diesel fuel with bio-diesel of sunflower or cottonseed oils derived from Greek feedstock. *Fuel,* 87**,** 147-157.

RAKOPOULOS, D. C., RAKOPOULOS, C. D., GIAKOUMIS, E. G., DIMARATOS, A. M. & KYRITSIS, D. C. (2010) Effects of butanol-diesel fuel blends on the performance and emissions of a high-speed DI diesel engine. *Energy Conversion Management,* 51**,** 1989-1997.

RAKOPOULOS, D. C., RAKOPOULOS, C. D., PAPAGIANNAKIS, R. G. & KYRITSIS, D. C. (2011) Combustion heat release analysis of ethanol or n-butanol diesel fuel blends in heavy-duty DI diesel engine. *Fuel,* 90**,** 1855-1867.

REN, Y., HUANG, Z., MIAO, H., DI, Y., JIANG, D., ZENG, K., LIU, B. & WANG, X. (2008) Combustion and emissions of a DI diesel engine fuelled with diesel-oxygenate blends. *Fuel,* 87**,** 2691-2697.

RICHTER, H. & HOWARD, J. (2000) Formation of polycyclic aromatic hydrocarbons and their growth to soot - a review of chemical reaction pathways. *Progress in Energy and Combustion Science,* 26**,** 565-608.

RODRÍGUEZ-FERNÁNDEZ, J., OLIVA, F. & VÁZQUEZ, R. A. (2011) Characterization of the diesel soot oxidation process through an optimized thermogravimetric method. *Energy & Fuels,* 25**,** 2039-2048.

RODRÍGUEZ-FERNÁNDEZ, J., TSOLAKIS, A., AHMADINEJAD, M. & SITSHEBO, S. (2009) Investigation of the deactivation of a NOx-reducing hydrocarbon-selective catalytic reduction (HC-SCR) catalyst by thermogravimetric analysis: effect of the fuel and prototype catalyst. *Energy & Fuels,* 24**,** 992-1000.

ROUNCE, P., TSOLAKIS, A., RODRÍGUEZ-FERNÁNDEZ, J., YORK, A. P. E., CRACKNELL, R. F. & CLARK, R. H. (2009) Diesel engine performance and emissions when first generation meets next generation biodiesel. *SAE Paper*.

SARAVANAN, N. & NAGARAJAN, G. (2008) An experimental investigation of hydrogen-enriched air induction in a diesel engine system. *International Journal of Hydrogen Energy,* 33**,** 1769-1775.

SARAVANAN, N., NAGARAJAN, G., DHANASEKARAN, C. & KALAISELVAN, K. M. (2007) Experimental investigation of hydrogen port fuel injection in DI diesel engine. *International Journal of Hydrogen Energy,* 32**,** 4071-4080.

SAXENA, P. & WILLIAMS, F. A. (2006) Testing a small detailed chemical-kinetic mechanism for the combustion of hydrogen and carbon monoxide. *Combustion and Flame,* 145**,** 316-323.

SCHMIDT, K. & VAN GERPEN, J. (1996) The Effect of Biodiesel Fuel Composition on Diesel Combustion and Emissions. *SAE Paper*.

SCHÖNBORN, A., LADOMMATOS, N., WILLIAMS, J., ALLAN, R. & ROGERSON, J. (2009) The influence of molecular structure of fatty acid monoalkyl esters on diesel combustion. *Combustion and Flame,* 156**,** 1396-1412.

SENATORE, A., CARDONE, M., ROCCO, V. & PRATI, M. V. (2000) A comparative analysis of combustion process in D.I. diesel engine fueled with biodiesel and diesel fuel. *SAE Paper*.

SENTHIL KUMAR, M., RAMESH, A. & NAGALINGAM, B. (2003) Use of hydrogen to enhance the performance of a vegetable oil fuelled compression ignition engine. *International Journal of Hydrogen Energy,* 28**,** 1143-1154.

SERDARI, A., FRAGIOUDAKIS, K., TEAS, C., ZANNIKOS, F., STOURNAS, S. & LOIS, E. (1995) Effect of biodiesel addition to diesel fuel on engine performance and emissions. *Journal of Propulsion and Power,* 15**,** 224-231.

SHI, X., YU, Y., HE, H., SHUAI, S., WANG, J. & LI, R. (2005) Emission characteristics using methyl soyate-ethanol-diesel fuel blends on a diesel engine. *Fuel,* 84**,** 1543-1549.

SHIN, B., CHO, Y., HAN, D., SONG, S. & CHUN, K. M. (2011) Hydrogen effects on NOx emissions and brake thermal efficiency in a diesel engine under low-temperature and heavy-EGR conditions. *International Journal of Hydrogen Energy,* 36**,** 6281-6291.

SINGHYADAV, V., SONI, S. L. & DILIP, S. (2012) Performance and emission studies of direct injection C.I. engine in duel fuel mode (hydrogen-diesel) with EGR. *International Journal of Hydrogen Energy,* 37**,** 3807-3817.

SONG, C.-L., ZHOU, Y.-C. & HUANG, R.-J. (2007) Influence of ethanol diesel blended fuels on diesel exhaust emissions and mutagenic and genotoxic activities of particulate extracts. *Journal of Hazardous Materials,* 149**,** 355-363.

SONG, J., ALAM, M., BOEHMAN, A. L. & KIM, U. (2006) Examination of the oxidation behavior of biodiesel soot. *Combustion and Flame,* 146**,** 589-604.

SONG, J., CHEENKACHORN, K., WANG, J., PEREZ, J., BOEHMAN, A. L., YOUNG, P. J. & WALLER, F. J. (2002) Effect of oxygenated fuel on combustion and emissions in a light-duty turbo diesel engine. *Energy & Fuels,* 16**,** 294-301.

STAAT, F. & GATEAU, P. (1995) The effects of rapeseed oil methyl ester on diesel engine performance, exhaust emissions and long term behaviour-a summary of three years of experimentation. *SAE Paper*.

STRAUSS, S., WASIL, J. R. & EARNEST, G. S. (2004) Carbon monoxide emisions from marine outboard engines. *SAE Paper*.

SUAREZ, P. A. Z., MOSER, B. R., SHARMA, B. K. & ERHAN, S. Z. (2009) Comparing the lubricity of biofuels obtained from pyrolysis and alcoholysis of soybean oil and their blends with petroleum diesel. *Fuel,* 88**,** 1143-1147.

SUKJIT, E. & DEARN, K. D. (2011) Enhancing the lubricity of an environmentally friendly Swedish diesel fuel MK1. *Wear,* 271**,** 1772-1777.

SUKJIT, E., HERREROS, J. M., DEARN, K. D., GARCÍA-CONTRERAS, R. & TSOLAKIS, A. (2012) The effect of the addition of individual methyl esters on the combustion and emissions of ethanol and butanol -diesel blends. *Energy,* 42**,** 364-374.

SUKJIT, E., HERREROS, J. M., DEARN, K. D., TSOLAKIS, A. & THEINNOI, K. (2013) Effect of hydrogen on butanol-biodiesel blends in compression ignition engines. *International Journal of Hydrogen Energy,* 38**,** 1624-1635.

SULEK, M. W., KULCZYCKI, A. & MALYSA, A. (2010) Assessment of lubricity of compositions of fuel oil with biocomponents derived from rape-seed. *Wear,* 268**,** 104-108.

SZYBIST, J. P., BOEHMAN, A. L., TAYLOR, J. D. & MCCORMICK, R. L. (2005a) Evaluation of formulation strategies to eliminate the biodiesel NOx effect. *Fuel Processing Technology,* 86**,** 1109-1126.

SZYBIST, J. P., KIRBY, S. R. & BOEHMAN, A. L. (2005b) NO_X emissions of alternative diesel fuels: A comparative analysis of biodiesel and FT diesel. *Energy & Fuels,* 19**,** 1484-1492.

TOMITA, E., KAWAHARA, N., PIAO, Z., FUJITA, S. & HAMAMOTO, Y. (2001) Hydrogen combustion and exhaust emissions ignited with diesel oil in a dual fuel engine. *SAE Paper*.

TSOLAKIS, A. (2006) Effects on particle size distribution from the diesel engine operating on RME-biodiesel with EGR. *Energy & Fuels,* 20**,** 1418-1424.

TSOLAKIS, A., HERNANDEZ, J. J., MEGARITIS, A. & CRAMPTON, M. (2005) Dual fuel diesel engine operation using H2. Effect on Particulate Emissions. *Energy & Fuels,* 19**,** 418-425.

TSOLAKIS, A. & MEGARITIS, A. (2004) Catalytic exhaust gas fuel reforming for diesel enginesî€”effects of water addition on hydrogen production and fuel conversion efficiency. *International Journal of Hydrogen Energy,* 29**,** 1409-1419.

TSOLAKIS, A., MEGARITIS, A. & WYSZYNSKI, M. L. (2003) Application of exhaust gas fuel reforming in compression ignition engines fueled by diesel and biodiesel fuel mixtures. *Energy & Fuels,* 17**,** 1464-1473.

TSOLAKIS, A., MEGARITIS, A., WYSZYNSKI, M. L. & THEINNOI, K. (2007) Engine performance and emissions of a diesel engine operating on diesel-RME (rapeseed methyl ester) blends with EGR (exhaust gas recirculation). *Energy,* 32**,** 2072-2080.

TURNS, S. R. (1996) *An Introduction to Combustion: Concepts and Applications,* New York, McGraw-Hill.

TURRIO-BALDASSARRI, L., BATTISTELLI, C. L., CONTI, L., CREBELLI, R., DE BERARDIS, B., IAMICELI, A. L., GAMBINO, M. & IANNACCONE, S. (2004) Emission comparison of urban bus engine fueled with diesel oil and 'biodiesel' blend. *Science of the Total Environment,* 327**,** 147-162.

TZANETAKIS, T., MOLOODI, S., FARRA, N., NGUYEN, B., MCGRATH, A. & THOMSON, M. J. (2011) Comparison of the spray sombustion characteristics and emissions of a wood-derived fast pyrolysis liquid-ethanol blend with number 2 and number 4 fuel oils in a pilot-stabilized swirl burner. *Energy & Fuels,* 25**,** 4305-4321.

ULLMAN, T. L., SPREEN, K. B. & MASON, R. L. (1994) Effects of cetane number, cetane improver, aromatics, and oxygenates on 1994 heavy-duty diesel engine emissions. *SAE Paper*.

VALENTINO, G., CORCIONE, F. E., IANNUZZI, S. E. & SERRA, S. (2012) Experimental study on performance and emissions of a high speed diesel engine fuelled with n-butanol diesel blends under premixed low temperature combustion. *Fuel,* 92**,** 295-307.

VARDE, K. S. & FRAME, G. A. (1983) Hydrogen aspiration in a direct injection type diesel engine-its effect on smoke and other engine performance parameters. *International Journal of Hydrogen Energy,* 8**,** 549-555.

WADUMESTHRIGE, K., ARA, M., SALLEY, S. O. & SIMON NG, K. Y. (2009) Investigation of lubricity characteristics of biodiesel in petroleum and synthetic fuel. *Energy & Fuels,* 23**,** 2229-2234.

WADUMESTHRIGE, K., NG, K. Y. S. & SALLEY, S. O. (2010) Properties of butanol-biodiesel-ULSD ternary mixtures. *SAE Paper*.

WEI, D. P., KORCEK, S. & SPIKES, H. A. (1996) Comparison of the lubricity of gasoline and diesel. *SAE Paper*.

WEISKIRCH, C., KAACK, M., BLEI, I. & EILTS, P. (2008) Alternative fuels for alternative and conventional diesel combustion systems. *SAE Paper*.

WESTBROOK, C. K., PITZ, W. J. & CURRAN, H. J. (2006) Chemical kinetic modeling study of the effects of oxygenated hydrocarbons on soot emissions from diesel engines. *Journal of Physical Chemistry A,* 110**,** 6912-6922.

WHITE, C. M., STEEPER, R. R. & LUTZ, A. E. (2006) The hydrogen-fueled internal combustion engine: a technical review. *International Journal of Hydrogen Energy,* 31**,** 1292-1305.

WILLIAMS, A., MCCORMICK, R. L., HAYES, R. R., IRELAND, J. & FANG, H. L. (2006) Effect of Biodiesel Blends on Diesel Particulate Filter Performance. *SAE Paper*.

XING-CAI, L., JIAN-GUANG, Y., WU-GAO, Z. & ZHEN, H. (2004) Effect of cetane number improver on heat release rate and emissions of high speed diesel engine fueled with ethanol-diesel blend fuel. *Fuel,* 83**,** 2013-2020.

YI, H. S., MIN, K. & KIM, E. S. (2000) The optimised mixture formation for hydrogen fuelled engines. *International Journal of Hydrogen Energy,* 25**,** 685-690.

YOON, S. H., SUH, H. K. & LEE, C. S. (2009) Effect of spray and EGR rate on the combustion and emission characteristics of biodiesel fuel in a compression ignition engine. *Energy & Fuels,* 23**,** 1486-1493.

YU, R. C. & SHAHED, S. M. (1981) Effects of injection timing and exhaust gas recirculation on emissions from a DI diesel engine. *SAE Paper*.

YÜCESU, H. S. & İLKILIÇ, C. (2006) Effect of cotton seed oil methyl ester on the performance and exhaust emission of a diesel engine. *Energy Sources,* Part A 28**,** 389-398.

ZHENG, M., MULENGA, M. C., READER, G. T., WANG, M., TING, D. S. K. & TJONG, J. (2008) Biodiesel engine performance and emissions in low temperature combustion. *Fuel,* 87**,** 714-722.

ZOLDY, M., HOLLO, A. & THERNESZ, A. (2010) Butanol as a diesel extender option for internal combustion engines. *SAE Paper*.